

THE CATHOLIC UNIVERSITY OF AMERICA

Chronic Alcohol Consumption Impairs Clathrin-Mediated Endocytosis
And Microtubule-Dependent Nuclear Translocation in Hepatocytes

A DISSERTATION

Submitted to the Faculty of the

Department of Biology

School of Arts and Sciences

Of The Catholic University of America

In Partial Fulfillment of the Requirements

For the Degree

Doctor of Philosophy

By

David Jaime Fernandez

Washington, D.C.

2012

Chronic Alcohol Consumption Impairs Clathrin-mediated Endocytosis And Microtubule-dependent Nuclear Translocation in Hepatocytes

David J. Fernandez, Ph.D.

Director: Pamela L. Tuma, Ph.D.

Although alcoholic liver disease is clinically well described, the molecular basis for alcohol-induced hepatotoxicity is not well understood. We therefore sought to further explore a known protein trafficking defect caused by chronic alcohol exposure: receptor internalization from the hepatocyte plasma membrane, as well as a hypothesized defect in microtubule-dependent nuclear translocation of transcription factors. We hypothesized that both of these protein trafficking defects are caused by ethanol-induced protein hyperacetylation. Previously, we determined that the clathrin-mediated internalization of asialoglycoprotein receptor (ASGP-R) was impaired in ethanol-treated WIF-B cells, whereas the internalization of a glycosylphosphatidylinositol (GPI)-anchored protein thought to be internalized via a caveolae/raft-mediated pathway was not changed. ASGP-R internalization was also impaired by trichostatin-A (TSA), a drug that induces global protein hyperacetylation, providing evidence that hyperacetylation is indeed associated with a defect in this process. We proposed that clathrin-mediated endocytosis was selectively impaired by ethanol. Thus, we examined the internalization of a panel of proteins and compounds internalized by different mechanisms in control and ethanol-treated WIF-B cells. Markers known to be internalized via clathrin-mediated mechanisms were impaired whereas the internalization of a known marker for caveolae/raft-mediated endocytosis

was not altered after ethanol exposure. Fluid phase internalization of Lucifer Yellow was not impaired in ethanol-treated WIF-B cells. Similarly, non-vesicle-mediated uptake and subsequent apical delivery of fluorescein diacetate was not altered. We conclude that clathrin-mediated endocytosis is selectively impaired by ethanol exposure.

Previously we found that alcohol exposure led to increased microtubule acetylation and stability in WIF-B cells and in livers from ethanol-fed rats. Because microtubules are known to regulate nuclear translocation of transcription factors, and dynamic microtubules are required for translocation of some transcription factors, we examined whether alcohol-induced microtubule acetylation and impairs nuclear translocation. Representing factors that undergo directed nuclear delivery, we examined the growth hormone-induced translocation of Signal Transducer and Activator of Transcription 5B (STAT5B) and the interleukin 6 (IL-6) -induced translocation of STAT3. Representing factors that are sequestered in the cytoplasm by microtubule attachment until ligand activation, we examined the Transforming Growth Factor- β (TGF- β) -induced translocation of Smad2/3. Ethanol exposure impaired the translocation of STAT3 and STAT5B, but not Smad2/3. STAT5B translocation was decreased to similar extents by addition of taxol or trichostatin A, agents that promote microtubule acetylation in the absence of alcohol. Thus, the alcohol-induced impairment of STAT nuclear translocation can be explained by increased microtubule acetylation. Only ethanol-treatment impaired STAT5B activation, indicating microtubule acetylation is not important for its activation by

Janus Kinase 2 (Jak2). Nuclear exit was unchanged in treated cells, indicating this process is also independent of microtubule acetylation and stability. Together, these results raise the exciting possibility that deacetylase agonists may be effective therapeutics for the treatment of alcoholic liver disease.

This dissertation by David J. Fernandez fulfills the dissertation requirement for the doctoral degree in the Department of Biology approved by Pamela L. Tuma, Ph.D., as Director, and by J. Michael Mullins, Ph.D., and John E. Golin, Ph.D., as Readers.

Pamela L. Tuma, Ph.D., Director

J. Michael Mullins, Ph.D., Reader

John E. Golin, Ph.D., Reader

DEDICATION

First and foremost, I dedicate this dissertation in thanks to the Blessed Trinity for giving me the strength to persevere. I also dedicate this to my amazing family, who've encouraged me every step of the way, to just keep going...

TABLE OF CONTENTS

List of Illustration	vi
Abbreviations	viii
Acknowledgements	xii
Introduction	
The liver	1
Alcoholic liver disease	4
WIF-B cells	10
Known Ethanol-induced Impairments in Protein Trafficking	14
Ethanol-induced Impairment of Clathrin-mediated Endocytosis	17
Signaling pathways	22
Materials and Methods	
Reagents and Antibodies	28
Ethanol Treatment of Rats	29
Cell culture, virus production and infection	29
Indirect Immunofluorescence Microscopy	30
Antibody trafficking in live cells	31
Cholera toxin internalization	31
Lucifer Yellow and HRP internalization	32
Fluorescein diacetate labeling	33
Cell fractionation	33
Immunoblotting	33
Liver Fractionation	34
Ligand addition and washout	34
Statistical Analysis	35
Part I: Ethanol selectively impairs clathrin-mediated internalization in polarized hepatic cells	36
Ethanol impairs clathrin-mediated, but not caveolae/raft-mediated internalization	38
Ethanol does not impair fluid phase or non-vesicle-mediated internalization	42
Clathrin coated assemblies accumulate at the plasma membrane in ethanol-treated cells	45
Ethanol impairs the endocytosis of apical residents with no known internalization signals	47
Conclusions and Implications of Part I	54

Part II: Hepatic microtubule acetylation and stability induced by chronic alcohol exposure impair nuclear translocation of STAT3 and STAT5B, but not Smad2/3	55
STAT and Smad steady state distributions and nuclear translocation are differentially dependent on microtubules	57
Ethanol impairs nuclear translocation of the STATs, but not Smad2/3	61
Decreased nuclear STAT5B is observed in livers from ethanol-fed rats	66
Expression of EGF-R, a target of STAT5B, is decreased in ethanol-treated cells	67
Increased microtubule acetylation and stability impair STAT5B nuclear translocation	68
STAT5B activation by Jak2 and nuclear exit are independent of microtubule acetylation and stability	72
Ethanol selectively impairs Jak2 activation	79
Conclusions and Implications of Part II	81
Discussion	82
Chronic ethanol exposure impairs clathrin-mediated endocytosis in hepatocytes	82
Ethanol-induced modifications of the clathrin machinery	83
Are single spanning apical proteins internalized via clathrin-mediated mechanisms?	86
Impaired clathrin-mediated internalization may explain nutritional deficiencies in patients	87
Impact of impaired clathrin-mediated internalization on liver function	88
Chronic ethanol exposure impairs microtubule-dependent nuclear translocation in hepatocytes	89
Ethanol selectively impairs directed nuclear translocation	90
Ethanol, but not taxol or TSA, impairs STAT5B activation	92
Clinical implications	93
References	95

LIST OF ILLUSTRATIONS

Figure 1	General Structure of the Liver	3
Figure 2	The progression of alcoholic liver disease	5
Figure 3	Ethanol metabolism	7
Figure 4	WIF-B cells are a good model for studying hepatotoxicity	12
Figure 5	Known defects in protein trafficking	16
Figure 6	The Jak/STAT pathway	23
Figure 7	The Smad pathway	26
Figure 8	Clathrin-mediated internalization is impaired in ethanol-treated cells	40
Figure 9	Caveolae/raft-mediated internalization is not impaired in ethanol-treated cells	42
Figure 10	Fluid phase endocytosis is not impaired in ethanol-treated cells	43
Figure 11	The non-vesicle-mediated uptake and subsequent canalicular delivery of fluorescein diacetate is not altered in ethanol-treated cells	45
Figure 12	Clathrin coated assemblies accumulate at the plasma membrane in ethanol-treated cells	47
Figure 13	Internalization of single spanning apical proteins with no known sorting information is impaired in ethanol-treated cells	50
Figure 14	Internalization of the single spanning apical residents is clathrin-dependent	53

Figure 15	Microtubule depolymerization enhances Smad2/3 nuclear delivery, but impairs STAT translocation	59
Figure 16	Microtubule depolymerization enhances Smad2/3, but impairs STAT5B nuclear translocation after ligand stimulation	61
Figure 17	Ethanol-exposure alters the steady state distributions of STAT5B and STAT3, but not Smad2/3	63
Figure 18	Ethanol exposure inhibits the ligand-stimulated translocation of STAT5B, but not Smad2/3	65
Figure 19	Decreased nuclear STAT5B is observed in livers from ethanol-fed rats	67
Figure 20	Ethanol-induced microtubule acetylation leads to increased cytosolic STAT5B	70
Figure 21	Ethanol-induced microtubule acetylation can explain impaired STAT5B nuclear translocation	72
Figure 22	Ethanol impairs STAT5B phosphorylation after GH addition	74
Figure 23	Ethanol, but not taxol or TSA, impairs STAT5B phosphorylation after GH addition	76
Figure 24	Ethanol does not impair STAT5B dephosphorylation or nuclear exit	78
Figure 25	Ethanol, but not taxol or TSA, impairs Jak2 phosphorylation after GH addition	80
Figure 26	Ethanol impairs vesicle fission	86
Figure 27	Ethanol impairs microtubule-dependent nuclear translocation	91

ABBREVIATIONS

4MP	4-methylpyrazole
5'NT	5' nucleotidase
AceCS2	acetyl-CoA synthetase 2
ADH	alcohol dehydrogenase
ALDH	acetylaldehyde dehydrogenase
AP2	adaptor protein 2
APN	aminopeptidase N
ASGP-R	asialoglycoprotein receptor
ATP	adenosine triphosphate
BC	bile canaliculus
BMP	bone morphogenic protein
BSA	bovine serum albumin
CHC	clathrin heavy chain
c-myc	cellular myelocytomatosis virus protein
CTxB	cholera toxin subunit B
CYP2E1	cytochrome P450 2E1
DMEM	Dulbecco's modified Eagle medium
DNA	deoxyribose nucleic acid
DPPIV	dipeptidyl peptidase IV
DTT	dithiothreitol

EE	early endosome
EGF	epidermal growth factor
EGF-R	epidermal growth factor receptor
EGTA	ethylene glycol tetraacetic acid
ER	endoplasmic reticulum
EtOH	ethanol
FBS	fetal bovine serum
FDA	fluorescein diacetate
FITC	fluorescein isothiocyanate
GH	growth hormone
GPI	glycophosphatidylinositol
GTP	guanosine triphosphate
HA	hemagglutinin
HAT	histone acetyltransferase
HDAC	histone deacetylase
HNE	4-hydroxy-2-nonenal
HRP	horse radish peroxidase
IB	immunoblot
IL-6	interleukin 6
Jak	Janus kinase
LDL	low density lipoprotein
LY	Lucifer Yellow

MAP	microtubule-associated protein
Map2cN	nuclear isoform of microtubule-associated protein 2
MDA	malondialdehyde
MIZ-1	myc-interacting zinc finger protein 1
nz	nocodazole
p53	protein 53
PAGE	polyacrylamide gel electrophoresis
PBS	phosphate buffered saline
PEM	Pipes/EGTA/MgSO ₄
PGC-1 α	peroxisome proliferator-activated receptor- γ coactivator 1 α
PMSF	phenylmethanesulfonylfluoride
PPAR γ	peroxisome proliferator activated receptor γ
pIgA-R	polymeric IgA receptor
PIP ₂	phosphatidylinositol 4,5-bisphosphate
pSTAT5B	phosphorylated STAT5B
PTM	post-translational modification
RE	recycling endosome
ROS	reactive oxygen species
SDS	sodium dodecyl sulfate
SEM	standard error or the mean
SH2	SRC homology 2
Smad	homologue of SMA and mothers against decapentaplegic

SOCS2	suppressor of cytokine signaling 2
SREPB-1c	sterol regulatory element binding protein 1c
STAT	signal transducer and activator of transcription
TGF- α	transforming growth factor α
TGF- β	transforming growth factor β
TGN	<i>trans</i> -Golgi network
Tf-R	transferrin receptor
TNF- α	tumor necrosis factor α
TSA	trichostatin A
WH	whole homogenate
WIF-B	human fibroblast (WI-38) fused with rat hepatoma (Fao)
WO	washout

ACKNOWLEDGEMENTS

I thank God every day for helping me get through this difficult period.

I thank Dr. Pamela Tuma, my advisor. I learned more from her than she will ever know, and not the least of which was how to think like a scientist. One of my favorite lessons with regards to thinking critically was “just because it’s published in XYZ journal, doesn’t necessarily make it correct.” This sort of thinking, of believing in who we are and what we can do, instilled confidence in me, which has carried over to other areas of my life. I thank her for letting me be myself, and allowing me to wear shorts and t-shirts nearly every day I was in her lab. I also thank Dr. Tuma for coming closer than anyone ever has in instilling a bit of high culture in my life.

I extend a special thanks to Dr. Mullins and Dr. Golin, for not only agreeing to be on my committee, but also for always being available for chatting and joking with me. I’ve never felt that they were too busy for me, and I am grateful for having gotten to know them on a professional as well as personal level.

I am very proud of the CUA Biology Department, and am grateful to have been a member. I think the entire faculty is outstanding. It may be a small department, but it produces some first-class science.

Where would I be without the support of the other members of the Tuma Lab, both past and present? Grad school is incredibly stressful, and I am sure I would have cracked if not for being able to have less-than-serious conversations with these fantastic people! I will miss Dr. Sai Prasad Ramnarayanan, Dr. Blythe Shepard, Dr. Julie In, Dr. Ben Kalu, and future Drs. Anneliese Striz, Alfonso Lopez-Coral, Jenn Groebner, and Julia Omotade. I am also thankful for my friendship with Dr. Vishal Kottadiel, and all of our great conversations.

Last but not least, I thank my loving family. Without their constant encouragement and support, I am sure I would have just stayed on the Metro Red Line all the way to the end of the line on some days...

INTRODUCTION

Alcoholic liver disease is clinically well described, but the molecular basis for alcohol-induced hepatotoxicity is not well understood. The fact that the liver is so heavily impacted by chronic alcohol consumption warrants closer examination of the organ itself, which will allow for a greater understanding of the pathology of alcoholic liver disease. The liver is the major site of ethanol metabolism, and thus sustains the most injury from chronic alcohol consumption.

The Liver:

Located in the upper right quadrant of the abdomen, the liver is the largest internal organ in the body, normally weighing about three pounds in adults (Seeley, et al., 2002). Structurally, the liver is divided into two major lobes and two minor lobes, and located inferiorly to the bulk of the organ is the porta, or region where ducts, nerves, and blood vessels are found that functionally connect the liver to the rest of the body (Seeley, et al., 2002). The two main blood vessels of the porta are the hepatic artery and the hepatic portal vein. The hepatic artery conducts oxygen-rich blood that has recently traversed the lungs, to the liver, which is then distributed to its cells by smaller arteries and other blood vessels. The hepatic portal vein also carries blood to the liver, but it is oxygen-poor. Rather this blood is laden with nutrients, which are brought from the digestive tract. As such, the liver is ideally placed to fulfill its crucial role as the body's main processing center for nutrients and toxic xenobiotics. Indeed, the liver functions to aid in digestion;

glycogen, fat, vitamin, and mineral storage; detoxification of harmful xenobiotics; and synthesis of several important blood proteins (Seeley, et al., 2002).

The aforementioned processes occur mostly in the hepatocyte, a highly specialized epithelial cell type, and the most prevalent cell type in the liver. Like the liver itself, this unique cell type is optimally structured and oriented to perform its roles. Specifically, the hepatocyte contacts at least two blood sinusoids by its basolateral membrane. Similarly, a tightly regulated cell polarity allows for the maintenance of an apical membrane, which encloses a portion of the tubular network that forms the bile canaliculi (Tuma and Hubbard, 2001). As seen in Figure 1, the bile canaliculi are actually formed from the apical membranes of adjacent hepatocytes. These two apical membrane domains, separated by tight junctions, are functionally distinct as well. At the basolateral surface, the membrane is composed of many microvilli, which increase the surface area of this membrane, and thus allow for more efficient transport of materials across it, and into or out of the blood. As such, this domain is highly active with regards to exocytosis and endocytosis, to allow bulk exchange with the bloodstream (Schachter, et al., 2001). A high concentration of receptors is found in the basolateral domain, so as to allow the hepatocyte to take up (in the case of crucial factors or nutrients) or respond to (in the case of ligands) important molecules carried in the bloodstream. On the other hand, while the apical membrane comprises less than 15% of the hepatocyte's surface, there is present a high concentration of ATP-dependent transporters, ion channels, and enzymes, which collectively allow this domain to be the site of bile and metabolized xenobiotic secretion, as well as nucleotide salvage (Ujhazy, et al., 2001).

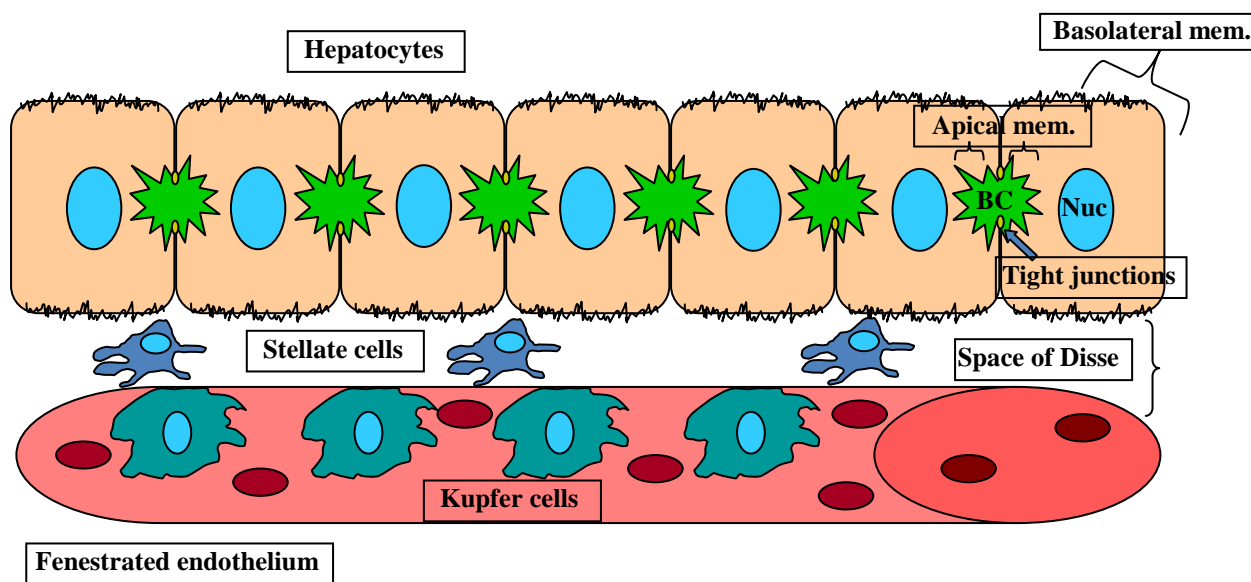


Figure 1. General Structure of the Liver. Hepatocytes are arranged in cords or sheets, with their basolateral membranes facing the blood sinusoids. These sinusoids are composed of fenestrated endothelial cells, to which the resident macrophages (Kupfer cells) adhere. In between the hepatocytes basolateral membrane and the fenestrated endothelial cells are the hepatic stellate cells, which reside in the space of Disse. The hepatocytes basolateral membranes are kept structurally distinct from the apical membranes by tight junctions. The apical membranes of adjacent hepatocytes form the bile canaliculi (BC), a tubular network into which bile is secreted. (modified from conatuspharma.com/images/img_liver_fig01.jpg)

Though hepatocytes constitute the majority of the liver by mass and cell type, as previously mentioned, they are aided and kept intact by other specialized cells (Figure 1). As the liver is so highly-perfused with blood, and functionally serves to filter this blood before it passes through the remainder of the body, it is essential to have an efficient means of eliminating dangerous foreign particles or organisms found in the blood. To accomplish this, the liver contains specialized macrophages called Kupffer cells (Figure 1, dark blue cells). Exclusively residing in the liver, these cells attach to the fenestrated endothelial cells of the blood sinusoids. Kupffer cells act like other macrophages,

engulfing potentially harmful materials such as bacteria, or apoptotic bodies scavenged from the remains of erythrocytes, hepatocytes, or neutrophils (Liu, et al., 2010).

However, once activated, Kupffer cells produce pro-inflammatory cytokines, such as interleukin-6, tumor necrosis factor- α , interleukin-1, and oncostatin M, that can act as chemottractants as well as induce the proliferation and activation of another specialized liver cell called the hepatic stellate cell (Rojkind, et al., 2001 and Liu, et al., 2010).

Normally, hepatic stellate cells reside both outside the fenestrated endothelial cells and the hepatocytes, in a gap known as the space of Disse (Figure 1, smaller blue cells) (Rojkind, et al., 2001). Combined with triglycerides, vitamin A is stored within these cells as fat droplets. However, upon activation, these cells shift from vitamin A storage to pro-inflammatory cytokine production, including a positive feedback loop involving interleukin-6 that leads to further activation. Ultimately, hepatic stellate cell activation results in collagen deposition, which plays a critical role in the progression of liver injury during inflammation (Rojkind, et al., 2001).

Alcoholic Liver Disease:

Approximately 75% of all Americans consume alcohol and 100,000 deaths per year are attributed to alcohol consumption. Of those deaths, greater than 20,000 are caused by cirrhosis of the liver, the 12th largest cause of death in Americans. Clearly, alcoholic liver disease is a major biomedical health concern in the United States. However, the progression to alcoholic liver disease involves a stepwise continuum, as seen in Figure 2.

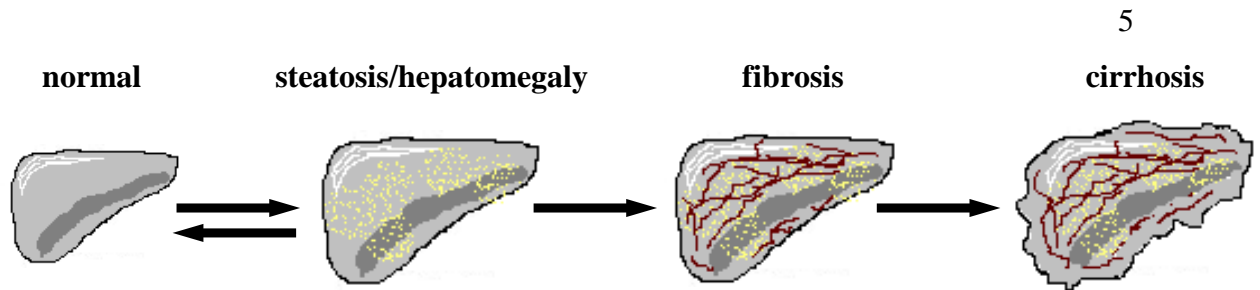


Figure 2. The progression of alcoholic liver disease. During the progression of ALD, fat accumulates in the liver, and the organ becomes enlarged. Further infiltration by immune cells and inflammation leads to hepatic stellate cell activation. Activated hepatic stellate cells may then deposit collagen and fibronectin, leading to fibrosis. Finally, as scar tissue replaces functional hepatocytes, the liver becomes cirrhotic. (modified from wikidoc.org/images/7/76/Stage_of_liver_damage.JPG)

Around 90% of individuals who drink regularly develop fatty liver, or steatosis, which is generally asymptomatic and reversible (Figure 2, second panel) (O’Shea, et al., 2010). Of these, about a third of individuals will progress to alcoholic hepatitis, which involves chronic inflammation of the liver (O’Shea, et al., 2010). While this stage may also be asymptomatic, it represents a critical juncture in the development of the terminal disease: progression from this point to fibrosis and eventually cirrhosis is not reversible and usually fatal (Diehl, 2001). During these later stages, fibrosis (scar tissue deposits) and activation of hepatic stellate cells occurs (Figure 2, third panel), which leads to additional inflammation of the organ, including infiltration of immune cells that leads to substantial hepatic apoptosis. Activated hepatic stellate cells produce collagen and fibronectin deposits, which further damages normal hepatic function. As the damaged and apoptotic hepatocytes are replaced by scar tissue, which impairs their proper functioning, the liver has then become cirrhotic (Figure 2, last panel). Complications commonly associated with liver cirrhosis include hepatic encephalopathy, ascites (a build-up of fluid in the

peritoneal cavity), jaundice, and hepatorenal syndrome (an impairment of proper kidney function) (Rahimi, et al., 2012). Despite considerable research efforts aimed at understanding the progression of the disease, the specific mechanisms leading to alcohol-induced tissue damage remain elusive. Defining these cellular mechanisms is critical for the development of more effective treatments for patients suffering from the disease. This information will also benefit our understanding and treatment of other liver diseases.

Ethanol metabolism:

Ethanol enters the liver via the bloodstream, where it is then quickly metabolized to acetylaldehyde by the cytosolic enzyme alcohol dehydrogenase (ADH), which resides mainly in the hepatocyte but may also function to metabolize ethanol in the male intestine and stomach (Figure 3, left side). Acetylaldehyde is then metabolized to acetate by the mitochondrial enzyme aldehyde dehydrogenase (ALDH), which is the crucial step because acetylaldehyde is highly reactive. Acetate is highly water-soluble, and is excreted in the urine. Alternatively, acetylaldehyde is produced by ethanol metabolism in the endoplasmic reticulum (ER) via the cytochrome p450 2E1 (CYP2E1) enzyme (Figure 3, right side) (Tuma and Casey, 2003). Compounding the production of acetylaldehyde, ethanol metabolism via the CYP2E1 pathway produces highly toxic reactive oxygen species (ROS), which can lead to oxidative stress and ultimately apoptosis (Tuma and Casey, 2003). As their name implies, ROS are indeed highly reactive, and can form intermediates when bound to lipids, as shown in Figure 3. Such intermediates include malondialdehyde (MDA) and 4-hydroxy-2-nonenal (HNE), which can further covalently

bind with proteins, lipids, and even DNA, leading to a disruption of proper hepatocyte function. (Brooks, et al.,1997; Tuma and Casey, 2003; Tuma, et al.,1987).

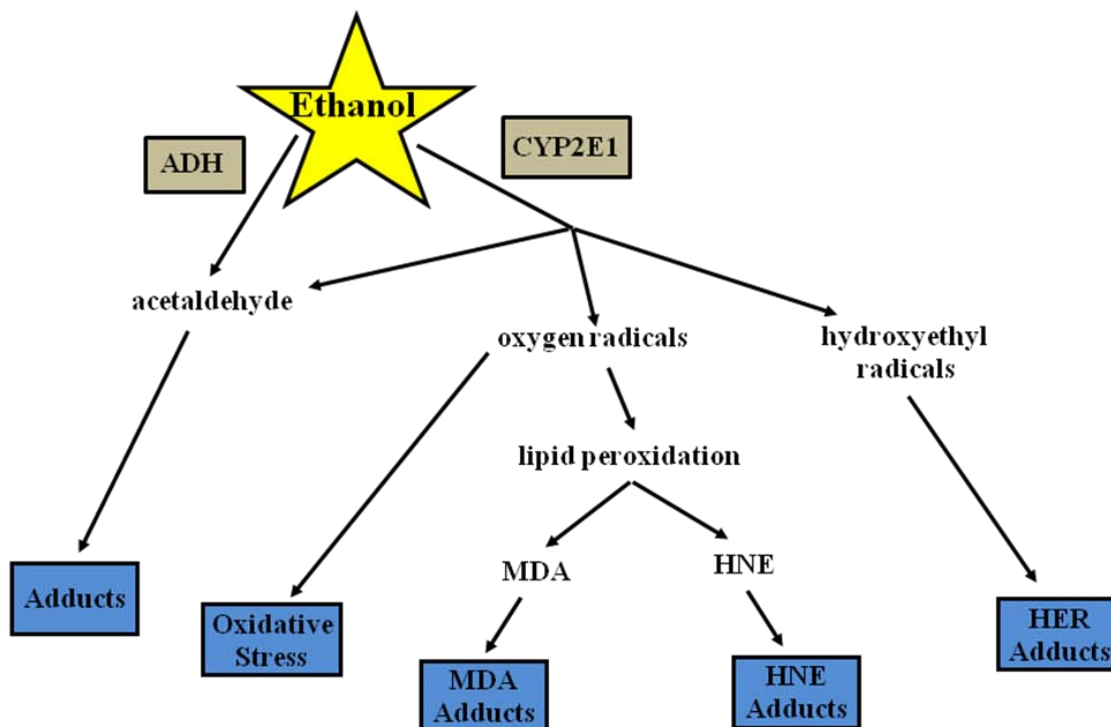


Figure 3. Ethanol metabolism. Ethanol is metabolized in the hepatocyte cytosol by alcohol dehydrogenase (ADH), leading to acetaldehyde production. Acetaldehyde is then metabolized into acetate by aldehyde dehydrogenase (ALDH). Alternatively, ethanol may be metabolized in the hepatocyte ER by cytochrome p450 2E1 (CYP2E1), producing acetaldehyde, oxygen radicals, and hydroxyethyl radicals. All of these intermediates are highly reactive, and can covalently modify proteins, DNA, and lipids. These modifications may alter normal hepatocytes functions. (modified from Tuma and Casey, 2003).

Ethanol-induced tubulin modifications:

Many proteins can be post-translationally modified by intermediates produced by ethanol metabolism. In fact, ethanol metabolism induces many post-translational modifications (PTM) of the natural repertoire, including acetylation, phosphorylation, methylation, and ubiquitination. Our studies focused mainly on acetylation, which is a PTM that may rival

phosphorylation in scope and function (Kouzarides, 2000). As protein phosphorylation is tightly regulated by the reciprocal actions of kinases and phosphatases, so acetylation is controlled by the functions of histone acetyltransferases (HATs) and histone deacetylases (HDACs) (Kouzarides, 2000; Plevoda and Sherman, 2002). Histones were the first proteins known to be acetylated and deacetylated by these enzymes, and so were named as such. While most HATs and HDACs reside in the nucleus, one Particular HDAC is solely cytosolic, and is expressed in the liver: HDAC6 (Grozinger et al., 1999; Hubbert et al., 2002; Matsuyama et al., 2002; Shepard et al., 2008; Zhang et al., 2008; Zhang et al., 2003). One of HDAC6's main substrates is α -tubulin, and importantly, α -tubulin is known to be hyperacetylated in ethanol-exposed cells (Glozak et al., 2005; Kannarkat et al., 2006; Shepard et al., 2008; Shepard et al., 2009b; Zhang et al., 2008; Zhang et al., 2003). This point, along with more details about protein acetylation during ethanol metabolism, will now be addressed.

Many proteins are known to be adducted by acetaldehyde, including tubulin, actin, calmodulin, hemoglobin, hepatic enzymes and plasma proteins (Jennet, et al., 1989; Mauch, et al., 1986; Mauch, et al., 1987; Medina, et al., 1985; Stevens, et al., 1981; Xu, et al., 1989). In general, acetaldehyde is thought to form stable adducts with the ϵ -amino group of lysine residues (Tuma, et al., 1991; Tuma, et al., 1987). One of the best-studied target proteins for acetaldehyde adduction is α -tubulin (Tuma, et al., 1991). In order to fully appreciate the consequences of acetaldehyde adduction on α -tubulin, it is first useful to understand the basic structure and functions of microtubules. Microtubules are polymers comprised of repeating units of α - and β -tubulin heterodimers. These

heterodimers form protofilaments, and 13 protofilaments, assembled in parallel to each other, constitute the hollow tube of a microtubule. Microtubules (along with actin microfilaments and keratin intermediate filaments) form the main components of the cytoskeleton. Additionally, microtubules provide a “track” on which vesicles and proteins can move, depending on their associated motor proteins. Movement along microtubules is dependent on their orientation, which is highly ordered. In polarized cells such as hepatocytes, microtubule orientation is such that their minus ends are proximal to the apical plasma membrane, while their plus ends face the basolateral plasma membrane (Meads and Schroer, 1995).

There are two main populations of microtubules: dynamic and stable. Stable microtubules generally have a longer half-life, are more resistant to microtubule poisons such as cold and nocodazole, and have specific post-translational modifications on the α -tubulin subunit, such as acetylation, C-terminal tyrosine removal, polyglutamylation, and polyglycylation (Westermann and Weber, 2003). *In vitro*, α -tubulin was found to be preferentially modified on a highly reactive lysine (Szasz, et al., 1982; Szasz, et al., 1986) in a time and concentration dependent manner (Jennett, et al., 1987; Jennett, et al., 1989). It was later revealed that α -tubulin is acetylated on lysine-40 (Westermann and Weber, 2003). *In vitro* polymerization assays using low acetaldehyde:tubulin dimer levels further revealed that adduction drastically impaired microtubule formation (Jennett, 1980). This impairment occurred at substoichiometric amounts of acetaldehyde (0.2 mol acetaldehyde/mol tubulin) (Smith, et al., 1992) suggesting that low levels of adduction can have far reaching effects on microtubule function. The defect in tubulin

polymerization was also examined in isolated hepatocytes from alcohol-fed rats (Yoon, et al., 1998). After removing nocodazole from the medium (a reversible, microtubule depolymerizing agent), microtubule regrowth was found to be significantly impaired in ethanol-treated hepatocytes consistent with impaired polymerization seen *in vitro*. Ethanol-treated WIF-B cells exhibited a similar tubulin phenotype where microtubule regrowth after nocodazole washout was impaired (Kannarkat, et al., 2006).

Steady state microtubules in alcohol-treated WIF-B cells were also found to be more stable and acetylated 2-3-fold more than in control cells (Kannarkat, et al., 2006). This post-translational modification is characteristic of stable microtubule populations (Westermann and Weber, 2003). These results were confirmed in livers from ethanol-fed rats and in ethanol-treated liver slices indicating the findings have physiologic importance (Kannarkat, et al., 2006). Because microtubule hyperacetylation is prevented by the ADH inhibitor 4-methylpyrazole (4-MP) in WIF-Bs and liver slices, and potentiated by cyanamide (in WIF-Bs), increased acetylation and stability require alcohol metabolism and are likely mediated by acetaldehyde. Thus, ethanol metabolism impairs tubulin polymerization, but once microtubules are formed they are hyperstabilized.

WIF-B cells:

Traditionally, animal models have been used to describe physiological responses to alcohol consumption. Although these studies have provided a wealth of information, there are disadvantages to using animal models. Not only is there considerable physiologic variation among animals, it is also difficult to quickly alter experimental

parameters (e.g., addition or withdrawal of inhibitors, changes in temperature) that are required for mechanistic studies. In addition, inhibitors or other experimental reagents are introduced to all organs of the animal's body where they may interfere with defining hepatic-specific responses or may produce severe side effects. Because these experimental barriers prevent good mechanistic studies in animals, many researchers have turned to *in vitro* systems. The challenge here has been to maintain cells in culture that retain their hepatocyte-specific characteristics that are required for proper liver function (e.g., cell surface polarity with canalicular and sinusoidal plasma membrane domains, bile acid transport, albumin and lipoprotein production, efficient ethanol metabolism, etc.). Several *in vitro* systems have been developed, but three hold the most promise: isolated hepatocytes, HepG2 hepatoma cells stably expressing exogenous alcohol dehydrogenase (ADH) (Clemens, et al., 1995) and the polarized, hepatic WIF-B cells (Shanks et al., 1994).

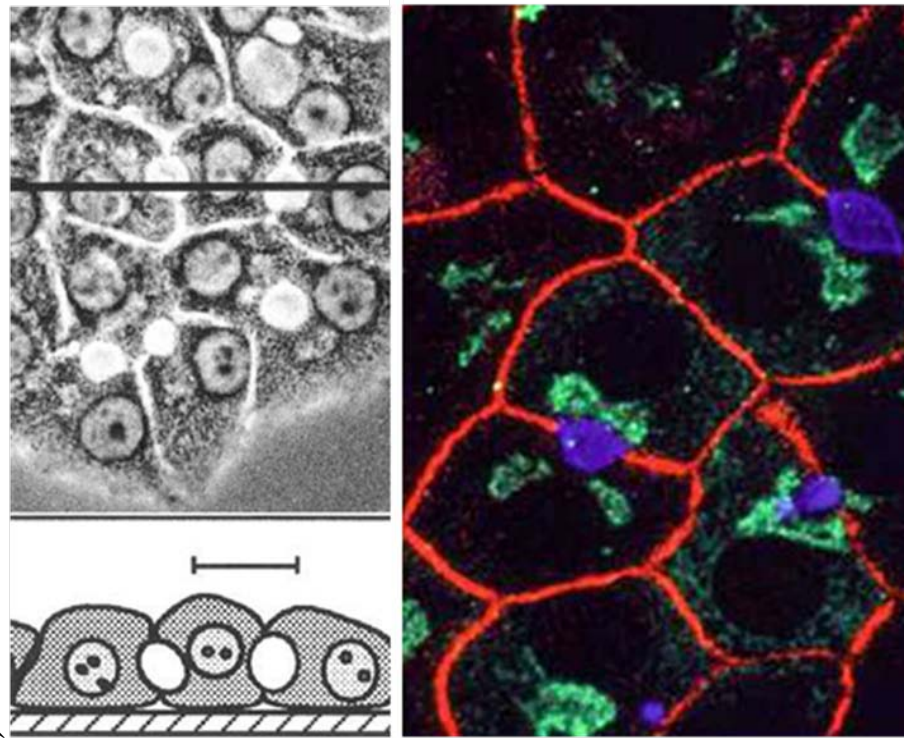


Figure 4. WIF-B cells are a good model for studying hepatotoxicity. About 70-95% of WIF-B cells are polarized in culture (left panel, top). Adjacent polarized WIF-B cells come together to form bile canaliculi (BCs) (left panel, top and bottom). The BC is comprised of the apical membranes of these cells (stained in blue). The apical membranes are separated from the basolateral membranes (stained in red) by tight junctions. The Golgis are stained in green (right panel).

Although isolated hepatocytes have been the most popular model system for the past 30 years, they may not be the most suitable system. Within hours of culture, they lose their liver-specific phenotype. Not only is their cell surface polarity lost, but also lost is the expression of many liver specific proteins, including expression of ADH. Similarly, only 10% of HepG2 cells are polarized in culture and many of their liver-specific functions are lost. In contrast, WIF-B cells, when cultured on plastic or glass coverslips, enter a terminal differentiation program. After 7-10 days in culture, 70-95% of WIF-B cells become fully differentiated and exhibit phase-lucent structures that are

functionally and compositionally analogous to the bile canaliculi (BC) (Figure 4, top left panel) (Shanks, et al., 1994). These phase-lucent BCs can be seen in Figure 4 in between adjacent cells, and are a hallmark of polarized WIF-B cells, functioning as bile canaliculi *in situ*. A drawing representing a cross-section of polarized WIF-B cells can be seen in Figure 4, bottom left panel, in which it can be seen that the cells form 3-dimensional BCs with adjacent cells. Domain-specific membrane proteins are localized in WIF-B cells as they are in hepatocytes *in situ* and liver-specific functions are maintained (Griffo, et al., 1993).

Importantly, WIF-B cells efficiently metabolize ethanol into acetaldehyde using ADH and cytochrome P450 2E1 (CYP 2E1) (Schaffert, 2004). Like hepatocytes *in situ*, ethanol-treated WIF-B cells have a reduced redox state and have increased triglyceride levels corresponding to the clinically observed fatty liver (Schaffert, et al., 2004). Ethanol-treated WIF-B cells also exhibit two-fold more ROS and caspase-3 activation, and this corresponds with increased cell death by necrosis and Fas-mediated apoptosis (McVicker, et al., 2009). Our recent studies have also shown that WIF-B cells display alcohol-induced defects in cellular processes as described *in situ* or in isolated hepatocytes. These impairments include (so far) decreased microtubule polymerization (Kannarkat, et al., 2006), defects in ASGP-R trafficking and albumin secretion (Joseph, et al., 2007). Furthermore, we determined that microtubules in both WIF-B cells and in livers from alcohol-fed rats were hyperacetylated (Kannarkat, et al., 2006). We believe these properties argue strongly that WIF-B cells are an excellent model for the

examination of alcohol-induced hepatotoxicity and will allow for meaningful mechanistic studies to be performed.

Known Ethanol-induced Impairments in Protein Trafficking:

To date, numerous proteins are known to have alcohol-induced alterations in their dynamics. As seen in Figure 5, the two main transport pathways that appear to be affected are: transport of newly synthesized secretory or membrane glycoproteins from the Golgi to the basolateral membrane (Figure 5, #3) and clathrin-mediated endocytosis from the sinusoidal surface (Figure 5, #1) (Shepard, et al., 2009). Additionally, studies performed in WIF-B cells that used 201-F, a novel drug that specifically depolymerizes dynamic microtubules (leaving only stable, acetylated ones behind), showed that secretion (Figure 5, #3), transcytosis (Figure 5, #2), and nuclear translocation (Figure 5, #4) were impaired (Pous, et al., 1998; Phung-Kostas, et al., 2005).

The liver synthesizes the majority of serum proteins and lipoproteins and is characterized by robust constitutive secretion from the basolateral surface. In general, proteins destined for the secretory pathway encode a signal sequence that directs their docking and co-translational entry into the endoplasmic reticulum (ER). During transit through the ER, secretory proteins are step-wise glycosylated, properly folded and eventually packaged into coatamer II-coated vesicles for delivery to the *cis*-Golgi. During transit through the Golgi, the secretory proteins are further modified (e.g., sulfation or phosphorylation) and their carbohydrates further trimmed and modified. In the *trans*-Golgi network (TGN), the newly synthesized proteins are terminally glycosylated by the

addition of N-acetylglucosamine, galactose, sialic acid and/or fucose moieties. While the mechanistic details regulating sorting at the TGN are not fully understood, secreted proteins are packaged into discrete vesicles, delivered to the basolateral surface and released (Saucan and Palade, 1994).

That ethanol causes a defect in the delivery of secreted proteins was elucidated mainly by studies involving the radiolabeling of leucine residues in newly synthesized proteins. A decrease in radiolabeled leucine or terminal sugars was found outside of the hepatocyte, while an increase in this radioactive signal was detected within the cell, indicating a defect in secretion of newly synthesized proteins, occurring at the TGN. In further studies, the addition of acetaldehyde also impaired hepatocyte secretion, providing evidence that ethanol metabolism is required for this impairment (Volentine et al., 1987). In fact, studies using cyanamide showed that this secretion defect could be potentiated, but largely prevented when cells were treated with 4-MP (Sorrell et al., 1977; Volentine et al., 1987; Volentine et al., 1984).

Thus, the evidence is strong that ethanol impairs hepatic protein secretion and glycoprotein delivery, and these defects are largely mediated by acetaldehyde. It is also important to note that surface delivery of secretory proteins is a microtubule-dependent process that is mediated by a host of other molecules (De Matteis, et al., 2008; McNiven, et al., 2006; Ponnambalam, et al., 2003; Rodriguez-Boulan, et al., 2005).

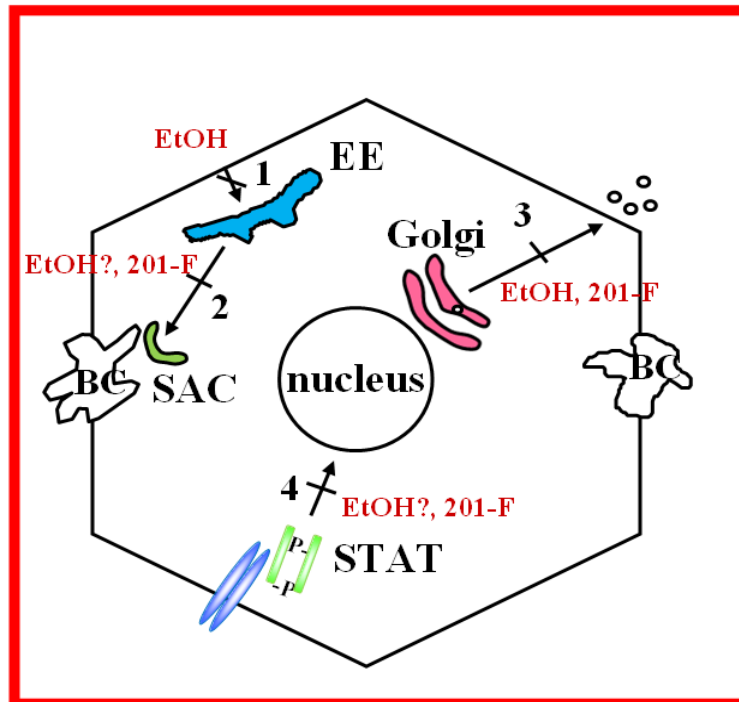


Figure 5. Known defects in protein trafficking. Alcohol-induced defects in hepatic trafficking. Secretion and delivery of newly synthesized basolateral proteins is impaired in ethanol-exposed hepatocytes (3). Also, three major steps in the itineraries of various receptors are impaired by ethanol metabolism: transport of newly synthesized receptors from the Golgi to the basolateral membrane (3); receptor internalization from the plasma membrane (1); and recycling of receptors from recycling endosomes back to the cell surface. As indicated, some of these steps are also impaired by the dynamic microtubule depolymerizing drug, 201-F. *EE* early endosome; *BC* bile canaliculus.

Albumin

Serum albumin is a plasma protein that is synthesized and secreted in high quantities by hepatocytes. In the blood, albumin plays an important role in the maintenance of osmotic pressure and serves as a carrier for small hydrophobic molecules including hormones and unconjugated bilirubin (Hankins, et al., 2006). Because decreased serum albumin levels can be associated with liver injury, it was of Particular interest to directly determine whether alcohol exposure led to impaired albumin secretion. Chronic ethanol exposure in

rats led to a significant increase in hepatic retention of both albumin and its precursor form, proalbumin, with a reciprocal decrease in secretion (Baraona, et al., 1977; Tuma, et al., 1981). More recent studies in both rat liver slices and polarized, hepatic WIF-B cells have also determined that ethanol exposure impairs albumin secretion (Joseph, et al., 2008; Klassen, et al., 2008). As for bulk secretion, addition of 4-MP to precision cut liver slices prevented the impairment, indicating that the defect requires ethanol metabolism and is likely mediated by acetaldehyde (Klassen, et al., 2008).

Ethanol-induced Impairment of Clathrin-mediated Endocytosis:

Endocytosis serves as the interface between the cell and its external environment and is vital to many cellular processes including intercellular communication, nutrition, cell motility and signal transduction. Endocytosis includes several diverse mechanisms by which molecules are internalized at the plasma membrane and are packaged into discrete transport vesicles. There are at least three major internalization routes in mammalian cells: clathrin-mediated, caveolae/raft-mediated, and non-clathrin/non-raft mediated (Conner, et al., 2003; Doherty, et al., 2009; Mayor, et al., 2007) that are characterized by specific molecular players, cargoes and regulators. In general, the ligands and receptors that display alcohol-induced internalization defects are internalized via clathrin-mediated pathways. In contrast, internalization of markers of caveolae/raft-mediated and fluid phase endocytosis and nonvesicle-mediated uptake are not changed by ethanol exposure. In this section, we will list and discuss which ligands, receptors and other markers have been examined for defects in endocytosis.

ASGP-R

Much of our understanding of the alcohol-induced defects in endocytosis comes from studies examining the trafficking of asialoglycoproteins (ASGP) and their receptor, the ASGP receptor (ASGP-R), in control and ethanol treated hepatic cells. After synthesis, ASGP-R is delivered to the basolateral plasma membrane where it is available to bind circulating ligands. Upon ligand binding, the receptor-ligand complex is internalized via clathrin-mediated endocytosis and is delivered to early endosomes. The ligand-receptor complex is then delivered to recycling endosomes where the ligand dissociates due to the acidic environment. The ligand is then transported to the lysosome for degradation, while the receptor recycles back to the basolateral plasma membrane for further rounds of ligand binding. At least three steps in the itinerary of ASGP-R have been shown to be impaired by ethanol metabolism: transport of newly synthesized ASGP-R from the Golgi to the basolateral plasma membrane (Figure 5, #3), receptor internalization from the basolateral plasma membrane (Figure 5, #1), and recycling of the receptors from recycling endosomes back to the cell surface (McVicker, et al., 1999). These phenomena have been observed in a number of model systems after chronic and acute ethanol exposure, including isolated rat hepatocytes, WIF-B cells, and intact perfused rat liver (Casey, 1987; Casey, 1990; Clemens, 1996; (Sharma and Grant, 1986)Tworek, et al., 1996). Addition of 4-MP (an ADH inhibitor) prevented the endocytic defect in both HepG2 cells stably expressing alcohol dehydrogenase and in WIF-B cells indicating the effect requires ethanol metabolism and is likely mediated by acetylaldehyde (Clemens, et al., 1996; Joseph, et al., 2008).

Other well-characterized receptors

The clathrin-mediated internalization of a number of other well-characterized receptors has also been shown to be impaired by ethanol exposure. For example, transferrin via the transferrin receptor has been shown to be impaired in isolated rat hepatocytes after acute ethanol treatment (Beloqui, et al., 1986). As for ASGP-R, addition of 4-MP to rat hepatocytes prevented impaired transferrin receptor internalization, suggesting that the defect requires ethanol metabolism. The internalization of another known clathrin-mediated endocytosis marker, chylomicron remnants via the LDL-receptor, was also shown to be impaired in rat hepatocytes (Lakshmanan, et al., 1986). Together, these results indicate that the well-described internalization defect of ASGP-R is not specific to that receptor, but rather is a general result of impaired clathrin-mediated endocytosis. To test this hypothesis, we sought to examine a panel of proteins internalized by either clathrin-dependent or clathrin independent mechanisms, in control or ethanol-treated WIF-B cells (see Part I).

Other internalization pathways are not impaired by ethanol exposure

In general, fluid-phase endocytosis and caveolae/lipid raft-mediated internalization are not likely impaired by ethanol exposure. Although not as extensively studied as clathrin-internalized receptors and ligands, there are a handful of studies that have examined markers of other internalization routes. For example, in rat livers, the fluid phase internalization of Lucifer Yellow was not changed by ethanol treatment (Camacho, et al., 1996). Similarly, the internalization of the GPI-anchored protein, 5' nucleotidase (5'NT), (a marker for raft-mediated internalization) was not changed in ethanol-treated WIF-B

cells (Joseph, et al., 2008). Together, these results indicate that ethanol exposure *selectively* impairs clathrin-mediated endocytosis, which is the main hypothesis to be addressed in Part I of this dissertation.

Cytokines, growth factors and hormones

The internalization and/or serum clearance of many cytokines, growth factors, and hormones has been shown to be impaired by ethanol consumption. The list so far includes: TGF- α , TNF- α , IL-6, EGF, and insulin (all in rat hepatocytes), growth hormone (GH) and insulin (in cirrhotic patients), and glucagon (in isolated rat liver plasma membranes) (Casey, et al., 1992; Dalke, et al., 1990; Nygren, et al., 1985; O'Rourke, et al., 1997; Rifkin, et al., 1983; Tuma, et al., 1991; Tuma, et al., 1996). Remarkably, most of these molecules are known to be internalized by clathrin-mediated endocytosis (Carpentier, et al., 1992; Carpentier, et al., 1993; Escobar, et al., 2006; Mosselmans, et al., 1988; Sachse, et al., 2001; Sorkin, et al., 2009; Thiel, et al., 1998; van Kerkhof, et al., 2001; Watanabe, et al., 1984). At present, it is not well-established whether the impaired internalization of these various ligands requires ethanol metabolism, but based on the receptor defects described above, the prediction is that it does.

Furthermore, many of these growth factors and cytokines are present in increased amounts in the alcoholic patient's circulation yet their biological effects are diminished (Lieber, 2003; Mezey, 1980). An interesting paradox has been described for signaling via the GH, TNF- α and IL-6 pathways (Hoek and Pastorino, 2002; Hoek and Pastorino, 2004). The circulating levels of each of these cytokines or growth factors are increased

in alcoholic patients and in ethanol-fed animals (Hoek and Pastorino, 2002; Hoek and Pastorino, 2004) where they exert proinflammatory responses. However, all of these ligands are also known to promote hepatoprotective activities and are required for liver regeneration (Gao, 2005; Hoek and Pastorino, 2002; Hoek and Pastorino, 2004; Taub, 2003). The puzzle is why the hepatoprotective and hepatomitogenic effects of GH, TNF- α and IL-6 are selectively lost in alcohol-treated hepatocytes despite their high circulating levels.

One possible explanation for impaired hepatic signaling is defects in their receptor internalization. The simple hypothesis is that decreased cytokine retrieval leads to decreased signaling, and thus, decreased hepatoprotection. Because alcohol-induced defects in basolateral delivery of the newly synthesized receptors and receptor recycling also lead to decreased cell surface receptor numbers (McVicker, et al., 1999), another intriguing hypothesis is that one or both of these steps is impaired in the receptors' itineraries. However, as generally these cytokines and growth factors exert their biological response via signaling pathways, it is also possible that an impairment in these networks may also lead to impaired signaling. This hypothesis becomes especially interesting when considering that proper signal relay throughout these pathways relies on proper protein trafficking, and that critical steps in many of these pathways require microtubules (further discussed below).

One such crucial step is the nuclear translocation of specific transcription factors downstream of several signaling pathways. As such, the prediction is that ethanol-

induced microtubule hyperacetylation may impair proper nuclear translocation of such transcription factors. To test this, we chose to examine the GH-induced Jak - STAT pathway in ethanol treated WIF-B cells. As mentioned, GH is a potent hepatomitogenic growth factor that is in higher-than-normal circulating levels in the chronic alcoholic, but its signaling is impaired. The focus of Part II of this dissertation aims to shed further light on this interesting clinical paradox. However, not all signaling pathways rely on microtubules for directed nuclear translocation. We therefore also aimed to examine the Smad pathway as one such example. This was done to determine if ethanol selectively impairs the microtubule-dependent nuclear translocation of transcription factors, and if this impairment is mediated by ethanol metabolism and microtubule hyperacetylation.

Signaling pathways

The Jak – STAT pathway

As mentioned, this clinical paradox found in the alcoholic involves signaling through receptors and their intercellular components. Of particular interest are signaling pathways that involve extracellular ligands that bind to receptors on the cell membrane, and elicit a phosphorylation cascade, leading to trafficking of the cognate transcription factor into the nucleus where it can bind to the appropriate promoter and activate transcription of target genes. As seen in Figure 6, one such pathway is the Jak-STAT pathway, whereby ligand binding at a receptor cross-links adjacent receptors, allowing two Jak proteins to cross-phosphorylate each other (Alberts, et al., 2008). This phosphorylation fully activates these kinases, allowing them to phosphorylate the

receptor itself on tyrosine residues. Two molecules of the cognate transcription factors, the STATs, are then recruited to these phosphotyrosine residues and bind them by their SH2 domains (Alberts, et al., 2008). The Jaks then phosphorylate the adjacent STAT molecules on tyrosine residues, allowing them to dissociate from the receptor and bind each other's phosphotyrosine residues by their reciprocal SH2 domains (Alberts, et al., 2008). The STAT dimer then translocates through the cytoplasm into the nucleus, where it can, with the help of other regulatory proteins, bind to cytokine response elements in target genes, and activate transcription (Alberts, et al., 2008).

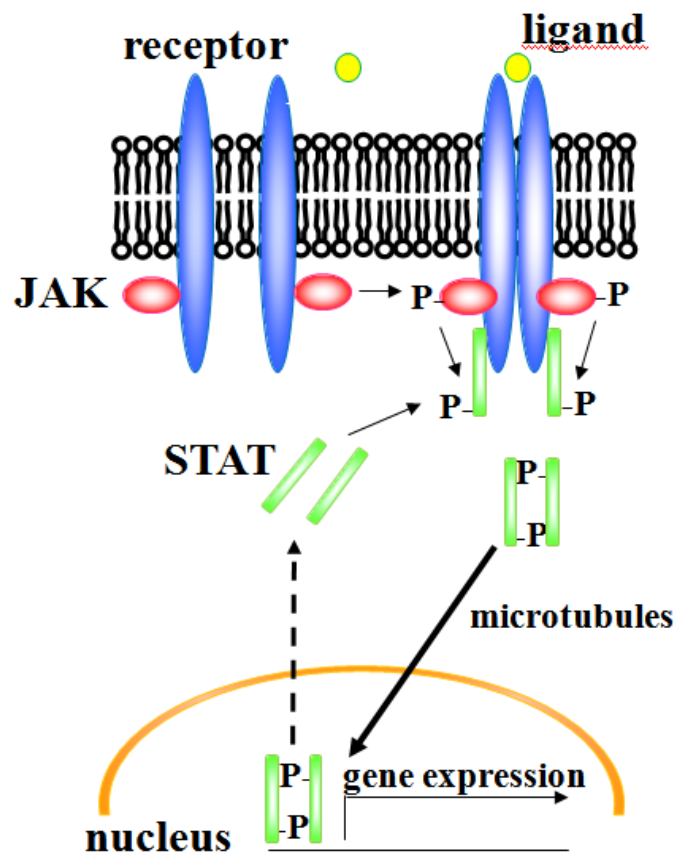


Figure 6. The Jak/STAT pathway. Ligand binding leads to receptor dimerization, which causes a conformational change, thus recruiting Jak to the receptor. After binding to the receptor, two Jak molecules cross-phosphorylate each other on tyrosine residues, leading to full activation. Activated Jak then phosphorylates the receptor on a tyrosine residue, recruiting STAT

binding via its SH2 domain. After Jak phosphorylation on a tyrosine residue, two STAT molecules depart from the complex as a dimer, bound via reciprocal phosphotyrosine residues by their SH2 domains. The activated dimer then uses microtubules for directed nuclear translocation, where it can bind DNA at specific response elements, activating target gene transcription.

The role of microtubules in STAT nuclear translocation

Though the paradigm of cytokine stimulation leading to nuclear translocation of STAT family members has been established, the mechanism of translocation has only somewhat recently been elucidated. In Figure 6, this process is represented as being microtubule-dependent (solid arrow), in part due to the following: Studying adipocytes, Gleason, et al found that microtubules were involved in this process, since stabilizing them with taxol (paclitaxel) lead to an impairment of nuclear translocation of STATs without altering their tyrosine phosphorylation (Gleason, et al., 2004). They concluded that the microtubule population must be dynamic in order to support nuclear translocation of STATs. A similar finding occurred a year later, reported by Phung-Kostas, whereby it was shown that in WIF-B cells, the growth hormone-mediated nuclear translocation of STAT5B (the liver-specific isoform of STAT5) was dependent on dynamic microtubules, and that this process was mediated by the minus-end directed microtubule motor protein dynein (Phung-Kostas, et al., 2005). Further, it was shown in MCF-7 human breast cancer cells that microtubules facilitated STAT5 nuclear translocation after epidermal growth factor (EGF) stimulation, while perturbations to the actin cytoskeleton had no effect (Lopez-Perez, et al., 2006). Additionally, STAT1, p53, glucocorticoid receptor, and retinoblastoma protein, have all been shown to use microtubules for directed

transport to the nucleus, and treatment with nocodazole impairs their nuclear translocation (Campbell and Hope, 2003). Taken together, it is clear that STATs, and in particular STAT5, rely on an intact and dynamic microtubule network for efficient nuclear translocation.

The Smad pathway

Another critical signaling pathway found in hepatocytes as well as nearly every other cell type, is the Smad pathway. Signaling via this pathway generally involves the TGF- β /activin superfamily or the bone morphogenic protein (BMP) superfamily, of ligands (Alberts, et al., 2008). Upon TGF- β binding to a type-II TGF- β receptor homodimer, a type-I receptor homodimer is then recruited to form a heterotetramer receptor complex, allowing the type-II receptor to phosphorylate the type-I receptor on a serine or threonine residue (depending on which combination of type-I and type-II receptors comprise the complex) (Alberts, et al., 2008). Once phosphorylated, the type-I receptor recruits and subsequently phosphorylates Smad 2 or Smad 3, which can then disengage the receptor and bind with Smad 4 (not known to be phosphorylated). This oligomer then translocates into the nucleus, where similarly to STATs, it will bind other regulatory proteins and DNA, activating target genes (Alberts, et al., 2008). In Figure 7, this step is shown to be microtubule-independent (dotted arrow), or at least, microtubules are not thought to facilitate directed nuclear transport after ligand stimulation, which will be further discussed in the next section.

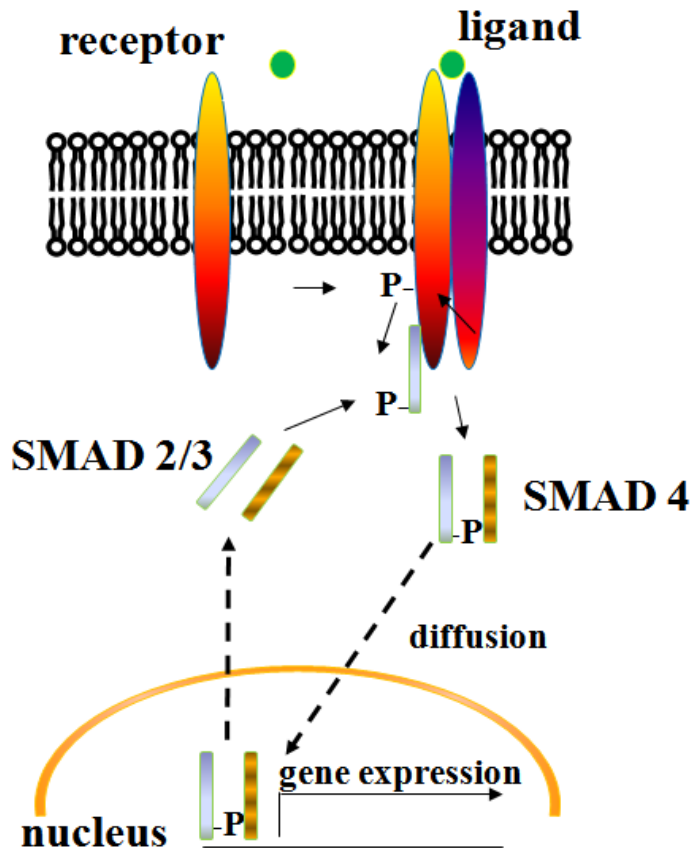


Figure 7. The Smad pathway. Ligand binding to a type-II receptor causes dimerization with a type-I receptor. The type-II receptor then phosphorylates the type-I receptor on a serine or threonine residue. This recruits Smad 2 or 3, which is then phosphorylated and thus activated. Activated Smad 2 or 3 then binds Smad 4, and the complex diffuses into the nucleus, where it binds DNA at specific response elements, activating target gene transcription.

The role of microtubules in Smad nuclear translocation

It is reasonable to suspect microtubules play a role in Smad nuclear translocation, and indeed there is evidence to support this. However, it appears that the role is very different from that in the Jak-STAT pathway, where the microtubule network serves as tracks along which motor proteins can transport these transcription factors long distances. In the case of the Smad pathway, Dong demonstrated that Smads 2, 3, and 4 bind

microtubules in several epithelial and endothelial cell lines, but that this served as a cytoplasmic sequestration mechanism (Dong, et al., 2000). Further, they showed that when microtubules (but not filamentous actin) were disrupted with chemical agents such as nocodazole or colchicine, Smad 2/3 phosphorylation and subsequent nuclear translocation was enhanced, an effect that could be inhibited by pre-treating cells with taxol (Dong, et al., 2000). A similar finding was described by Gong, in which taxol or another microtubule-stabilizing agent epothilone B enhanced cytosolic Smad 3 association with β 2-tubulin, and increased the inhibitory effect of cGMP on its nuclear translocation in pulmonary artery smooth muscle cells (Gong, et al., 2011). Furthermore, c-myc and myc-interacting zinc finger protein (MIZ-1) have been shown to use microtubules in a similar fashion (Campbell and Hope, 2003). From these studies, it is clear that microtubules play distinct roles in nuclear translocation, depending on the signaling pathway in which they are acting. This distinction will be further addressed in Part II of this dissertation.

MATERIALS AND METHODS

Reagents and Antibodies. F12 (Coon's) medium, FITC-conjugated cholera toxin B (CTxB), Lucifer Yellow and fluorescein diacetate, taxol, TSA, 4-methylpyrazole (4-MP), and Nuclei EZ Prep kits were purchased from Sigma–Aldrich (St. Louis, MO). Nuclei were purified according to the manufacturer's instructions. HEPES was from HyClone (Logan, UT). Transferrin receptor (Tf-R) monoclonal antibodies (CL071AP) were from Cedarlane Laboratories (Burlington, NC) clathrin heavy chain antibodies (Clone X22) were from Novus Biologicals (Littleton, CO) and antibodies against dynamin-2 were from BD Biosciences (San Jose, CA). Fetal bovine serum was from Gemini Bio-Products (Woodland, CA) and HEPES was from HyClone (Logan, Utah). Alexa-466 and -568-conjugated secondary antibodies were purchased from Invitrogen (Carlsbad, CA). Antibodies against dipeptidyl peptidase IV (DPP IV), hemagglutinin (HA) and polymeric IgA-receptor (pIgA-R) were all kindly provided by Dr. Ann Hubbard (Johns Hopkins School of Medicine, Baltimore, MD). Recombinant adenoviruses encoding V5/His6 epitope-tagged full-length DPP IV or pIgA-R and full-length HA were also all provided by A. Hubbard and have been described in detail (Bastaki, 2002). Antibodies against STAT5B (C-17), STAT3 (K-15) and Smad2/3 (FL-425) were purchased from Santa Cruz Biotechnology (Santa Cruz, CA). Anti-pSTAT5B (C7E5) and Jak2 (D2e12) antibodies were purchased from Cell Signaling Technologies (Beverly, MA), and anti-pJak2 antibodies were from Upstate Biotech (Temecula, CA). Recombinant GH, interleukin-6 (IL-6) and TGF- β were purchased from Shenandoah Biotechnology (Warwick,

PA). Alexa-conjugated secondary antibodies were purchased from Invitrogen (Carlsbad, CA).

Ethanol Treatment of Rats. Male Wistar rats (Charles River Laboratories, Wilmington, MA) were pair-fed control and ethanol Lieber-DeCarli liquid diets (Dyets, Inc., Bethlehem, PA) for 5 weeks as described (Lieber and DeCarli, 1989). At time of sacrifice, livers were excised and frozen at -70°C .

Cell culture, virus production and infection. WIF-B cells were grown in a humidified 7% CO_2 incubator at 37°C as described (Shanks, 1994). Briefly, cells were grown in F12 medium, pH 7.0, supplemented with 5% FBS, 10 μM hypoxanthine, 40 nM aminopterin and 1.6 μM thymidine. Cells were seeded onto glass coverslips at 1.3×10^4 cells/cm² and grown for 8-12 days until they reached maximum density and polarity. In general, cells were treated on day 7 with 50 mM ethanol in medium buffered with 10 mM Hepes, pH 7.0 for 72 h as described (Shaffert, 2004).

Recombinant adenoviruses encoding V5/His6 epitope-tagged DPP IV or V5/myc-tagged pIgA-R or untagged HA that were generated using the Cre-Lox system (Bastaki et al., 2002) were provided by Dr. A. Hubbard (Johns Hopkins University School of Medicine, Baltimore, MD). The tetracycline repressible dynamin wild type and K44A dominant negative recombinant adenoviruses were provided by Drs. S. Schmid and H. Damke (Scripps, La Jolla, CA). For alcohol studies, WIF-B cells were infected after 48 h of ethanol treatment for 60 min at 37°C as described (Bastaki et al., 2002). The cells

were washed with complete medium and incubated an additional 18 - 20 h in the continued absence or presence of ethanol to allow protein expression. For the dynamin mutant analysis, cells were coinfecting for 30 min at 37°C with recombinant adenovirus Particles encoding the tetracycline repressible transactivator and wildtype or K44A dominant negative dynamins under the control of the tetracycline responsive element. After washing, the cells were incubated an additional 18-24 h to allow dynamin expression. For triple infections, cells were simultaneously incubated for 30 min at 37°C with dynamin wildtype or mutant virus, the transactivator and virus encoding full length DPPIV or pIgA-R and allowed to express as above.

Indirect Immunofluorescence Microscopy. WIF-B cells were fixed on ice with chilled phosphate buffered saline (PBS) containing 4% paraformaldehyde for 1 min and permeabilized with ice-cold methanol for 10 min. Cells were processed for indirect immunofluorescence as described previously (Ihrke, 1993). Alexa-conjugated secondary antibodies were used at 5 µg/ml. Cells were visualized by epifluorescence using an Olympus BX60 Fluorescence Microscope (OPELCO, Dulles, VA). Images were taken with a Coolsnap HQ2 digital camera (Photometrics, Tucson, AZ) and IPLabs image analysis software (Biovision, Exton, PA). Adobe Photoshop (Adobe Systems Inc., Mountain View, CA) was used to compile Figures.

To quantitate the relative distributions of the membrane proteins, random fields from each slide were visualized by epifluorescence and digitized as described (Nyasae et al., 2003; Ramnarayanan et al., 2007). From micrographs, the average pixel intensity of

selected regions of interest (ROI) placed at the apical or basolateral surface of the same WIF-B cell (for pIgA-R, DPP IV and HA) or selected regions of interest placed in the nucleus or cytoplasm of the same cell (for STAT3, STAT5B, and Smad2/3) were measured using the Measure ROI tool of the ImageJ software (National Institutes of Health). For Tf-R, the average pixel intensity at recycling endosomes or plasma membrane of the same cell was measured. The averaged background pixel intensity was subtracted from each value and the ratio of apical to basolateral membrane (for pIgA-R, DPP IV and HA) or intracellular to basolateral membrane fluorescence intensity (for Tf-R) was determined.

Antibody trafficking in live cells. Cells were continuously labeled with anti-Tf-R antibodies (1:25) for 30 min at 37⁰C in complete medium. Cells were washed 3 times for 2 min each in chilled complete medium, were fixed and labeled with Alexa-conjugated secondary antibodies. To monitor internalization of apical markers, cells were surface labelled with antibodies specific to DPPIV (1:50), APN (1:50) or pIgA-R (1:25) for 15-30 min at 4⁰C. Because tight junctions restrict access of the antibodies to the apical PM, only antigens at the basolateral surface were labeled. Cells were washed 3 times for 2 min on ice with chilled medium and then reincubated with prewarmed complete medium. Antibodies with bound antigens were chased for 45 or 90 min at 37⁰C. Cells were washed and processed as described above.

Cholera toxin internalization. Control or treated WIF-B cells were rinsed 3 times with prewarmed serum-free medium then continuously incubated with 0.5 – 1.0 µg/ml FITC-

CTxB in complete serum-free medium for 60 min at 37°C. Cells were washed 3 times for 2 min each with PBS, fixed and visualized directly by epifluorescence. Intracellular vs. surface fluorescence intensities were measured as described above.

Lucifer Yellow and HRP internalization. Control or treated WIF-B cells were rinsed 3 times with prewarmed serum-free medium then continuously incubated with 1.0 mg/ml Lucifer Yellow in serum-free medium for 30 min at 37°C. After rinsing with prewarmed medium, live cells were imaged directly by epifluorescence. To quantitate amounts of Lucifer Yellow internalized, intracellular fluorescence was monitored using a plate reader. After internalization and washing, cells were scraped from coverslips in 100 µl PBS containing 0.1% Triton X-100, and 50 µl of each sample was placed in a 96-well dish. Fluorescence was detected with the plate reader emission wavelength set at 428 nm and emission at 536 nm. Levels of internalized Lucifer Yellow were determined relative to a standard curve of known concentrations.

Control or dynamin expressing WIF-B cells were incubated for 2h with 5 mg/ml HRP at 37°C. Cells were washed 3 times for 2 min each with chilled medium, then fixed as described above and immunolabeled with anti-HRP antibodies. Cells were visualized by epifluorescence and images collected from random fields. From micrographs, dynamin expressing cells were scored for the absence or presence of intracellular HRP labeling and percent positive cells calculated.

Fluorescein diacetate labeling. Control or treated cells were rinsed 3 times with prewarmed complete medium then continuously incubated with 0.5 $\mu\text{g}/\text{ml}$ fluorescein diacetate in complete medium for 20 min at 37°C. After rinsing with prewarmed medium, live cells were imaged directly by epifluorescence. To determine the percentage of bile canalicular (BC) structures labeled, random fields from each slide were visualized by epifluorescence or phase contrast and digitized. From phase micrographs, the total number of BCs was counted, and from the corresponding epifluorescence image, the number of labeled BCs was calculated (labeled BCs/total BCs). High, medium and low fluorescence labeling intensities of BCs were also scored from the same micrographs.

Cell fractionation. WIF-B cells grown on 10 cm dishes were rinsed with PBS, detached with trypsin for 2 min at 37°C and pelleted by centrifugation. Cells from two dishes were pooled, resuspended in 5 ml ice-cold swelling buffer (1 mM MgCl_2 , 1 mM DTT, 1 mM EGTA) and incubated 5 min on ice. Cells were pelleted by centrifugation and resuspended in 500 μl of PEM (100 mM Pipes, 1 mM EGTA, 1 mM MgSO_4 , pH 6.6) with added protease inhibitors (1 $\mu\text{g}/\text{ml}$ each of leupeptin, antipain, PMSF and benzamidine) and Dounce-homogenized with a tight fitting pestle for 20 strokes. The homogenate was centrifuged for 60 min at 4°C at 150,000 x g to prepare cytosolic and total membrane fractions. The fractions proteins were immunoblotted for clathrin heavy chain and dynamin-2 and the relative distributions were determined by densitometry.

Immunoblotting. Samples were immunoblotted with antibodies against clathrin heavy chain (1:2000), dynamin-2 (1:1000), STAT5B (1:5,000-10,000), STAT3, Smad2/3, EGF-

R or pSTAT5B (all 1:1000) diluted in PBS containing 5% (w/v) milk and 0.1% (v/v) Tween-20. Anti-Jak2 and -pJak2 antibodies (both 1:1000) were diluted in PBS containing 1% (w/v) BSA and 0.1% (v/v) Tween-20 and incubated overnight at 4°C. Immunoreactivity was detected using enhanced chemiluminescence (PerkinElmer, Crofton, MD).

Liver Fractionation. Livers were Dounce-homogenized in 0.25 M sucrose containing 10 mM Tris and 2 µg/ml each of leupeptin, antipain, PMSF and benzamidine. Homogenates (20% w/v) were centrifuged at 900 x g at 4°C for 5 min. The resultant supernatant was centrifuged at 150,000 x g at 4°C for 60 min to prepare the cytosolic and non-nuclear membranes. The nuclear pellet was washed by resuspending to volume and centrifuging at 14,200 x g at 4°C for 10 min. Samples were mixed with 2X sample buffer and boiled for 3 min.

Ligand addition and washout. Cells were treated with 50 nM GH or 500 pM TGF-β for up to 30 min at 37°C. Samples were processed for indirect immunofluorescence microscopy or lysed with SDS-PAGE sample buffer at the indicated times. For washout experiments, after 30 min of GH addition, pre-warmed medium was added to dilute the ligand 40-fold, and cells were incubated up to an additional 30 min at 37°C and processed for indirect immunofluorescence.

Statistical Analysis. Results were expressed as the mean \pm S.E.M. Comparisons between control and ethanol-treated cells were made using the Student's *t* test for paired data. *P* values of ≤ 0.05 were considered significant.

**Part I: Ethanol selectively impairs clathrin-mediated
internalization in polarized hepatic cells**

Although alcoholic liver disease is clinically well-described, the molecular basis for alcohol-induced hepatotoxicity is not well understood. Previously, we determined that the clathrin-mediated internalization of asialoglycoprotein receptor was impaired in ethanol-treated WIF-B cells whereas the internalization of a glycosphosphatidylinositol-anchored protein thought to be endocytosed via a caveolae/raft-mediated pathway was not changed suggesting that clathrin-mediated endocytosis is selectively impaired by ethanol. To test this possibility, we examined the internalization of a panel of proteins and compounds internalized by different mechanisms in control and ethanol-treated WIF-B cells. We determined that the internalization of markers known to be internalized via clathrin-mediated mechanisms was impaired. In contrast, the internalization of markers for caveolae/raft-mediated endocytosis, fluid phase internalization or non-vesicle-mediated uptake was not impaired in ethanol-treated cells. We further determined that clathrin heavy chain accumulated at the basolateral surface in small puncta in ethanol-treated cells while there was decreased dynamin-2 membrane association. Interestingly, the internalization of resident apical proteins that lack any known internalization signals was also disrupted by ethanol suggesting that these proteins are internalized via clathrin-mediated mechanisms. This conclusion is consistent with our findings that dominant negative dynamin-2 overexpression impaired internalization of known clathrin markers and single spanning apical residents, but not of markers of fluid phase or raft-mediated internalization. Together these results indicate that ethanol exposure selectively impairs

hepatic clathrin-mediated internalization by preventing vesicle fission from the plasma membrane

RESULTS OF PART I

Ethanol impairs clathrin-mediated, but not caveolae/raft-mediated internalization

We first examined the steady state distributions of two well-characterized markers known to be constitutively internalized by clathrin-mediated endocytosis: transferrin receptor (Tf-R), a protein that recycles between the basolateral membrane and recycling endosomes in the presence or absence of ligand, and polymeric IgA-receptor (pIgA-R), a transcytosing protein that traverses the basolateral membrane en route to the canalicular surface. In control cells, the majority of Tf-R was present on intracellular, perinuclear structures corresponding to recycling endosomes (Fig. 8A, a) while pIgA-R mainly distributed to the apical membrane (Fig. 8A, c). In ethanol treated cells, a striking increase in staining at or near the basolateral membrane was observed for both markers (Fig. 8A, b and d). Such a shift in distribution is consistent with impaired receptor internalization.

To quantitate our morphological observations, we measured Tf-R and pIgA-R relative distributions from micrographs using our previously published method (Nyasae et al., 2003; Ramnarayanan et al., 2007). The fluorescence intensities of selected regions of interest placed at intracellular vs. basolateral populations of Tf-R or at apical vs. basolateral populations of pIgA-R were measured. The averaged background intensity was subtracted from each value and the ratio of intracellular to basolateral membrane (for Tf-R) or apical to basolateral membrane fluorescence intensity (for pIgA-R) was determined. For both receptors, their corresponding ratios were decreased to only ~40%

of control values in ethanol treated cells indicating more receptors were present at the basolateral surface consistent with decreased internalization. These decreased values are consistent with those determined previously for ASGP-R in ethanol-treated WIF-B cells (56% of control) (Joseph, et al., 2008)

To confirm directly that clathrin-mediated internalization was impaired in ethanol treated cells, we monitored the trafficking of antibody-labeled Tf-R. Live cells were continuously labeled with antibodies specific to external receptor epitopes for 30 min. Cells were fixed and the trafficked antigen-antibody complexes were detected with secondary antibodies. In control cells, significant Tf-R populations were detected in intracellular structures (Fig. 8C a) with very little basolateral labeling indicating that Tf-R was rapidly internalized. In contrast, in ethanol-treated cells (Fig. 8C, b), Tf-R was mainly detected at the basolateral surface indicating that the increased Tf-R steady state basolateral staining was due to impaired internalization.

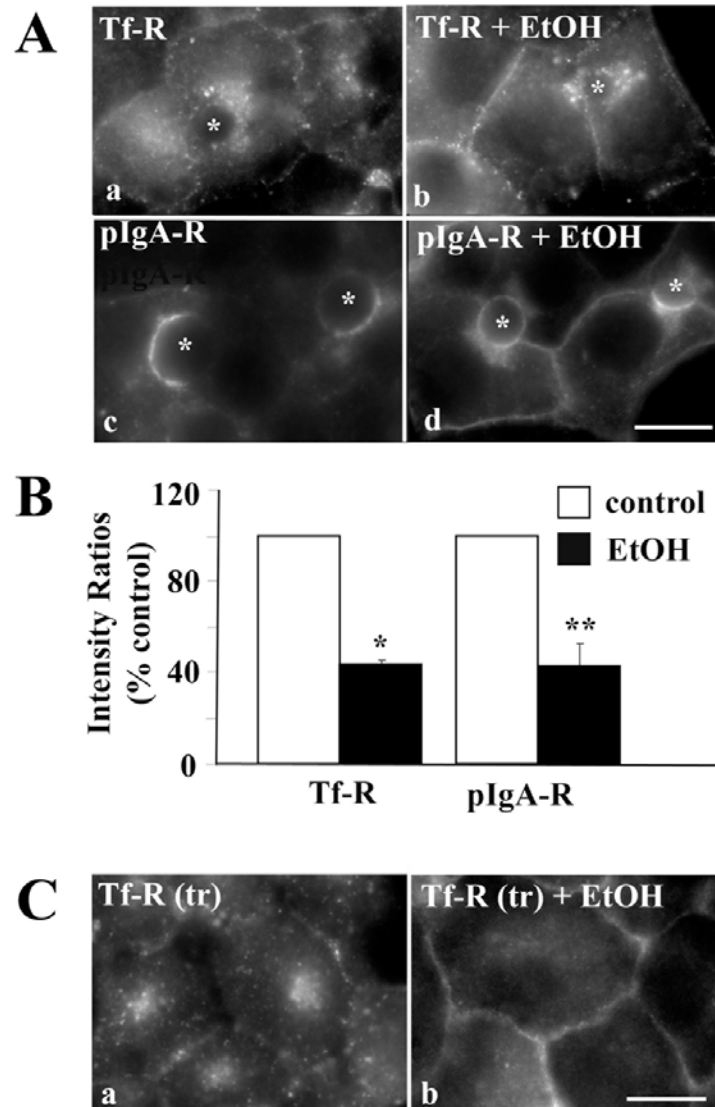


Figure 8. Clathrin-mediated internalization is impaired in ethanol-treated cells. **A**, WIF-B cells were treated in the absence (a, c) or presence (b, d) of ethanol (EtOH) and labeled for Tf-R (a, b) or pIgA-R (c, d). Asterisks are marking selected BCs. **B**, Random fields were visualized by epifluorescence and digitized. From micrographs, the average pixel intensity of each marker at selected regions of interest placed at the apical or basolateral membrane (for pIgA-R) or at the intracellular population and basolateral membrane (for Tf-R) of the same WIF-B cell was measured. The averaged background pixel intensity was subtracted from each value and the ratio of apical to basolateral or intracellular to basolateral fluorescence intensity was determined. In all cases, control ratios were set to 100%. Values are expressed as the mean \pm SEM. Measurements were done on at least three independent experiments. * $P < 0.0005$, ** $P < 0.03$ **C**, Cells were treated in the absence (a) or presence (b) of ethanol (EtOH). Live cells were continuously labeled with anti-Tf-R antibodies for 30 min in the continued absence or presence ethanol. Cells were fixed, permeabilized and labeled with secondary antibodies to detect the trafficked (tr) antibody-antigen complexes. Bar = 10 μ m

Our previous results showing that the internalization of the GPI-anchored protein, 5'NT, was not impaired in ethanol-treated cells suggested that caveolae/raft-mediated endocytosis was not altered by ethanol exposure. To test this hypothesis, we measured the internalization of FITC-conjugated cholera toxin B (CTxB). This subunit binds ganglioside M1, a known component of lipid rafts and is internalized via a caveolae/raft-mediated mechanism (Geny and Popoff, 2006). Once internalized, CTxB is delivered first to the Golgi and then to the ER (Geny and Popoff, 2006). As shown in Fig. 9A, there was no observable difference in CTxB internalization between control and ethanol-treated cells. In both cases, significant reticular ER-like staining was observed with some labeling detected at the basolateral surface (Fig. 9A). When quantitated, the intracellular to basolateral fluorescence intensity ratios were virtually identical (Fig. 9B) indicating endocytosis was not impaired. Thus, we conclude that caveolae/raft-mediated internalization is not altered in ethanol-treated cells.

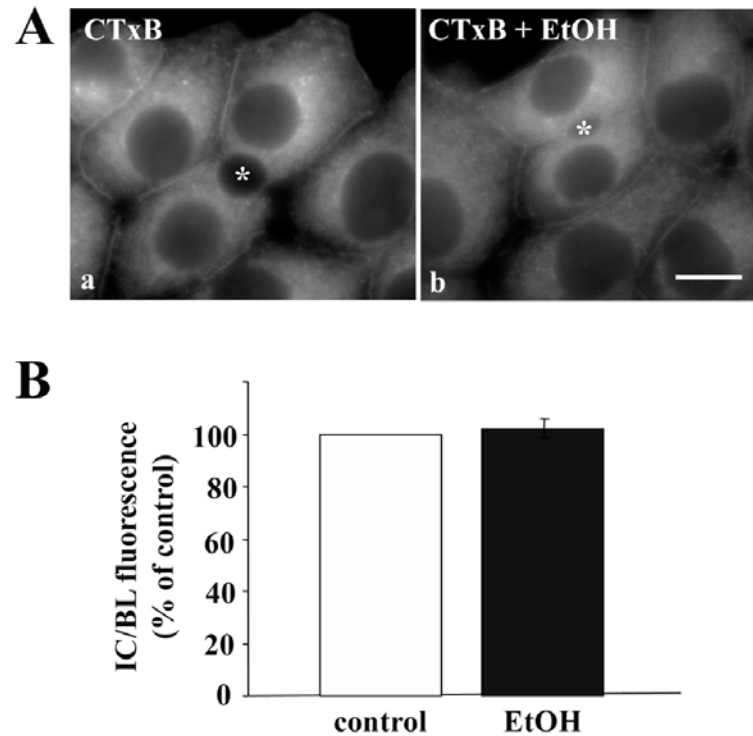


Figure 9. Caveolae/raft-mediated internalization is not impaired in ethanol-treated cells.

A, WIF-B cells were treated in the absence (a) or presence (b) of ethanol (EtOH). Cells were continuously labeled for 60 min at 37⁰C with 0.5 μg/ml CTxB. Cells were fixed and CTxB was visualized directly by epifluorescence. Asterisks are marking selected BCs. Bar = 10 μm **B**, The relative distributions of CTxB in control or ethanol-treated cells were quantitated as described in Figure 1B. Values are expressed as the mean ± SEM. Measurements were done on three independent experiments.

Ethanol does not impair fluid phase or non-vesicle-mediated internalization

To test whether fluid phase internalization is altered by ethanol treatment and to further confirm that WIF-B cells are a good model for studying mechanisms of hepatotoxicity, we monitored the internalization and lysosomal delivery of Lucifer Yellow in control and treated cells. As in isolated hepatocytes from ethanol-fed rats (Casey, et al., 1992), no change in Lucifer Yellow internalization was observed in ethanol-treated cells (Fig.

10A). After 30 min of uptake, Lucifer Yellow was detected in large intracellular structures corresponding to lysosomes in both control and ethanol-treated cells (Fig. 10A). We confirmed these morphological results by measuring total intracellular fluorescence. After incubation with Lucifer Yellow for 30 min, cells were detached from coverslips by addition of PBS containing 1.0% Triton X-100. The lysates were placed in a 96-well dish and fluorescence detected with a plate reader. In general, robust Lucifer Yellow internalization was observed in both control and ethanol-treated cells (range: ~65 – 210 ng/coverslip) (Fig. 10B). These results confirm that fluid phase internalization was not altered in ethanol-treated WIF-B cells.

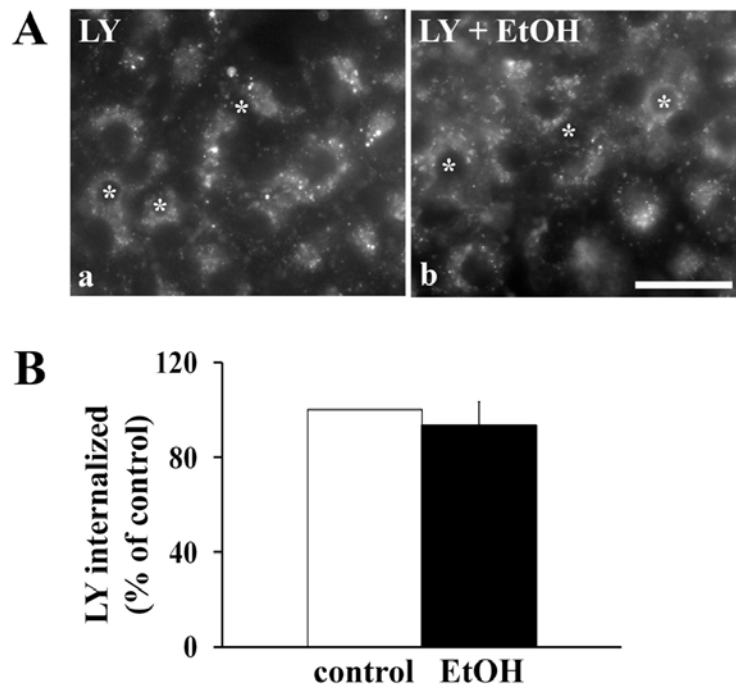


Figure 10. Fluid phase endocytosis is not impaired in ethanol-treated cells. **A**, WIF-B cells were treated in the absence (a) or presence (b) of ethanol (EtOH). Cells were continuously labeled for 30 min at 37°C with 1.0 mg/ml Lucifer Yellow (LY). Cells were washed and live cells were visualized immediately by epifluorescence. Bar = 10 μm **B**, Control or ethanol-treated cells were continuously labeled for 30 min at 37°C with 2.0 mg/ml Lucifer Yellow (LY). Cells

were detached from coverslips by addition of PBS containing 0.1% Triton X-100. The lysates were placed in a 96-well dish and fluorescence detected with a plate reader set at 428 nm excitation and 536 nm emission. Values are expressed as the mean \pm SEM. Measurements were done on four independent experiments.

We also examined non-vesicle-mediated internalization in control and ethanol-treated cells by monitoring the uptake of the organic anion, fluorescein diacetate. Once internalized, this anion diffuses across the cell and is secreted from the canalicular surface. In both control and ethanol-treated WIF-B cells, fluorescein diacetate was detected in the BC-like structures (Fig. 25A) indicating efficient internalization and subsequent apical secretion. These morphological observations were confirmed when we quantitated BC fluorescence. Virtually no difference in the number of labeled BCs was observed between control and ethanol-treated cells ($81.0 \pm 3.6\%$ vs. 78.7 ± 5.0 , respectively). Similarly, when scored for fluorescence intensity, virtually identical proportions of labeled BCs exhibited low, medium or high fluorescence levels (Fig. 11B). Thus, non-vesicle-mediated internalization was not impaired in ethanol-treated cells. These results further indicate that canalicular secretion was not impaired upon ethanol exposure.

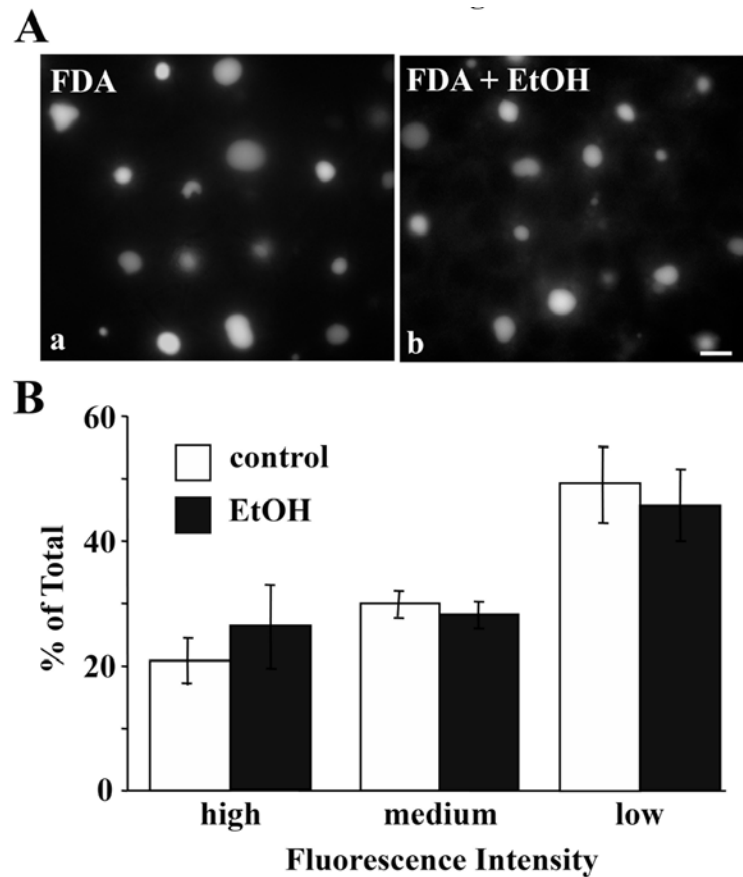


Figure 11. The non-vesicle-mediated uptake and subsequent canalicular delivery of fluorescein diacetate is not altered in ethanol-treated cells. **A**, WIF-B cells were treated in the absence (a) or presence (b) of ethanol (EtOH). Cells were continuously labeled for 20 min at 37°C with 0.5 µg/ml fluorescein diacetate (FDA). Cells were washed and live cells were visualized immediately by epifluorescence. Bar = 10 µm **B**, Labeled BCs were scored for low, medium or high fluorescence intensity and the percentages plotted. Values are expressed as the mean ± SEM. Measurements were done on three independent experiments.

Clathrin coated assemblies accumulate at the plasma membrane

in ethanol-treated cells

To more directly determine whether clathrin-mediated internalization was impaired by ethanol exposure, we examined the distributions of clathrin heavy chain, a major coat component of clathrin. In control cells, diffuse cytosolic and faint basolateral membrane

staining was observed with significant labeling of intracellular structures (likely Golgi) (Fig. 12A, a). Although the intracellular and cytosolic labeling was detected in ethanol-treated cell, there was a striking increase in staining of clathrin heavy chain at the basolateral membrane (Fig. 12A, b) in discrete puncta (see inset) suggesting that clathrin-coated vesicle fission was impaired.

We next immunoblotted cytosolic and total membrane fractions prepared from control or ethanol-treated cells for clathrin heavy chain or dynamin-2. Importantly, this dynamin isoform has recently been shown to selectively regulate clathrin-mediated endocytosis; it is not required for cholera toxin, caveolae or raft-mediated internalization (Liu, et al., 2008) Furthermore, dynamin-2 is thought to function in late stages of vesicle formation and fission. Comparison of the whole homogenate (WH) samples revealed that the levels of neither clathrin heavy chain nor dynamin-2 were changed by ethanol treatment indicating that impaired clathrin-mediated internalization was not simply due to decreased protein amounts. Although membrane association of clathrin heavy chain was maintained in ethanol-treated cells, (81.7 ± 6.6 vs. 82.9 ± 5.3 , control vs. ethanol, respectively), dynamin-2 membrane association was markedly decreased (Fig. 12B). In control cells, over 70% (71.6 ± 5.3) of dynamin-2 is membrane-associated. In contrast, only ~50% (54.2 ± 2.9) of dynamin-2 associates with membranes in ethanol-treated cell. These results suggest that clathrin-coated assemblies are formed at the plasma membrane, but vesicle fission is impaired, and that the impaired fission is due to decreased membrane recruitment of dynamin-2. These findings are remarkably consistent with the

increased basolateral staining observed for the markers of clathrin-mediated internalization.

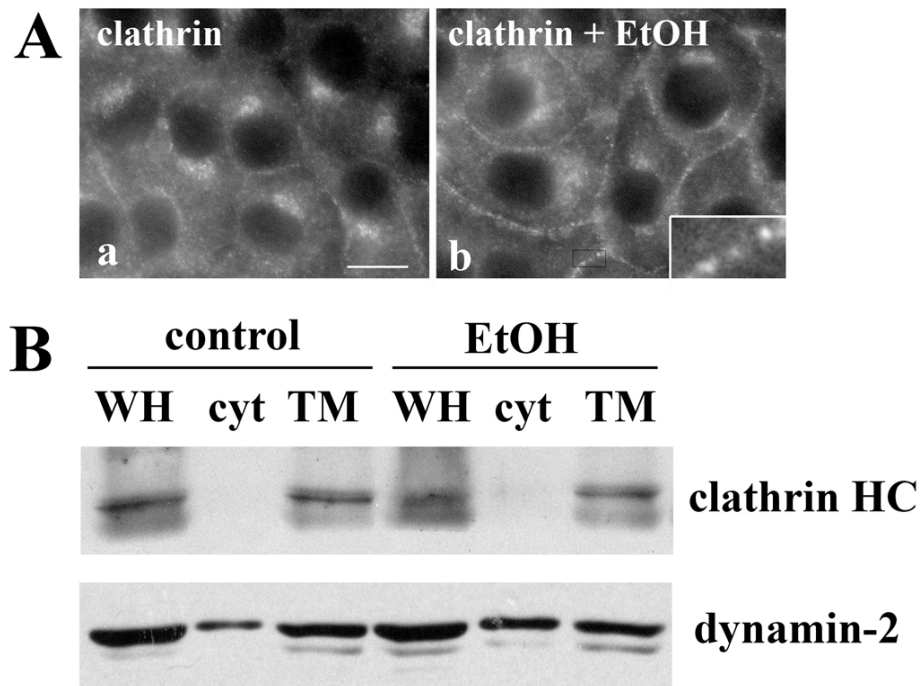


Figure 12. Clathrin coated assemblies accumulate at the plasma membrane in ethanol-treated cells. **A**, WIF-B cells were treated in the absence (a) or presence (b) of ethanol (EtOH) and labeled for clathrin heavy chain. The inset is an enlarged image of the indicated boxed-in area. Bar = 10 μ m **B**, Whole homogenate (WH), cytosolic (cyt) and total membrane (TM) fractions were prepared from control or ethanol-treated WIF-B cells and immunoblotted for clathrin heavy chain or dynamin-2 as indicated. The blots shown are representative of five independent experiments.

Ethanol impairs the endocytosis of apical residents with no known internalization signals

In hepatocytes, newly synthesized single spanning resident apical proteins take an indirect route to the apical surface. They are transported from the *trans*-Golgi network

(TGN) to the basolateral surface where they are selectively retrieved by endocytosis and transcytosed to the apical surface. However, unlike basolateral resident proteins, no specific targeting signal sequences have been identified that guide them along this circuitous pathway (Tuma and Hubbard, 2003). Our previous studies have also indicated that these apical residents are not internalized via caveolae/raft-mediated pathways (Nyasae, et al., 2003). Furthermore, the short cytoplasmic domains of the apical residents lack any known tyrosine- or dileucine-based clathrin-mediated internalization signal sequences (Tuma and Hubbard, 2003). Thus, our recent finding that the basolateral internalization of APN was impaired in ethanol-treated cells is intriguing (Joseph, et al., 2008).

To determine if internalization of other single spanning apical residents is impaired by ethanol exposure, we examined the steady state distributions of another ectoenzyme (dipeptidyl peptidase IV; DPP IV), and an exogenously expressed viral protein (hemagglutinin; HA) in control and treated cells. In control cells, both DPP IV and HA were present mainly at the apical surface (Fig. 13A, a and c). In contrast, a striking increase in staining at or near the basolateral membrane was observed for both markers in ethanol-treated cells (Fig. 13A, b and d). For both receptors, the apical to basolateral fluorescence intensity ratios were decreased in ethanol-treated cells (Fig. 13B). As for Tf-R and pIgA-R measurements, HA intensity ratio was 40% of that of control. Although the decreased ratio for DPP IV was less dramatic (80% of control), it was significant ($P < 0.02$).

To confirm directly that DPP IV internalization was impaired in ethanol-treated cells, we monitored the trafficking of a cohort of antibody-labeled DPP IV. Live cells were labeled with DPP IV antibodies specific to external epitopes at 4⁰C. After washing, the labeled DPP IV cohort was chased for 45 or 90 min at 37⁰C. Cells were fixed and labeled with secondary antibodies to detect the trafficked antigen-antibody complexes. In control cells, significant DPP IV staining was detected at the apical surface (Fig. 13C, a and c) indicating that DPP IV was rapidly internalized and transcytosed to the apical surface. In contrast, in ethanol-treated cells (Fig. 12C, b and d), basolateral DPP IV staining was observed with a reciprocal decrease in apical labeling. As for DPP IV at steady state, the apical to basolateral fluorescence intensity ratios were decreased, but to a much greater extent. After 45 min chase, the ratio was decreased to ~22% of control, and after 90 min, the ratio was ~30% of control. Thus, we conclude that the basolateral internalization of DPP IV was impaired in ethanol-treated cells.

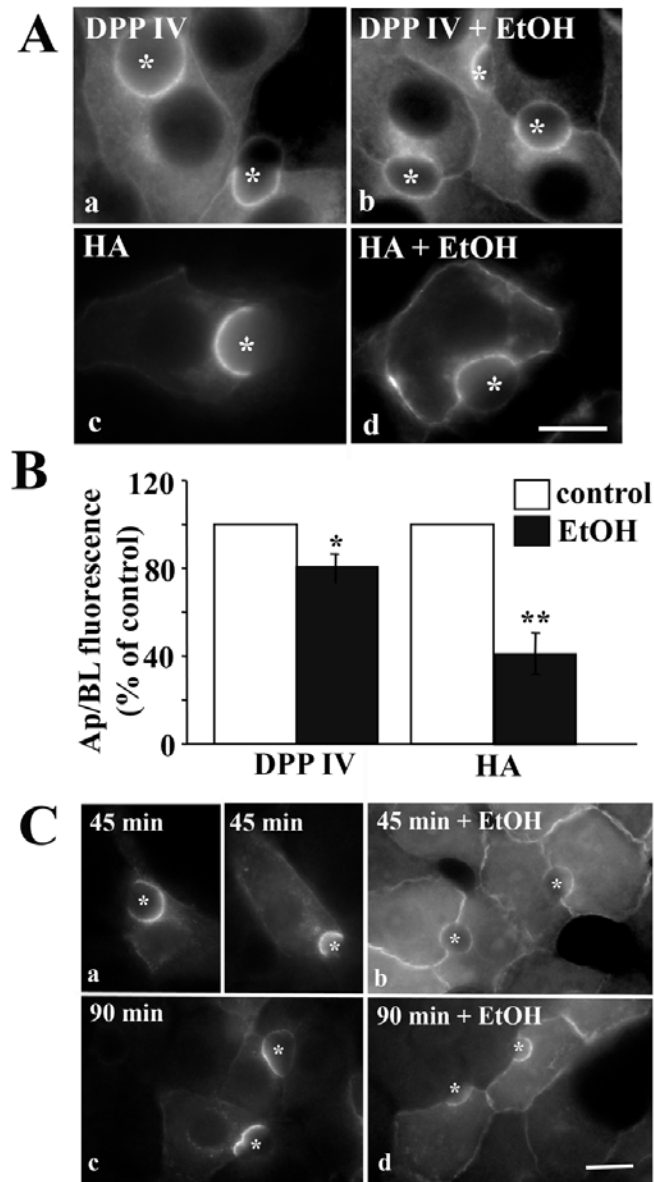


Figure 13. Internalization of single spanning apical proteins with no known sorting information is impaired in ethanol-treated cells. **A**, WIF-B cells were treated in the absence (a, c) or presence (b, d) of ethanol (EtOH) and labeled for DPP IV (a, b) or HA (c, d). Asterisks are marking selected BCs. Bar = 10 μ m **B**, WIF-B cells were treated as described in A and the relative distributions determined. Values are expressed as the mean \pm SEM. Measurements were done on at least three independent experiments. * $P < 0.05$; ** $P < 0.01$ **C**, Cells were treated in the absence (a) or presence (b) of ethanol (EtOH). Live cells were labeled with anti-DPP IV antibodies and the antigen-antibody complexes were chased for 45 or 90 min in the continued absence or presence ethanol. Cells were labeled with secondary antibodies to detect the trafficked (tr) complexes. Bar = 10 μ m

Because the internalization of DPP IV and HA (and APN) was impaired to a similar extent as ASGP-R, pIgA-R and Tf-R, we suggest that these apical residents are endocytosed via clathrin-mediated pathways. To test this, we examined internalization of DPP IV and APN in cells expressing wildtype or dominant negative (K44A) dynamin-2. Importantly, this dynamin isoform has recently been shown to selectively regulate clathrin-mediated endocytosis; it is not required for cholera toxin, caveolae or raft-mediated internalization (Liu, et al., 2008). Overexpression of the dominant negative dynamin-2 induced remarkably similar defects in endocytosis as observed in ethanol-treated cells. In Particular, the clathrin-mediated internalization of pIgA-R was drastically impaired. In cells overexpressing wild type dynamin-2, virtually all of the antibody-labeled receptor was chased to the apical surface (Fig. 14A, a). In contrast, in dynamin K44A overexpressing cells, virtually no pIgA-R apical labeling was observed (marked with an asterisk) with a reciprocal increase in basolateral staining indicating impaired internalization (Fig. 14A, b). When pIgA-R distributions were quantitated as described above, the ratio of apical to basolateral fluorescence intensity was only 5% of control indicating a near complete block in internalization (Fig. 14B).

The internalization of DPP IV and APN was also impaired in cells expressing dominant negative dynamin-2. As for pIgA-R in dynamin wildtype expressing cells, the majority of DPPIV and APN antigen-antibody complexes were chased to the apical surface (Fig. 14A, c and e) while in dynamin K44A expressing cells, virtually no apical labeling was observed for DPPIV (unlabeled BCs are marked with asterisks) whereas

decreased labeling was observed for APN (note the much brighter apical labeling in the BC of the adjacent, non-dynamin expressing cells) (Fig. 14A, d and f). As for pIgA-R, a reciprocal increase in basolateral labeling was observed in the dynamin K44A expressing cells (Fig. 14A, d and f). When quantitated, the apical to basolateral fluorescence intensities for APN and DPP IV were ~20 and 40% of control levels, respectively, indicating impaired internalization.

To verify that dynamin-2 selectively impairs clathrin-mediated internalization in WIF-B cells, we monitored the internalization of markers of other endocytic pathways. Like in ethanol treated cells, neither the fluid phase internalization of HRP (Fig. 14A, g and h and Fig. 14B) nor the caveolae/raft-mediated internalization of CTxB (Fig. 14B) was changed by dynamin K44A expression (Fig. 14B). Together these results indicate that the single spanning apical residents are basolaterally internalized via a clathrin-mediated pathway.

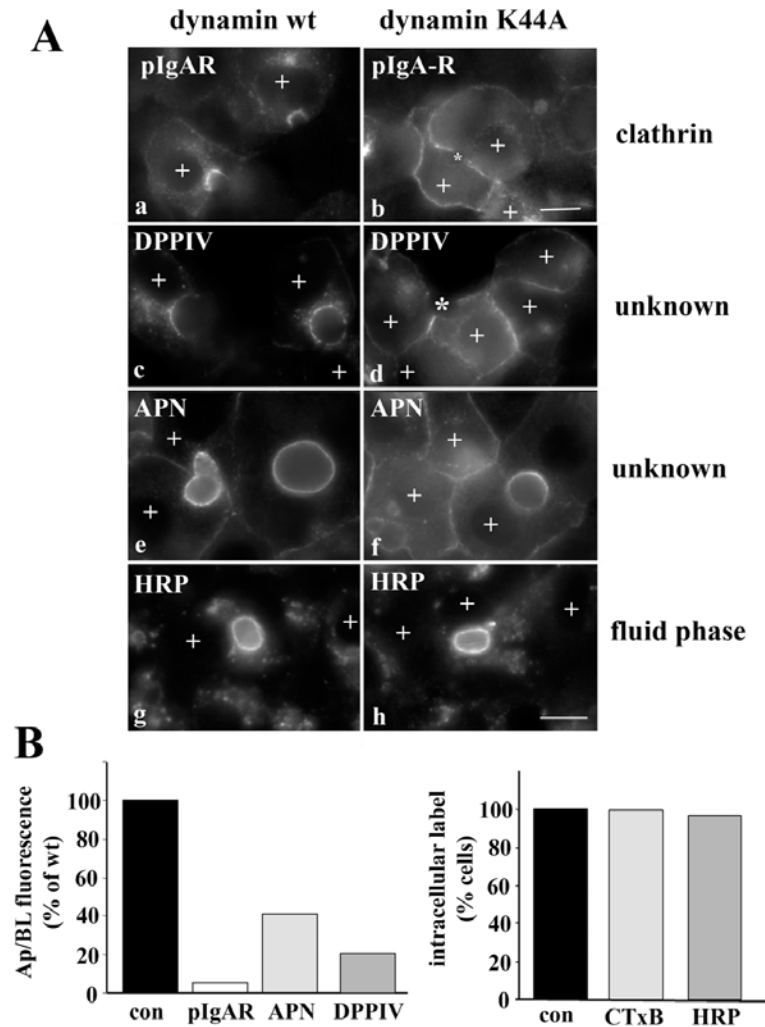


Figure 14. Internalization of the single spanning apical residents is clathrin-dependent. A, WIF-B cells were co-infected for 30 min at 37°C with recombinant adenovirus particles encoding the tetracycline repressible transactivator and wildtype (a, c, e and g) or K44A dominant negative dynamins (b, d, f, and h) under the control of the tetracycline responsive element. Cells were additionally infected with pIgA-R (a and b) or DPPIV (c and d) viruses. After washing, the cells were incubated an additional 18-24 h to allow dynamin expression. Live cells were labeled with anti-pIgA-R (a and b), anti-DPP IV (c and d) or anti-APN (e and f) antibodies and the antigen-antibody complexes chased for 90 min. Cells were also continuously labeled for 2 h with 5 mg/ml HRP in serum free medium (g and h). Cells expressing the recombinant dynamin adenoviruses are indicated with a “+” symbol. Asterisks in panels b and d are marking unlabeled BCs in cells overexpressing dynamin K44A. Bar = 10 μ m B, Cells were infected with wild type of K44A dynamin viruses as described in A, and internalization of the indicated markers was monitored by epifluorescence. Apical to basolateral fluorescence intensities were measured for pIgA-R, DPPIV and APN in dynamin expressing cells. For CTxB and HRP, dynamin-expressing cells were scored for the presence of labeled intracellular puncta, and percent positive cells calculated.

CONCLUSIONS AND IMPLICATIONS OF PART I

This study was initiated to determine whether clathrin-mediated endocytosis from the basolateral membrane is selectively impaired by ethanol exposure in polarized hepatic cells. To test this possibility, we examined endocytosis of a broad array of proteins and compounds that are known to be internalized by distinct mechanisms. As we hypothesized, the constitutive clathrin-mediated internalization of pIgA-R and Tf-R was significantly impaired in ethanol-treated WIF-B cells. In contrast, the caveolae/raft-mediated internalization of CTxB, the fluid phase uptake of Lucifer Yellow and the non-vesicle-mediated uptake of fluorescein diacetate were not impaired after ethanol exposure. Ethanol exposure led to the redistribution of clathrin heavy chain to puncta at the basolateral surface suggesting impaired vesicle fission. This conclusion is further substantiated by our findings that there is markedly less dynamin-2 associated with membranes in ethanol-treated cells. These findings are strikingly consistent with the increased basolateral staining observed for the markers of clathrin-mediated internalization. Interestingly, the internalization of single spanning apical membrane residents that contain no known internalization signaling information was significantly impaired suggesting these proteins may be endocytosed by a clathrin-mediated mechanism. This was confirmed in cells expressing dominant negative dynamin-2.

Part II: Hepatic Microtubule Acetylation and Stability Induced by Alcohol

Exposure Impair Nuclear Translocation of STATs 3 and 5B, but not Smad2/3

Alcoholic liver disease is clinically well-described, however the molecular basis for alcohol-induced hepatotoxicity is not well understood. Previously, we found that alcohol exposure led to increased microtubule acetylation and stability in polarized, hepatic WIF-B cells and in livers from ethanol-fed rats. Because microtubules are known to regulate transcription factor nuclear translocation, and that dynamic microtubules are required for translocation of at least a sub-set of these factors, we examined whether alcohol-induced microtubule acetylation and stability impairs nuclear translocation. We examined nuclear delivery of factors representing the two mechanisms by which microtubules regulate translocation. To represent factors that undergo directed delivery, we examined growth hormone-induced STAT5B translocation and interleukin-6-induced STAT3 translocation. To represent factors that are sequestered in the cytoplasm by microtubule attachment until ligand activation, we examined TGF- β -induced Smad2/3 translocation. We found that ethanol exposure selectively impaired the translocation of the STATs, but not Smad 2/3. STAT5B delivery was decreased to similar extents by addition of taxol (a microtubule stabilizing drug) or trichostatin A (a deacetylase inhibitor), agents that promote microtubule acetylation in the absence of alcohol. Thus, the alcohol-induced impairment of STAT nuclear translocation can be explained by increased microtubule acetylation and stability. Only ethanol-treatment impaired STAT5B activation, indicating that microtubules are not important for its activation by Jak2. Furthermore, nuclear exit was not changed in treated cells indicating this process is also independent of

microtubule acetylation and stability. Together, these results raise the exciting possibility that deacetylase agonists may be effective therapeutics for the treatment of alcoholic liver disease.

RESULTS OF PART II

STAT and Smad steady state distributions and nuclear translocation are differentially dependent on microtubules.

To confirm that microtubules play two distinct roles in nuclear translocation in WIF-B cells, we examined the steady state distributions of Smad2/3 (a microtubule sequestered factor) and STAT3 and STAT5B (actively transported factors) in nocodazole-treated cells. In control cells, Smad2/3 distributed equally between the cytosol and nucleus (Fig. 15A, a). Consistent with it being a sequestered factor, increased relative nuclear Smad2/3 was detected in nocodazole-treated cells (Fig. 15A, d). STAT5B was also detected in both the nucleus and cytosol in control cells, but unlike for Smad2/3, increased cytosolic staining was observed in nocodazole-treated cells (Fig. 15A, b and e). Although much less cytosolic STAT3 was detected in control cells than for STAT5B, increased cytosolic staining was also observed in nocodazole-treated cells (Fig. 15A c and f). This increased cytosolic staining for both STAT5B and STAT3 is consistent with them being actively-transported factors.

To directly assess the effects of microtubule depolymerization on nuclear translocation, we monitored the nuclear delivery of the transcription factors in cells activated by addition of their cognate ligands. Addition of TGF- β led to the dramatic redistribution of Smad2/3 to the nucleus. By 10 min, nuclear labeling was observed and by 30 min, near complete nuclear delivery occurred (Fig. 15B). Consistent with Smad2/3 being a sequestered factor, addition of nocodazole led to even more rapid nuclear

translocation. Within 10 min, robust nuclear labeling was observed (Fig. 15B). GH addition led to an even more rapid shift in STAT5B distributions. In control cells, increased nuclear labeling was observed by 5 min with peak delivery after 15 min (Fig. 15C). Consistent with STAT5B requiring intact microtubules for nuclear delivery, its nuclear translocation was impaired after GH addition in nocodazole-treated cells. Little increased nuclear staining was observed even after 15 min of activation. Similar results were observed for STAT3 upon IL-6 addition (unpublished results).

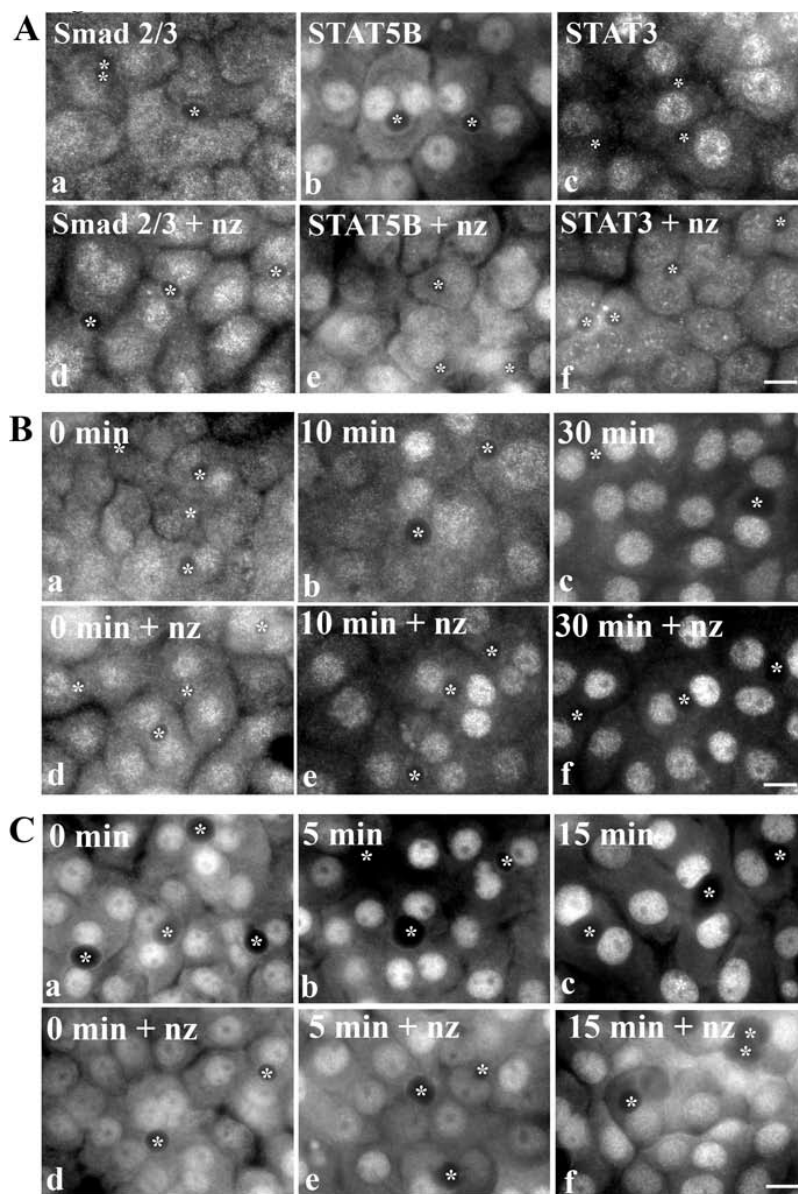


Figure 15. Microtubule depolymerization enhances Smad2/3 nuclear delivery, but impairs STAT translocation. (A) Cells were treated in the absence (a-c) or presence of 33 μ M nocodazole (nz) for 1 h (d-f). Cells were fixed and immunolabeled for Smad2/3 (a, d), STAT5B (b, e), or STAT3 (c, f). (B) Cells were pretreated in the absence (a-c) or presence of 33 μ M nocodazole (nz) for 1 h (d-f). 500 pM TGF- β was added (in the continued presence of nz) for the indicated times, cells were fixed and immunolabeled for Smad2/3. (C) Cells were pretreated in the absence (a-c) or presence of nocodazole (d-f) as in B. 50 nM GH was added for the indicated times, cells were fixed and immunolabeled for STAT5B. Asterisks are labeling selected bile canaliculi. Bar, 10 μ m.

To quantitate these differences, we measured relative Smad2/3 or STAT5B fluorescence intensities in the nucleus vs. cytoplasm. In control cells, a rapid increase in the ratios was observed for both transcription factors after ligand addition indicating increased nuclear translocation (Fig. 16A and B). At steady state (0 min), the Smad2/3 ratio was 1.10 increasing to 1.62 after TGF- β addition. Similarly, the ratios for STAT5B went from 1.24 to 1.68 after 15 min of GH addition. In nocodazole-treated cells, the Smad2/3 ratios were higher at each time point, peaking at 1.86, indicating enhanced delivery. In contrast, the STAT5B ratios were lower than control at each time point, staying at \sim 1.22. These data were confirmed biochemically in nuclei isolated from ligand-stimulated WIF-B cells. At steady state, 4.2% of Smad2/3 was nuclear whereas 12.3% was in nocodazole-treated cells (Fig. 16C). After 10 min TGF- β stimulation, the percent nuclear Smad2/3 increased to greater extents in nocodazole-treated cells than in control indicating enhanced delivery. In contrast, nocodazole decreased STAT5B nuclear delivery after GH stimulation at all time points tested (Fig. 16D). Together these results confirm that microtubules differentially regulate nuclear translocation in WIF-B cells.

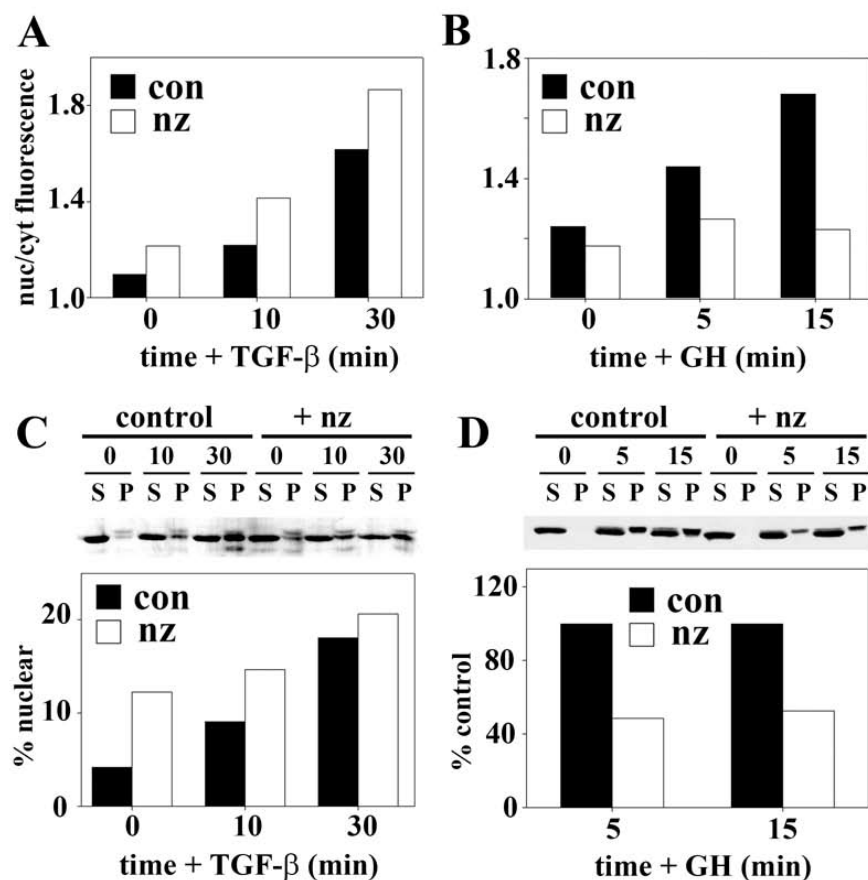


Figure 16. Microtubule depolymerization enhances Smad2/3, but impairs STAT5B, nuclear translocation after ligand stimulation. The ratio of nuclear-to-cytoplasmic fluorescence intensities was calculated for Smad2/3 (A) or STAT5B (B) in the experiments shown in Figures 15B and 15C, respectively. (C) Cells were treated in the absence or presence of 33 μ M nocodazole for 1 h. 500 pM TGF- β was added (in the continued presence of nocodazole) for the indicated times and nuclei were purified. Supernatants (S) and pelleted nuclei (P) were immunoblotted for Smad2/3. (D) Cells were pretreated in the absence or presence of nocodazole as in C. 50 nM GH was added for the indicated times, nuclei were purified and supernatants (S) and pelleted nuclei (P) were immunoblotted for STAT5B. Smad2/3 and STAT5B nuclear distributions were calculated and plotted.

Ethanol impairs nuclear translocation of the STATs, but not Smad2/3.

To determine whether ethanol exposure selectively impairs directed microtubule translocation, we first examined Smad2/3, STAT5B and STAT3 steady state distributions. Smad2/3 distributed equally between the cytosol and nucleus in control

and ethanol-treated cells (Fig. 17A) suggesting no change in its translocation. In contrast, much greater STAT5B and STAT3 cytoplasmic staining was observed in ethanol-treated cells (Fig. 17A). Quantification confirmed these observations. In control cells, the STAT5B nuclear-to-cytoplasmic ratio was 1.25 ± 0.01 and for STAT3, was 1.23 ± 0.03 (Fig. 17B). In ethanol-treated cells, decreased ratios were calculated for both STAT5B and STAT3 (1.08 ± 0.004 and 1.08 ± 0.01 , respectively) indicating decreased nuclear localization. Although the reduction was modest (~15%), it was statistically significant ($p \leq 0.01$). The Smad2/3 ratios were nearly identical in control and ethanol-treated cells (1.11 and 1.14, respectively; $n=2$) also confirming the morphological results. To confirm that the apparent change in STAT distributions was not due to altered protein levels, we immunoblotted lysates from control and ethanol-treated cells. As shown in Fig. 17C, their expression levels did not change.

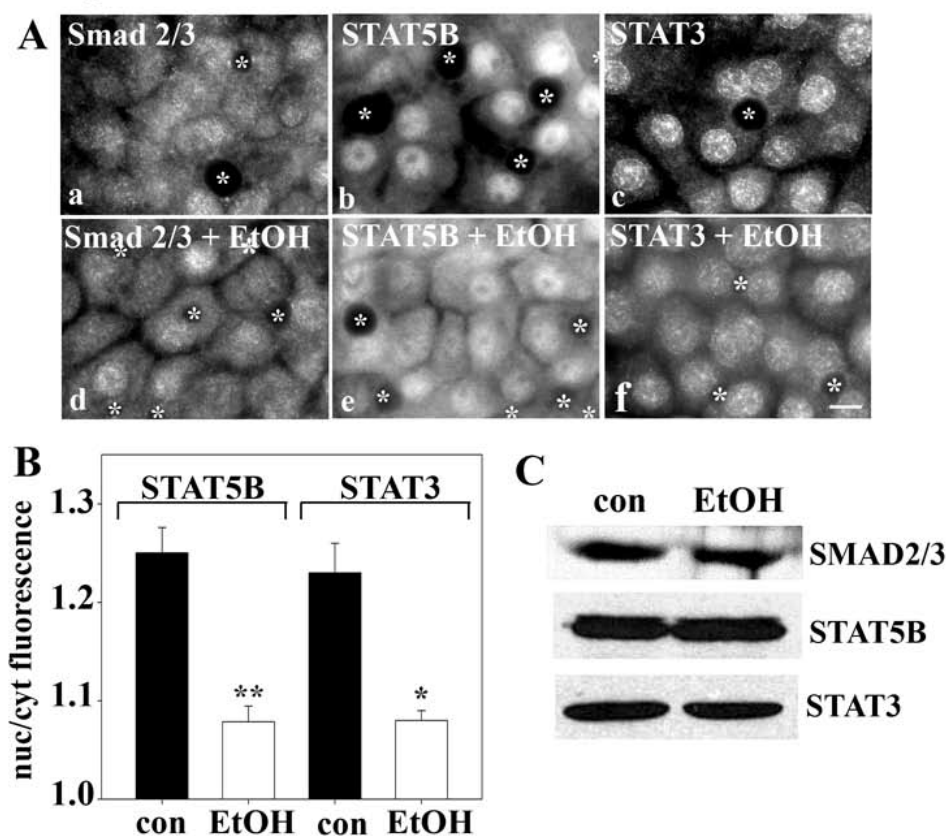


Figure 17. Ethanol-exposure alters the steady state distributions of STAT5B and STAT3, but not Smad2/3. (A) WIF-B cells were incubated in Hepes-buffered medium for 72 h in the absence or presence of 50 mM ethanol. Cells were fixed and were immunolabeled for Smad2/3, STAT5B or STAT3 as indicated. Selected bile canaliculi are labeled with asterisks. Bar, 10 μ m. (B) The ratio of nuclear-to-cytoplasmic fluorescence intensities was calculated for STAT5B or STAT3. Values represent the mean \pm SEM from at least three independent experiments. * $p \leq 0.05$, ** $p \leq 0.01$ (C) Control or ethanol-treated cells were immunoblotted for Smad2/3, STAT5B or STAT3 as indicated.

To directly determine whether ethanol exposure impairs translocation, we monitored nuclear delivery in ligand-activated cells. As above, TGF- β addition led to Smad2/3 nuclear delivery, and in ethanol-treated cells, similar kinetics of translocation were observed (Fig. 18A). In contrast, STAT5B nuclear delivery was markedly impaired in ethanol-treated cells. Even after 15 min of GH addition when peak nuclear delivery is seen in controls, substantial cytoplasmic staining was observed (Fig. 18B). Similar

results were observed for IL-6-induced STAT3 translocation (unpublished results).

Quantitation of the experiments shown confirms our observations. For each time point after TGF- β addition, nearly identical Smad2/3 nuclear-to-cytoplasmic ratios were measured (Fig. 18C, left). In contrast, decreased ratios were observed for STAT5B at each time point, indicating impaired delivery (Fig. 18C, right). From these results, we conclude that ethanol exposure selectively impairs directed microtubule-dependent nuclear translocation.

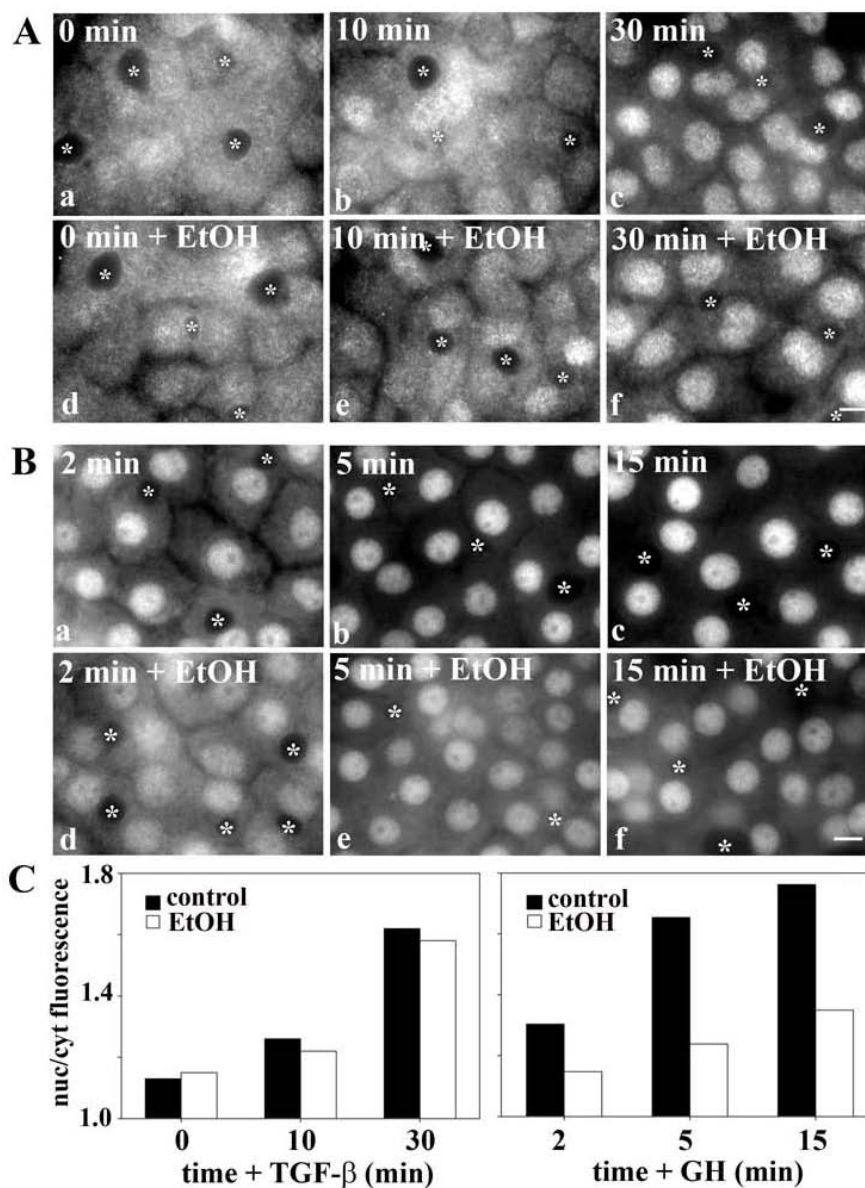


Figure 18. Ethanol exposure inhibits the ligand-stimulated translocation of STAT5B, but not Smad2/3. (A) Control (a-c) or ethanol-treated (d-f) cells were incubated with 500 pM TGF- β for the indicated times. Cells were fixed and immunolabeled for Smad2/3. (B) Control (a-c) or ethanol-treated (d-f) cells were incubated with 50 nM GH for the indicated times. Cells were fixed and immunolabeled for STAT5B. Asterisks are marking selected bile canaliculi. Bar, 10 μ m. (C) The ratio of nuclear-to-cytoplasmic fluorescence intensities was calculated for Smad2/3 (left) or STAT5B (right) in the experiments shown in A and B, respectively.

Decreased nuclear STAT5B is observed in livers from ethanol-fed rats.

Because more STAT5B is cytosolic than STAT3, nuclear translocation is more easily visualized and measured, thus we focused on STAT5B for the remaining studies. To confirm that our WIF-B observations have physiologic importance, we examined STAT5B in livers from ethanol-fed rats. As observed in WIF-B cells, STAT5B expression in rat livers was not changed by ethanol exposure (Fig. 19A); STAT5B expression in ethanol-treated livers was $95\% \pm 10.4\%$ of control levels ($n = 3$). To determine if alcohol feeding led to increased cytosolic STAT5B levels we examined its distributions in fractions containing isolated nuclei, cytosol or total non-nuclear membranes that were prepared according to our previously published methods (Shepard, et al., 2010). Importantly marker analysis confirmed the relative purity and equal loading of the fractions (Fig. 19B and see ref. 26 for further characterization). In control animals, $28.8 \pm 1.5\%$ of STAT5B was present in the nuclear fraction. In contrast, only $19.4 \pm 2.2\%$ of STAT5B was present in nuclei from ethanol-treated animals with a corresponding increase in the cytosol (from 43.8 ± 6.0 in control to $55.0 \pm 9.3\%$ in treated cells) (Figs. 19C and D). This STAT5B redistribution is remarkably similar to that observed in WIF-B cells confirming the physiologic importance of our findings.

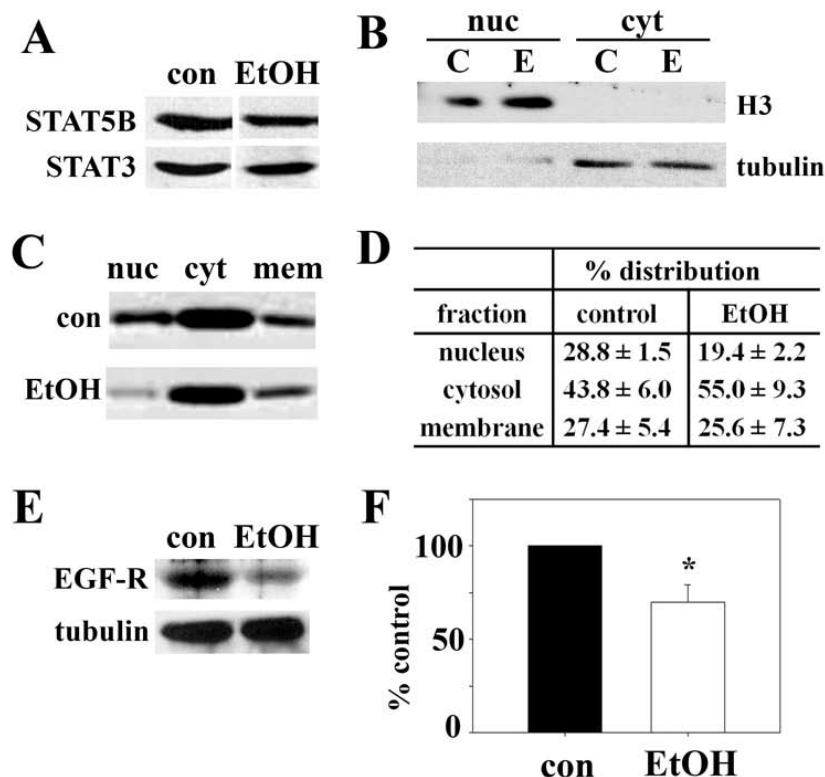


Figure 19. Decreased nuclear STAT5B is observed in livers from ethanol-fed rats. (A) Male Wistar rats were pair-fed control or ethanol Lieber-DeCarli liquid diets for 5 weeks. Liver whole homogenates from control or ethanol-fed rats were immunoblotted for Smad2/3, STAT5B or STAT3 as indicated. The blot is representative of three independent experiments. Liver whole homogenates from control (C) or ethanol-fed rats (E) were subfractionated to prepare nuclear (nuc), cytosolic (cyt) and non-nuclear membrane (mem) samples. (B) To assess fraction purity, cytosolic and nuclear fractions were immunoblotted for acetylated histone H3 (nuclear marker; H3) or α -tubulin (cytosolic marker). (C) The liver fractions were immunoblotted for STAT5B; a representative blot is shown. Immunoreactivity was measured using densitometry and plotted in D. Values represent the average \pm SEM from three independent pairs of rats. (E) Control or ethanol-treated cells were immunoblotted for EGF-R or tubulin (as a loading control) as indicated. (F) Immunoreactivity was measured using densitometry, and EGF-R levels were normalized to tubulin levels and calculated as percent of control. Values represent the average \pm SEM from four independent experiments (* $p \leq 0.46$).

Expression of EGF-R, a downstream target of STAT5B, is decreased in ethanol-treated cells.

To determine whether the ethanol-induced impairment in STAT5B nuclear translocation led to altered STAT5B-mediated signaling, we examined the protein expression levels of

EGF-R in control or ethanol-treated WIF-B cells. Importantly, expression of this receptor is known to be reduced in livers from STAT5B knockout mice and in livers from rats or mice chronically fed ethanol (Baik et al.; Deaciuc et al., 2004a; Deaciuc et al., 2004b). In control cells, EGF-R was robustly detected on immunoblots (Fig. 19E). However, in ethanol-treated cells, expression was significantly diminished. When quantitated, EGF-R protein expression was determined to be only $69.9 \pm 9.2\%$ ($p \leq 0.046$) of that in control cells when normalized to total α -tubulin expression (Fig. 19E) indicating that decreased STAT5 translocation is functionally significant.

Increased microtubule acetylation and stability impair STAT5B nuclear translocation.

To determine whether the altered STAT5B distributions required ethanol metabolism, we treated ethanol-exposed cells with the ADH inhibitor, 4-MP. Concomitant incubation with 4-MP prevented this redistribution, and more nuclear STAT5B was observed (Fig. 20A). Quantitation confirmed these observations. In control cells, the nuclear-to-cytoplasmic ratio was 1.28 ± 0.02 , and in ethanol-treated cells, the ratio dropped to 1.17 ± 0.03 % (Fig. 20B). In cells also treated with 4-MP, the ratio was nearly identical to that observed in controls (1.27 ± 0.02). Treatment with 4-MP alone had no effect on STAT5B distributions (ratio = 1.26 ± 0.01). Thus, impaired STAT5B nuclear translocation requires alcohol metabolism and is likely mediated by acetaldehyde.

To determine whether the ethanol-impaired STAT5B translocation was due to increased microtubule stability and acetylation, two agents were used in the absence of

ethanol. First, TSA was used as described (Joseph et al., 2008) to globally hyperacetylate cellular proteins (including tubulin) to the same extent as ethanol. Additionally, microtubules were specifically stabilized and acetylated using low taxol concentrations also as described (Phung-Koskas et al., 2005). Both treatments led to enhanced STAT5B cytoplasmic distributions (Fig. 20A). When quantitated, remarkably similar decreases in nuclear-to-cytoplasmic labeling were observed in taxol (1.09 ± 0.01 , 12.1% decrease) and TSA-treated cells (1.06 ± 0.01 , 14.8% decrease), and those values correspond well to that observed in ethanol-treated cells (1.08 ± 0.004 , 14.6% decrease) (Fig. 20C).

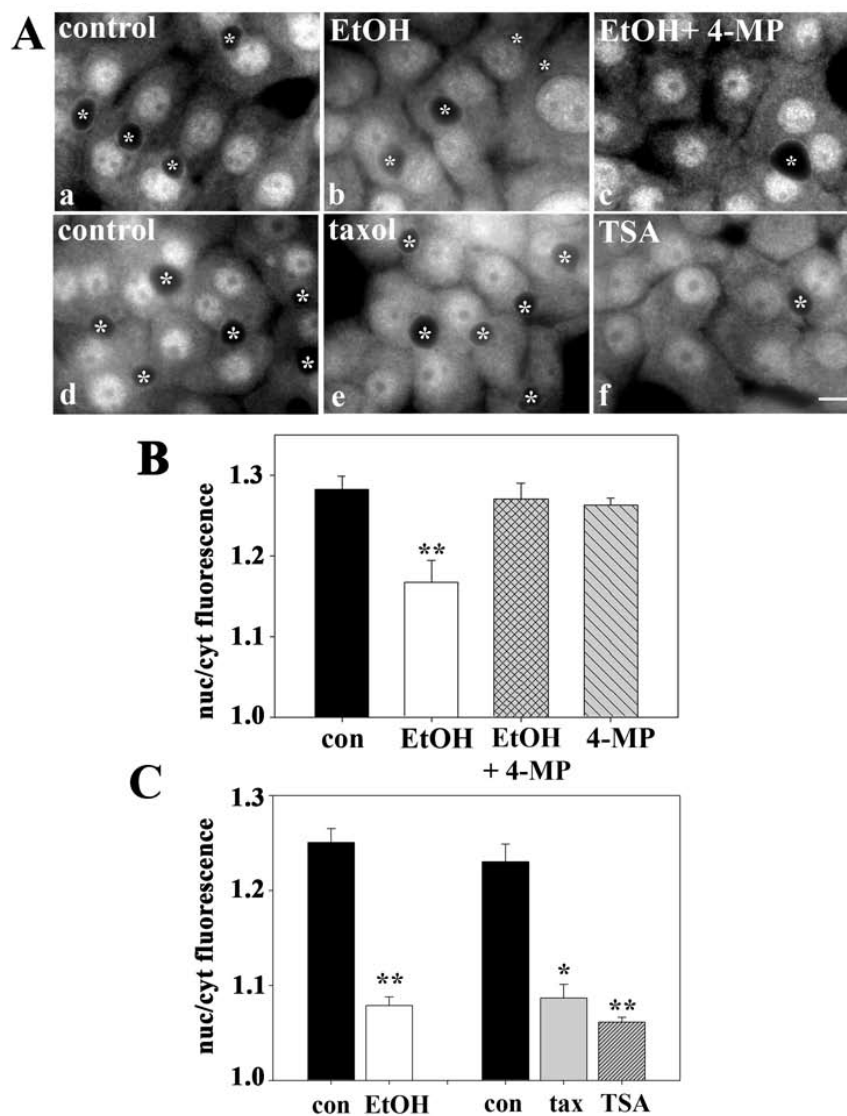


Figure 20. Ethanol-induced microtubule acetylation leads to increased cytosolic STAT5B. (A) Cells were treated with 50 mM ethanol alone (b) or with 1 mM 4-MP (c). Cells were also treated with 20 μ M taxol for 2 h (e) or 50 nM TSA for 30 min (f). Cells were fixed and immunolabeled for STAT5B. Asterisks are marking selected bile canaliculi. Bar, 10 μ m. The ratio of STAT5B nuclear-to-cytoplasmic fluorescence intensities was calculated in cells treated with ethanol and/or 4-MP (B) or ethanol, taxol or TSA (C). Values represent the mean \pm SEM from three independent experiments. * $p \leq 0.05$, ** $p \leq 0.01$.

To confirm these observations, we monitored STAT5B distributions after GH addition by immunoblotting purified nuclei. Increased STAT5B detection in nuclear

pellets was observed upon GH addition in control cells (Fig. 21A). However, this redistribution was attenuated and delayed in ethanol-treated cells. Similarly, in taxol (Fig. 21B) or TSA-treated (Fig. 21C) cells, much less STAT5B was recovered in the nuclear pellets after 5 and 15 min of GH addition. Because the amounts recovered in the pellets were less than expected based on our images, we immunoblotted the fractions for acetylated histone H3, an exclusively nuclear protein. All histone immunoreactivity was detected in the pelleted fractions in control and ethanol-treated cells, indicating full recovery (Fig. 21D). Even after darker exposures, histone H3 immunoreactivity was detected only in the pellet (unpublished results).

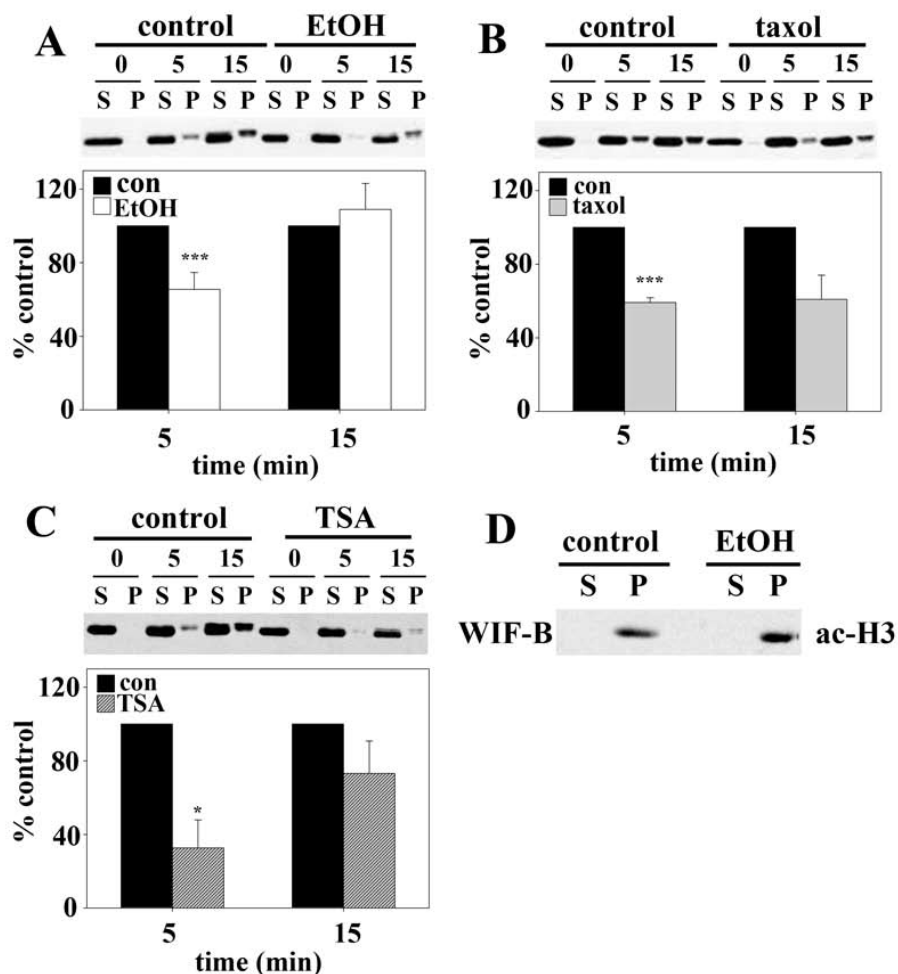


Figure 21. Ethanol-induced microtubule acetylation can explain impaired STAT5B nuclear translocation. Cells were treated with ethanol (A), 20 μ M taxol for 2 h (B) or 50 nM TSA for 30 min (C). In the continued presence of each agent, cells were incubated with 50 nM GH as indicated. Nuclei were purified and the pelleted nuclei (P) and resultant supernatants (S) were immunoblotted for STAT5B. Immunoreactivity was measured using densitometry and the relative STAT5B nuclear distribution calculated. Values were normalized to the percent of control nuclear distribution and represent the mean \pm SEM from at least three independent experiments. * $p \leq 0.05$, *** $p \leq 0.005$. (D) Nuclei were purified from control or ethanol-treated cells and the pelleted nuclei (P) and resultant supernatants (S) were immunoblotted for acetylated histone H3 (ac-H3).

STAT5B activation by Jak2 and nuclear exit are independent of microtubule acetylation and stability.

Because STAT5B nuclear translocation occurs after its ligand-stimulated phosphorylation, we examined whether impaired translocation was due to decreased activation. We monitored activation by immunolabeling cells for STAT5B phosphorylated on tyr694 (pSTAT5B) after GH addition. In cells without added ligand, little-to-no pSTAT5B was observed in either control or treated cells (Fig. 22A). After 2 min, diffuse cytoplasmic labeling was observed only in control cells. Not until 5 min, was cytosolic pSTAT5B detected in treated cells, while nuclear pSTAT5B was already detected in controls. By 15 min, virtually all pSTAT5B was nuclear in control cells, whereas a substantial cytosolic pool persisted in ethanol-treated cells.

These observations were confirmed biochemically by immunoblotting cell lysates for pSTAT5B. In control cells, pSTAT5B was detected after only 2 min, with peak phosphorylation at 5-15 min (Fig. 22B, top). After 30 min, pSTAT5B levels returned to near un-stimulated levels. As seen morphologically, STAT5B phosphorylation was decreased and delayed in ethanol-treated cells; pSTAT5B was not detected until after 5 min of GH addition, and persisted to 30 min (Fig. 22B, top). Immunoblots of purified nuclei confirmed these results. In control cells, substantial nuclear pSTAT5B was detected after 5 min of GH addition that remained high after 15 min. In contrast, the overall pSTAT5B levels and nuclear distribution were decreased (Fig. 22B, lower) in treated cells. STAT5B phosphorylation was also impaired in livers from ethanol-fed rats. As shown in Figure 22C, phosphorylation levels were reduced to only 45% of controls when normalized to tubulin. Importantly, these were the same fractions immunoblotted for total STAT5B in Figure 19A where levels did not change.

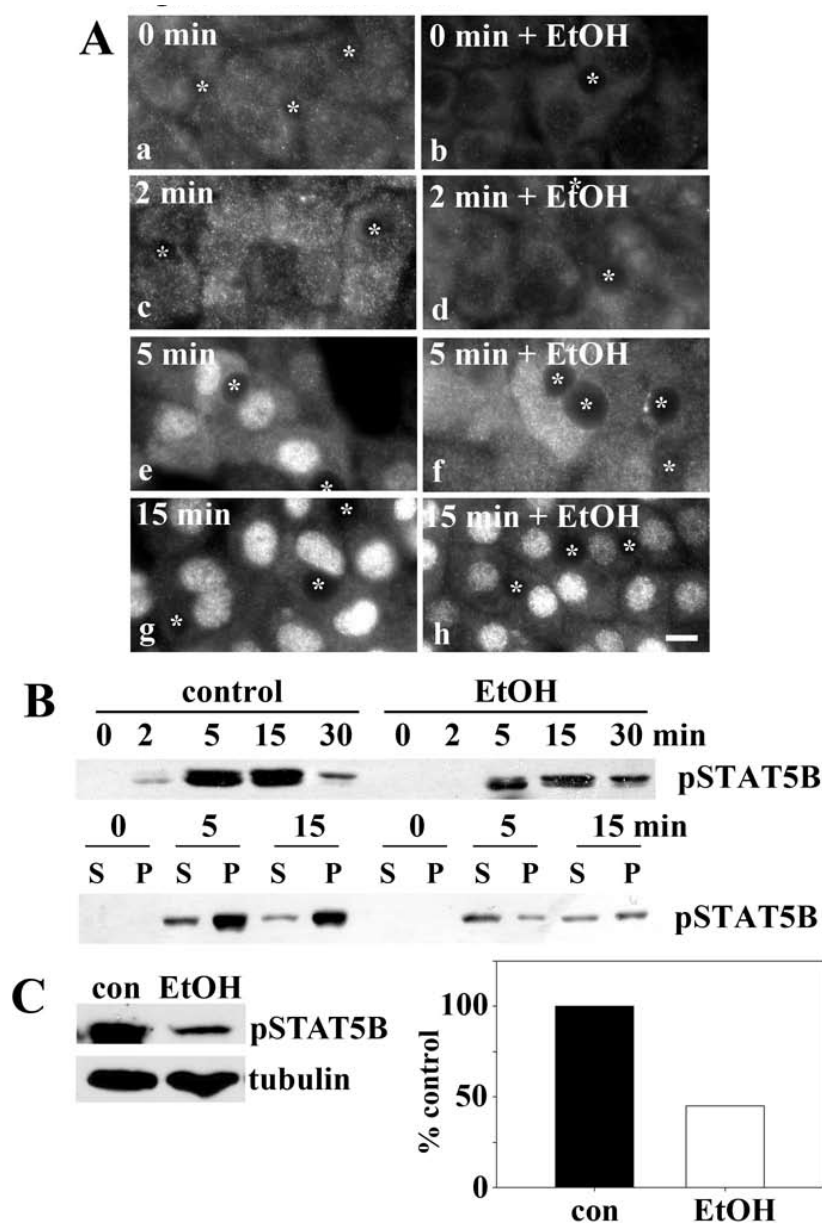


Figure 22. Ethanol impairs STAT5B phosphorylation after GH addition. (A) Control (a, c, e, g) or ethanol-treated (b, d, f, h) cells were incubated with 50 nM GH for the indicated times. Cells were fixed and immunolabeled for pSTAT5B (ph). Asterisks are marking selected bile canaliculi. Bar, 10 μ m. (B) Lysates (upper) or purified nuclei (bottom) from cells treated as in A and the pelleted nuclei (P) and resultant supernatants (S) were immunoblotted for pSTAT5B. (C) Liver whole homogenates from control or ethanol-fed rats were immunoblotted for pSTAT5B (p5B) or tubulin, as indicated. Relative levels of expression were determined from densitometric analysis of the immunoreactive species, normalized to tubulin levels and plotted as percent of control.

This impairment was strikingly similar to that found in ethanol-treated WIF-B cells, where peak STAT5B phosphorylation after 15 min of GH addition was reduced to 48% of control (Fig. 23A).

In contrast, pSTAT5B levels were nearly identical in control, taxol (Fig. 23B) or TSA-treated cells (Fig. 23C). Importantly, total STAT5B levels did not change with any of these treatments. To confirm that impaired nuclear translocation in ethanol-treated cells was activation-independent, but dependent on enhanced microtubule acetylation and stability, we examined pSTAT5B translocation in taxol-treated cells that have control pSTAT5B levels. In control cells, $17.5 \pm 1.5\%$ of pSTAT5B was nuclear by 5 min, compared to only $6.5 \pm 0.8\%$ in taxol-treated cells, and by 15 min, $51.7 \pm 7.7\%$ was nuclear in controls while only $34.9 \pm 8.4\%$ was nuclear in taxol-treated cells (Fig. 23D). Together these results indicate that ethanol impairs both STAT5B phosphorylation and subsequent translocation, and that only the latter step is microtubule-dependent.

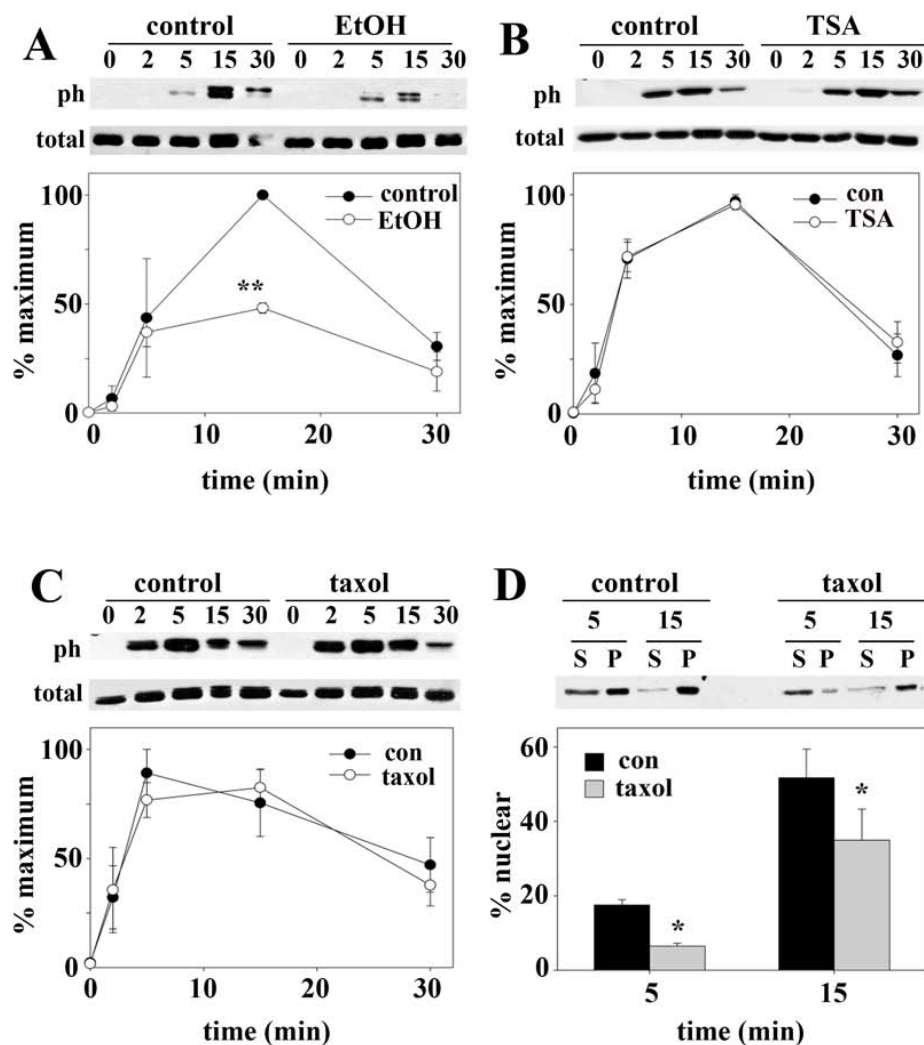


Figure 23. Ethanol, but not taxol or TSA, impairs STAT5B phosphorylation after GH addition. Cells were treated with ethanol (A), 20 μ M taxol for 2 h (B) or 50 nM TSA for 30 min (C). In the continued presence of each agent, cells were incubated with 50 nM GH for up to 30 min. Cell lysates were immunoblotted for pSTAT5B (ph) or total STAT5B. Immunoreactivity was measured by densitometry and plotted as the percent of maximal phosphorylation. Values are the mean \pm SEM from three independent experiments. (D) Cells were treated as in C and nuclei purified. Supernatants (S) and pelleted nuclei (P) were immunoblotted for pSTAT5B and its nuclear distribution calculated as percent total STAT5B. * $p \leq 0.05$, *** $p \leq 0.005$.

From these results, we further predict that nuclear exit and dephosphorylation, processes thought to be microtubule-independent, are not changed in ethanol-treated cells. For these experiments, cells were treated with GH for 30 min to fully translocate

STAT5B to the nucleus. The ligand was diluted 40-fold to biologically inactive concentrations by addition of prewarmed medium, and pSTAT5B was monitored for up to 30 min of withdrawal. In both control and ethanol-treated cells, robust nuclear pSTAT5B labeling was observed at 0 min of ligand withdrawal (Fig. 24). By 5 min, overall pSTAT5B signal was diminished with a subpopulation present in the cytoplasm reflecting dephosphorylation and nuclear exit, respectively. By 15 min, further decreased pSTAT5B staining was observed with increased cytoplasmic staining indicating additional nuclear exit and dephosphorylation in both control and ethanol-treated cells. Finally, by 30 min, pSTAT5B staining in both control and treated cells returned to unstimulated levels. Similar results were obtained using TSA (unpublished results). Thus, as predicted, nuclear exit and dephosphorylation are not impaired in ethanol-treated cells.

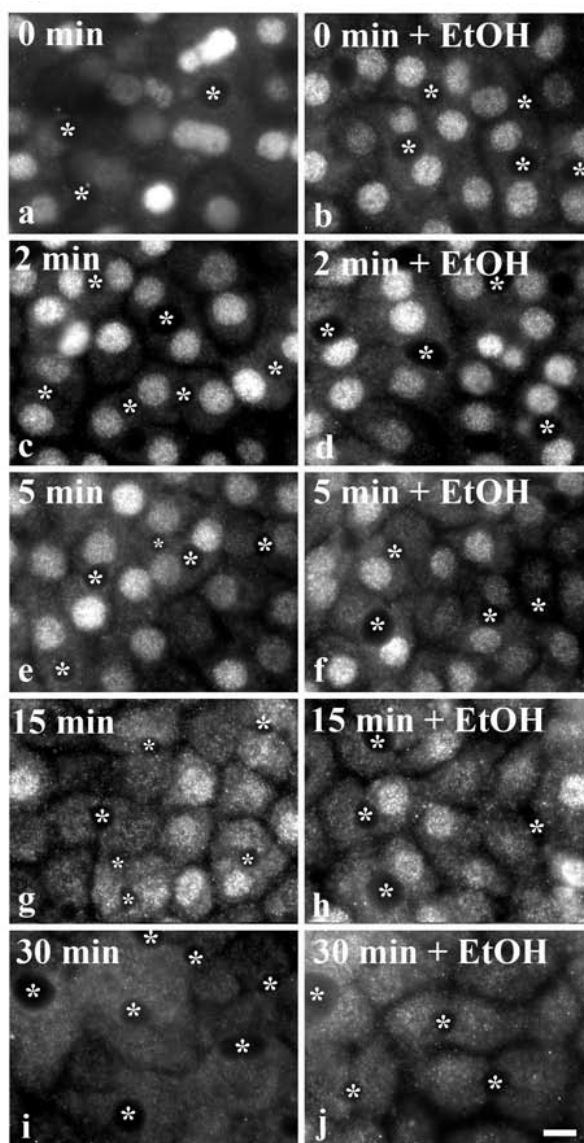


Figure 24. Ethanol does not impair STAT5B dephosphorylation or nuclear exit. Cells were treated in the absence (a, c,e, g,i) or presence of 50 mM ethanol for 72 h (b, d, f, h, j) at 37°C. In the continued presence of ethanol, cells were incubated with 50 nM GH for 30 min. Prewarmed medium was then added to dilute the ligand 40-fold thereby eliminating its ability to activate receptors, and cells were incubated for up to an additional 30 min at 37°C as indicated. Cells were fixed and cells immunolabeled for pSTAT5B. Asterisks are marking selected bile canaliculi. Bar, 10 μm

Ethanol selectively impairs Jak2 activation.

Since STAT5B phosphorylation was selectively impaired by ethanol treatment, we examined whether activation of its upstream tyrosine kinase, Jak2, was also selectively impaired by immunoblotting for pJak2. In control, taxol and TSA-treated cells, pJak2 levels and appearance were nearly identical (Fig. 25A). In all cases, increased pJak2 was observed after 2 min of GH addition, peaked at 5 min and began to diminish by 30 min. Importantly, peak Jak2 phosphorylation preceded peak STAT5B phosphorylation (5 vs. 15 min) consistent with its proposed role in STAT activation. In ethanol-treated cells, much less steady state pJak2 was observed and its activation was attenuated at each time point while total pJak2 levels remained unchanged (Fig. 25B). These results indicate that ethanol-selectively impairs Jak2 phosphorylation which can in turn, explain impaired STAT5B phosphorylation.

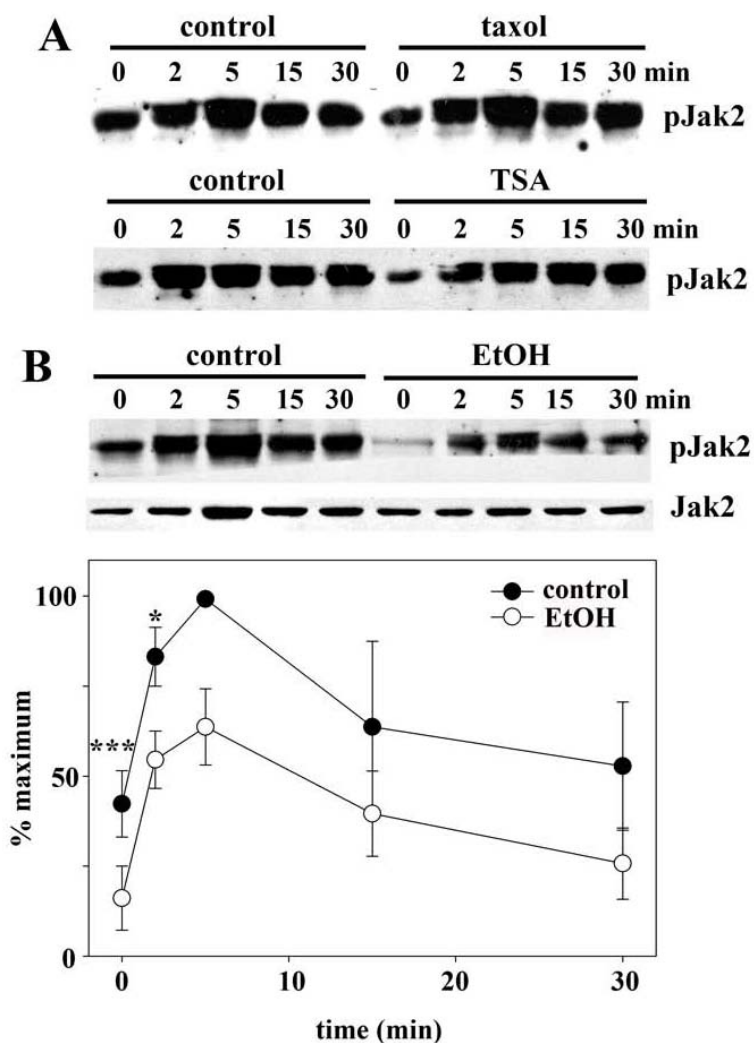


Figure 25. Ethanol, but not taxol or TSA, impairs Jak2 phosphorylation after GH addition. (A) Cells were treated with 20 μ M taxol for 2 h (upper panel) or 50 nM TSA for 30 min (lower panel). In the continued presence of each agent, cells were incubated with 50 nM GH for up to 30 min. Cell lysates were immunoblotted for pJak2. (B) Control or ethanol-treated cells were incubated with 50 nM GH for up to 30 min. Cell lysates were immunoblotted for total (bottom) or pJak2 (upper). (C) Immunoreactivity was measured by densitometry and plotted as the percent of maximal phosphorylation. Values represent the mean \pm SEM from three independent experiments. * $p \leq 0.05$, *** $p \leq 0.005$.

CONCLUSIONS AND IMPLICATIONS OF PART II

From these studies, we made several major observations. First, we confirmed that the two proposed models of microtubule-mediated nuclear translocation represented by Smad2/3 (sequestration) and STAT5B and STAT3 (directed delivery) operate in WIF-B cells. We determined that only the latter mechanism is impaired by ethanol treatment, and that the ethanol-induced impairment can be explained by increased microtubule acetylation and stability. We also found that the ethanol-induced defect in Jak2 activation and its subsequent activation of STAT5B is independent of microtubule acetylation and stability. Finally, we showed that nuclear STAT5B is decreased in livers from ethanol-fed rats indicating these observations have physiologic importance.

DISCUSSION

We undertook these studies to shed further light on the molecular mechanisms involved in hepatotoxicity due to chronic ethanol exposure. Since ethanol exposure or consumption has been shown to impair several key protein trafficking steps, we directed our studies at two important processes in the hepatocyte: clathrin-mediated internalization and nuclear translocation, to broaden our understanding of how ethanol impacts these hepatic functions. The list of proteins demonstrated to be acetylated in the presence of ethanol is continually growing. In addition to α -tubulin, this list includes: histone-H3, peroxisome proliferator-activated receptor- γ coactivator 1 α (PGC-1 α), p53, sterol regulatory element binding protein 1c (SREPB-1c), and acetyl-CoA synthetase 2 (AceCS) (Shepard and Tuma, 2009; Shepard, et al., 2010). It follows that our understanding of how these modified proteins (including α -tubulin/microtubules) impact proper hepatocyte function is also deepening. Eventually, understanding the molecular mechanisms involved in alcoholic liver disease will potentially allow the design of more effective therapeutics.

Chronic ethanol exposure impairs clathrin-mediated endocytosis in hepatocytes

We first sought to determine whether clathrin-mediated endocytosis from the basolateral membrane is selectively impaired by ethanol exposure in polarized hepatic cells. After examining the endocytosis of a broad array of proteins and compounds that are known to be internalized by distinct mechanisms, we confirmed that ethanol indeed selectively

impairs clathrin-mediated endocytosis in hepatocytes, as demonstrated by impairment of the constitutive clathrin-mediated internalization of pIgA-R and Tf-R (Fernandez, et al., 2009). In contrast, the caveolae/raft-mediated internalization of CTxB, the fluid phase uptake of Lucifer Yellow and the non-vesicle-mediated uptake of fluorescein diacetate were not impaired after ethanol exposure. We also showed evidence that ethanol exposure led to the redistribution of clathrin heavy chain to puncta at the basolateral surface, suggesting impaired vesicle fission, along with significantly less dynamin-2 associated with membranes in ethanol-treated cells. We then demonstrated that the internalization of single spanning apical membrane residents that contain no known internalization signaling information was significantly impaired, a result that was confirmed in cells expressing dominant negative dynamin-2, suggesting these proteins may be endocytosed by a clathrin-mediated mechanism (Fernandez, et al., 2009).

Ethanol-induced modifications of the clathrin machinery:

Clathrin-mediated internalization is a highly regulated process involving multiple proteins ((Conner and Schmid, 2003; Doherty and McMahon, 2009; Lee et al., 2009; Mayor and Pagano, 2007; McNiven and Thompson, 2006) McNiven, et al., 2006). In general, clathrin triskelions are recruited to and assembled at regions of the plasma membrane enriched in PIP₂. Adaptor protein (AP) complexes, such as AP2, are targeted to the membrane by their α -adaplin subunits and interact directly with sorting signals on internalized proteins (usually containing di-leucine or tyrosine-based motifs) via their μ 2 subunits. The large GTPase, dynamin, is thought to be recruited and assembled on the necks of coated pits where it likely mediates membrane fission and vesicle release. The

released vesicles are rapidly uncoated allowing for coat recycling and vesicle fusion with its target organelle.

At present, the specific mechanisms responsible for ethanol-induced defects in clathrin-mediated internalization are not known. Because the clathrin-mediated internalization of many unrelated proteins is impaired *in situ*, and in isolated hepatocytes, it is likely that a universal regulator of clathrin-mediated internalization is impaired, *not* the receptors themselves. Because impaired ASGP-R clathrin-mediated internalization required ethanol metabolism and is likely mediated by acetaldehyde (Joseph, et al., 2008), an exciting possibility is that the molecular machinery that drives clathrin-mediated endocytosis is more prone to adduction by acetaldehyde or other reactive metabolites than the molecules regulating other internalization routes. Clearly, this intriguing hypothesis requires more research.

A similar scenario may also evolve for proteins involved in vesicle budding and fission from the TGN. Basolateral resident proteins contain targeting information that likely promotes their recruitment into clathrin-coated vesicles at the TGN (Rodriguez-Boulan, et al., 2005). These basolateral targeting signals are similar to the signals required for clathrin-internalization and the majority are either tyrosine-based or contain a di-leucine motif (Rodriguez-Boulan, et al., 2005). Thus, one exciting possibility is that an alcohol-induced modification of the clathrin machinery also leads to defective vesicle fission at the TGN. Although constitutive secretory proteins are thought to bud from the TGN in different vesicle populations than transmembrane proteins (Saucan, et al., 1992)

it is not yet clear what factors are required for their formation. Because constitutive secretion is also impaired in ethanol-treated hepatic cells, one possibility is that at least some components of the clathrin machinery are shared, and that these components are readily modified by reactive alcohol metabolites. Clearly, this is a fertile area of investigation for future research.

Another possibility is that key components of the clathrin machinery may be hyperacetylated upon ethanol exposure leading to impaired internalization. This idea is supported by the findings that actin and cortactin, two members of the clathrin machinery, are known to be hyperacetylated in the presence of ethanol (Shepard and Tuma, 2009). Both of these proteins regulate late stages of clathrin coated vesicle budding from the plasma membrane and the TGN (Cao, et al., 2003; Cao, et al., 2005).

In general, cortactin is thought to promote actin polymerization at sites of vesicle formation and recruit dynamin to the necks of budding vesicles (Cao, et al., 2003; Cao, et al., 2005). Recently, it was shown that ethanol (as well as TSA) impairs internalization at a late stage of clathrin-mediated endocytosis, before vesicle fission. This defect likely results from a decreased dynamin recruitment to the necks of clathrin-coated invaginations, which results in a defect in subsequent vesicle budding (Shepard, et al., 2012) (Figure 26). At present, the exact mechanism by which cortactin, actin and dynamin function to promote vesicle release is not yet completely elucidated. However, acetylation of cortactin is known to prevent its association with actin (Zhang, et al., 2007). Taken together, these studies provide evidence that alcohol-induced

hyperacetylation leads to decreased interactions between actin and cortactin such that cortactin is no longer recruited to sites of clathrin-vesicle formation, which then inhibits dynamin recruitment and subsequent vesicle fission.

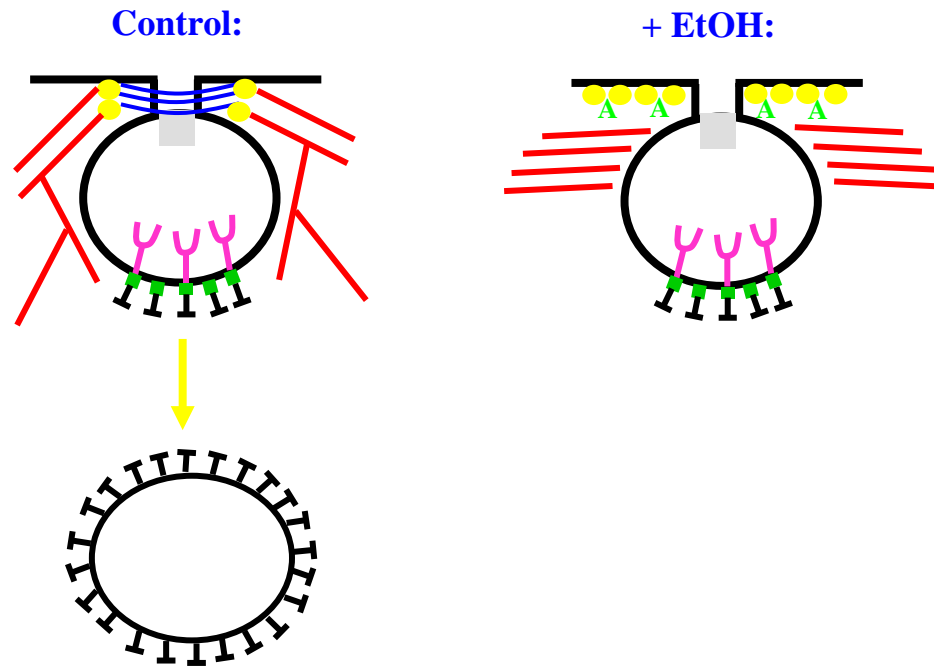


Figure 26. Ethanol impairs vesicle fission. In control cells (left panel), cortactin (shown in yellow) promotes actin polymerization (shown in red) and dynamin recruitment (shown in blue) to the neck of a budding endocytic vesicle. Dynamin facilitates vesicle fission and proper endocytosis. Ethanol (or TSA) treatment (right panel) leads to increased cortactin acetylation, likely preventing dynamin recruitment and subsequent vesicle fission. (Model made by Dr. Blythe Shepard)

Are single spanning apical proteins internalized via clathrin-mediated mechanisms?

In hepatocytes, newly synthesized single spanning apical resident proteins take the “indirect” route to the canalicular surface. They are transported from the TGN to the basolateral surface where they are retrieved by endocytosis and transcytosed to the apical surface (Tuma and Hubbard, 2003). Currently, little is known about how apical proteins are selectively retrieved from the basolateral membrane. Our previous studies indicated

that they are not likely internalized via caveolae/raft-mediated pathways (Nyasae, et al., 2003). When cholesterol or glycosphingolipids (raft components) were depleted from WIF-B cells, internalization was not changed. Furthermore, the short cytoplasmic domains (6-12 amino acids) of the apical residents lack any known tyrosine- or dileucine-based clathrin-mediated internalization signal sequences (Tuma and Hubbard, 2003). However, our finding that internalization of DPP IV, HA and APN were all impaired to a similar extent as ASGP-R, pIgA-R and Tf-R suggest that apical residents may be endocytosed via clathrin-mediated pathways. This is supported by our observation that overexpressed dominant negative dynamin-2 impaired internalization of pIgA-R, ASGP-R, DPP IV and APN, but not internalization of CTxB or HRP. However it remains to be determined whether the apical residents are actively recruited to clathrin-coated vesicles or if they are passive passengers.

Impaired clathrin-mediated internalization may explain nutritional deficiencies in patients:

Chronic alcohol consumption leads to many nutritional side effects. Much of this is due to the fact that an alcoholic often substitutes the calories from ethanol for the calories from food such that he/she becomes malnourished (Lieber, et al., 2003; Mezey, et al. 1980). This is further exacerbated by the decreased intestinal absorption of many compounds including dietary fats, fat soluble vitamins, essential amino acids, folic acid, glucose and minerals such as calcium, zinc, iron and magnesium (Tuma and Hubbard, 2003). In general, these defects are not likely due to impaired clathrin-mediated endocytosis. Most fat soluble vitamins associate with bile acid micelles and enter

passively across the membrane while most minerals are absorbed paracellularly or through specific transporters (e.g., copper and zinc). Thus, decreased absorption may be due to decreased bile production (for dietary fats and fat-soluble vitamins) or decreased paracellular permeability (for minerals).

However, there are some nutritional deficiencies that might be explained by impaired clathrin-mediated internalization. For example, Many alcoholics display serious vitamin B₁₂ deficiencies (Lieber, et al. 2003; Mezey, et al. 1980). Unlike many other hydrophobic vitamins, B₁₂ is internalized via clathrin-mediated mechanisms in the intestine, liver and kidney (Tuma and Hubbard, 2003).

Furthermore, vitamins A and D are scavenged via a mechanism operating in kidney proximal tubules (Tuma and Hubbard, 2003). These vitamins are retrieved from the urine by association with surface-associated megalin, and the megalin-A or -D complexes are internalized in clathrin-coated vesicles. Thus, one interesting prediction is that this clathrin-mediated scavenge mechanism is impaired in chronic alcoholics.

Impact of impaired clathrin-mediated internalization on liver function

Endocytosis serves as the interface between the hepatocyte and its external environment and is critical for intercellular communication and signal transduction. Endocytosis also functions to retrieve metabolites from the blood such that small impairments can lead to increased levels of circulating hormones, growth factors, cytokines and other ligands.

This is consistent with reports where increased levels of circulating interleukin-6,

transferrin and pIgA were observed in ethanol-fed rats (Potter, et al., 1985; van de Wiel, et al., 1987; Hoek, et al., 2002; Hoek and Pastorino, 2004). These results also are remarkably consistent with the observed defects in pIgA-R and Tf-R internalization reported here. Because these and other ligands are all associated with specific biological responses, small defects in their endocytosis can lead to alterations in hepatic homeostasis and metabolism which can promote liver injury. Thus, defining the mechanisms responsible for impaired clathrin-mediated endocytosis in ethanol-treated hepatocytes may have important clinical implications.

Chronic ethanol exposure impairs microtubule-dependent nuclear translocation in hepatocytes

In extending our studies to other possible impairments in protein trafficking, we examined selected signaling pathways known to be perturbed in the chronic alcoholic. More specifically, we studied two main pathways demonstrated to use microtubules in opposing manners: the Jak-STAT pathway which uses an intact microtubule network for efficient, concerted transcription factor nuclear delivery after ligand stimulation, and the Smad pathway, which uses microtubules for cytosolic sequestration of transcription factors. We found that the two proposed models of microtubule-mediated nuclear translocation represented by Smad2/3 (sequestration) and STAT5B and STAT3 (directed delivery) operate in WIB-cells. We determined that only the latter mechanism is impaired by ethanol treatment, and that the ethanol-induced impairment can be explained by increased microtubule acetylation and stability. We also found that the ethanol-

induced defect in Jak2 activation and its subsequent activation of STAT5B is independent of microtubule acetylation and stability. Finally, we showed that nuclear STAT5B is decreased in livers from ethanol-fed rats indicating these observations have physiologic importance (Fernandez, et al., 2012).

Ethanol selectively impairs directed nuclear translocation.

Microtubule depolymerization with nocodazole led to increased Smad2/3 nuclear delivery at steady state and in ligand-treated cells whereas it impaired STAT5B and STAT3 delivery. This confirms that Smad2/3 is a microtubule sequestered factor while STATs require microtubules for directed translocation in WIF-B cells. We further determined that only STAT translocation was impaired by ethanol exposure, and that taxol or TSA addition impaired STAT translocation to remarkably similar extents, suggesting that increased microtubule acetylation and stability can explain the observed defect.

What is responsible for this selective effect? The answer may be related to the differential dependence of the factors on microtubule-based motors for nuclear delivery (Fig. 27). Although it is not known what microtubule-associated protein (MAP)/motor is responsible for Smad2/3 microtubule sequestration, once it is released, it freely diffuses to the nucleus without microtubule assistance. In contrast, STAT5B translocation has been shown to require the minus-end directed microtubule motor, dynein (Campbell and Hope, 2003). Because dynein has been shown to preferentially bind acetylated

microtubules (Janke and Bulinski), a provocative explanation for our results is that its enhanced microtubule binding impedes microtubule-dependent translocation. From our studies with 4-MP, we further determined that impaired STAT5B nuclear translocation requires ethanol metabolism and is likely mediated by acetaldehyde. Because tubulin and purified hepatic MAPs and motors are known acetaldehyde-adducted proteins (Jennett et al., 1987), we predict that impaired translocation can be alternatively (additionally?) explained by adduct-induced changes in MAP or motor function.

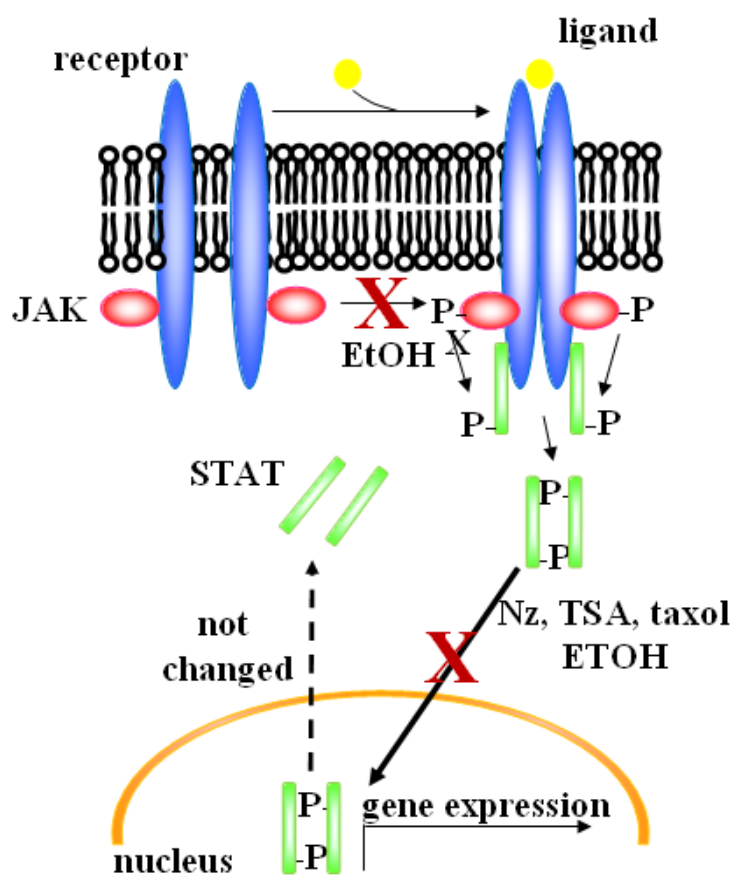


Figure 27. Ethanol impairs microtubule-dependent nuclear translocation. Ethanol exposure leads to a decrease in Jak2 phosphorylation, with a corresponding decrease in STAT5B phosphorylation. Additionally, nuclear translocation requires an intact and dynamic microtubule network, as depolymerization with nocodazole, or hyperacetylation/hyperstability

(EtOH/TSA/taxol) impairs microtubule-dependent nuclear translocation. Nuclear exit (non-microtubule-dependent) is not impaired.

Ethanol, but not taxol or TSA, impairs STAT5B activation.

We determined that only ethanol-exposure impairs STAT5B phosphorylation after GH activation. The kinetics and extent of STAT5B phosphorylation were not changed in taxol- or TSA-treated cells. In an effort to explain the selectivity of this defect, we examined Jak2 activation, the STAT5B activating kinase. We found that only ethanol exposure (not taxol or TSA) led to decreased Jak2 activation. The delayed and decreased Jak2 activation correlate remarkably with the delayed and decreased STAT5B phosphorylation, thus, we conclude that decreased pJak2 can explain the decreased STAT5B observed in our studies.

These results suggest that ethanol impairs GH-mediated signaling in at least two ways, with only translocation being microtubule-dependent. This is consistent with our findings that translocation of control pSTAT5B levels in taxol-treated cells is also impaired. This is also consistent with our observations that STAT5B nuclear exit and dephosphorylation were not changed in ethanol-treated cells, processes not thought to be microtubule-dependent. The open question is how does ethanol-exposure, in a non-microtubule-mediated fashion, lead to impaired Jak2 activation? Recently, it has been shown that the phospho-tyrosine phosphatase 1B (PTP1B) responsible for Jak2 dephosphorylation is up-regulated in ethanol-treated rat skeletal muscle (Gao et al.). Thus, one intriguing possibility is that in alcohol-exposed hepatocytes, PTP1B expression is also up-regulated, leading to decreased pJak2. Alternatively, critical GH-receptor

intracellular docking sites or other components of the signaling machinery may be particularly prone to adduction or acetylation preventing proper signaling complex formation. This is consistent with reports that STAT3 is an acetylated protein (Ray et al., 2005).

Clinical implications

High circulating GH amounts are present in alcoholic patients, yet its hepatoprotective activities are diminished (Shepard et al., 2010). One explanation for this paradox is that the ethanol-induced impairment of STAT5B nuclear translocation alters gene expression required for hepatoprotection. Our finding that the expression of the downstream target gene, epidermal growth factor receptor (EGF-R), is significantly decreased in ethanol-treated WIF-B cells, is perfectly consistent with this idea. Additionally, expression of other known STAT5B target genes, including EGF-R, suppressor of cytokine signaling 2 (SOCS2), CYP4A12 and CYP7B1 are decreased in hepatocytes from ethanol-fed rodents (Baik et al.; Deaciuc et al., 2004a; Deaciuc et al., 2004b). Also, the expression of peroxisome proliferator activated receptor γ (PPAR γ), a gene shown to be up-regulated in STAT5B knockout mice, is enhanced in ethanol-fed animals (Bardag-Gorce et al., 2006; Hosui and Hennighausen, 2008). We further suggest that the ethanol-induced down-regulation of numerous genes involved in hepatomitogenesis may represent not-yet-identified targets for GH/STAT5B-mediated signaling.

Finally, these studies suggest that modulating cellular acetylation levels is a unique therapeutic target for the treatment of alcoholic liver disease. To date, the acetylation of

numerous proteins is known to be enhanced by ethanol-treatment, and this list is expanding (Shepard and Tuma, 2009; Shepard, et al., 2010). Currently, many naturally-occurring and synthetic deacetylase agonists are in clinical trials for treatment of human diseases (Elliott and Jirousek, 2008). One such drug, resveratrol, has been shown to attenuate fatty liver and oxidative stress in alcohol-exposed mice (Ajmo et al., 2008). An exciting possibility is that specific deacetylase agonists or acetyltransferase antagonists will be useful in treating alcoholic liver disease.

REFERENCES

- Ajmo, J.M., X. Liang, C.Q. Rogers, B. Pennock, and M. You. 2008. Resveratrol Alleviates Alcoholic Fatty Liver in Mice. *Am J Physiol Gastrointest Liver Physiol*.
- Alberts, B, Johnson, A., Lewis, J., Raff, M., Roberts, K., Walter, P., 2008. Molecular Biology of the Cell., Garland Science, NY, New York.
- Baik, M., J.H. Yu, and L. Hennighausen. 2011. Growth hormone-STAT5 regulation of growth, hepatocellular carcinoma, and liver metabolism. *Ann N Y Acad Sci*. 1229:29-37.
- Baraona, E., Leo, M.A., Borowsky, S.A., Lieber, C.S. 1977. Pathogenesis of alcohol-induced accumulation of protein in the liver. *J Clin Invest* 60: 546-554.
- Bardag-Gorce, F., B.A. French, J. Dedes, J. Li, and S.W. French. 2006. Gene expression patterns of the liver in response to alcohol: in vivo and in vitro models compared. *Exp Mol Pathol*. 80:241-51.
- Bastaki, M., L.T. Braiterman, D.C. Johns, Y.H. Chen, and A.L. Hubbard. 2002. Absence of direct delivery for single transmembrane apical proteins or their "Secretory" forms in polarized hepatic cells. *Mol Biol Cell*. 13:225-37.
- Beloqui, O., R.M. Nunes, B. Blades, P.D. Berk, and B.J. Potter. 1986. Depression of iron uptake from transferrin by isolated hepatocytes in the presence of ethanol is a pH-dependent consequence of ethanol metabolism. *Alcohol Clin Exp Res*. 10:463-70.
- Brooks, P.J. 1997. DNA damage, DNA repair, and alcohol toxicity--a review. *Alcohol Clin Exp Res*. 21:1073-82.
- Camacho, K.B., Tuma, D.J., Casey, C.A. 1996. Zonal differences in ethanol-induced impairments in fluid-phase endocytosis in rat hepatocytes. *Alcohol Clin Exp Res* 20: 589-594.
- Campbell, E.M. and Hope, T.J. 2003. Role of the cytoskeleton in nuclear import. *Adv Drug Deliv Rev* 55: 761-771.
- Cao, H., J.D. Orth, J. Chen, S.G. Weller, J.E. Heuser, and M.A. McNiven. 2003. Cortactin is a component of clathrin-coated pits and participates in receptor-mediated endocytosis. *Mol Cell Biol*. 23:2162-70.
- Cao, H., S. Weller, J.D. Orth, J. Chen, B. Huang, J.L. Chen, M. Stamnes, and M.A. McNiven. 2005. Actin and Arp1-dependent recruitment of a cortactin-dynamin complex

to the Golgi regulates post-Golgi transport. *Nat Cell Biol.* 7:483-92.

Carpentier, J.L. 1992. Insulin-induced and constitutive internalization of the insulin receptor. *Horm Res* 38: 13-18

Carpentier, J.L., Paccaud, J.P., Backer, J., Gilbert, A., Orci, L., Kahn, C.R., Baecker, J. 1993. Two steps of insulin receptor internalization depend on different domains of the beta-subunit. *J Cell Biol* 122: 1243-1252.

Casey, C.A., Kragoskow, S.L., Sorrell, M.F., Tuma, D.J. 1990. Effect of chronic ethanol administration on total asialoglycoprotein receptor content and intracellular processing of asialoorosomuroid in isolated rat hepatocytes. *Biochim Biophys Acta* 1052: 1-8

Casey, C.A., Camacho, K.B., Tuma, D.J. 1992. The effects of chronic ethanol administration on the rates of internalization of various ligands during hepatic endocytosis. *Biochim Biophys Acta* 1134: 96-104.

Casey, C.A., Kragoskow, S.L., Sorrell, M.F., Tuma, D.J. 1987. Chronic ethanol administration impairs the binding and endocytosis of asialo-orosomuroid in isolated hepatocytes. *J Biol Chem* 262: 2704-2710.

Clemens, D.L., C.M. Halgard, J.R. Cole, R.M. Miles, M.F. Sorrell, and D.J. Tuma. 1996. Impairment of the asialoglycoprotein receptor by ethanol oxidation. *Biochem Pharmacol.* 52:1499-505.

Clemens, D.L., C.M. Halgard, R.R. Miles, M.F. Sorrell, and D.J. Tuma. 1995. Establishment of a recombinant hepatic cell line stably expressing alcohol dehydrogenase. *Arch Biochem Biophys.* 321:311-8.

Conner, S.D., and S.L. Schmid. 2003. Regulated portals of entry into the cell. *Nature.* 422:37-44.

Dalke, D.D., Sorrell, M.F., Casey, C.A., Tuma, D.J. 1990. Chronic ethanol administration impairs receptor-mediated endocytosis of epidermal growth factor by rat hepatocytes. *Hepatology* 12: 1085-1091.

Deaciuc, I.V., D.E. Doherty, R. Burikhanov, E.Y. Lee, A.J. Stromberg, X. Peng, and W.J. de Villiers. 2004a. Large-scale gene profiling of the liver in a mouse model of chronic, intragastric ethanol infusion. *J Hepatol.* 40:219-27.

Deaciuc, I.V., X. Peng, N.B. D'Souza, S.I. Shedlofsky, R. Burikhanov, I.V. Voskresensky, and W.J. de Villiers. 2004b. Microarray gene analysis of the liver in a rat model of chronic, voluntary alcohol intake. *Alcohol.* 32:113-27.

- De Matteis, M.A., and A. Luini. 2008. Exiting the Golgi complex. *Nat Rev Mol Cell Biol.* 9:273-84.
- Diehl, A.M. 2001. Nonalcoholic fatty liver disease: implications for alcoholic liver disease pathogenesis. Review in *Alcohol Clin Exp Res.* May;25
- Doherty, G.J., and H.T. McMahon. 2009. Mechanisms of Endocytosis. *Annu Rev Biochem.*
- Dong, C., Li, Z., Alvarez, R. Jr., Feng, X.H., Goldschmidt-Clermont, P.J. 2000. Microtubule binding to Smads may regulate TGF beta activity. *Mol Cell.* Jan;5(1):27-34.
- Elliott, P.J., and M. Jirousek. 2008. Sirtuins: novel targets for metabolic disease. *Curr Opin Investig Drugs.* 9:371-8.
- Escobar, G.A., McIntyre, R.C., Jr., Moore, E.E., Gamboni-Robertson, F., Banerjee, A., 2006. Clathrin heavy chain is required for TNF-induced inflammatory signaling. *Surgery* 140: 268-272.
- Fernandez, D.J., B.L. McVicker, D.J. Tuma, and P.L. Tuma. 2009. Ethanol selectively impairs clathrin-mediated internalization in polarized hepatic cells. *Biochem Pharmacol.* 78:648-55.
- Fernandez D.J., D.J. Tuma, P.L. Tuma. 2012. Microtubule acetylation and stability induced by chronic alcohol exposure impair nuclear translocation of STAT3 and STAT5B, but not Smad 2/3, in polarized hepatic cells. *American Journal of Physiology* (in revision)
- Gao, B. 2005. Cytokines, STATs and liver disease. *Cell Mol Immunol.* 2:92-100.
- Gao, L., X. Zhang, F.R. Wang, M.F. Cao, X.J. Zhang, N.N. Sun, J. Zhang, and J.J. Zhao. 2010. Chronic ethanol consumption up-regulates protein-tyrosine phosphatase-1B (PTP1B) expression in rat skeletal muscle. *Acta Pharmacol Sin.* 31:1576-82.
- Geny, B., and Popoff, M.R. 2006. Bacterial protein toxins and lipids: pore formation or toxin entry into cells. *Biol Cell* 98:667-78.
- Gleason EL, Hogan JC, and Stephens JM. 2004. Stabilization, not polymerization, of microtubules inhibits the nuclear translocation of STATs in adipocytes. *Biochem Biophys Res Commun* 325: 716-718.
- Glozak, M.A., N. Sengupta, X. Zhang, and E. Seto. 2005. Acetylation and deacetylation of non-histone proteins. *Gene.* 363:15-23.

Gong, K., Xing, D., Li, P., Hilgers, R.H., Hage, F.G., Oparil, S., Chen, Y.F. 2011. cGMP inhibits TGF-beta signaling by sequestering Smad3 with cytosolic beta2-tubulin in pulmonary artery smooth muscle cells. *Mol Endocrinol.* Oct;25(10):1794-803.

Griffo, G., Hamon-Benais, C., Angrand, P.O., Fox, M., West, L., Lecoq, O. 1993. HNF4 and HNF1 as well as a panel of hepatic functions are extinguished and reexpressed in parallel in chromosomally reduced rat hepatoma-human fibroblast hybrids. *J Cell Biol* 121:887-98.

Grozinger, C.M., C.A. Hassig, and S.L. Schreiber. 1999. Three proteins define a class of human histone deacetylases related to yeast Hda1p. *Proc Natl Acad Sci U S A.* 96:4868-73.

Hankins, J. 2006. The role of albumin in fluid and electrolyte balance. *J Infus Nurs* 29: 260-265.

Hoek, J.B., and J.G. Pastorino. 2002. Ethanol, oxidative stress, and cytokine-induced liver cell injury. *Alcohol.* 27:63-8.

Hoek, J.B., and J.G. Pastorino. 2004. Cellular signaling mechanisms in alcohol-induced liver damage. *Semin Liver Dis.* 24:257-72.

Hosui, A., and L. Hennighausen. 2008. Genomic dissection of the cytokine-controlled STAT5 signaling network in liver. *Physiol Genomics.* 34:135-43.

Hubbert, C., A. Guardiola, R. Shao, Y. Kawaguchi, A. Ito, A. Nixon, M. Yoshida, X.F. Wang, and T.P. Yao. 2002. HDAC6 is a microtubule-associated deacetylase. *Nature.* 417:455-8.

Ihrke, G., E.B. Neufeld, T. Meads, M.R. Shanks, D. Cassio, M. Laurent, T.A. Schroer, R.E. Pagano, and A.L. Hubbard. 1993. WIF-B cells: an in vitro model for studies of hepatocyte polarity. *J Cell Biol.* 123:1761-75.

Jennett, R.B., M.F. Sorrell, E.L. Johnson, and D.J. Tuma. 1987. Covalent binding of acetaldehyde to tubulin: evidence for preferential binding to the alpha-chain. *Arch Biochem Biophys.* 256:10-8.

Jennett R.B., Sorrell M.F., Saffari-Fard A., Ockner J.L., Tuma D.J., 1989. Preferential covalent binding of acetaldehyde to the alpha-chain of purified rat liver tubulin, *Hepatology* 9: 57-62.

- Jennett R.B., Tuma D.J., Sorrell M.F., 1980. Effect of ethanol and its metabolites on microtubule formation, *Pharmacology* 21: 363-368.
- Joseph, R.A., B.D. Shepard, G.T. Kannarkat, T.M. Rutledge, D.J. Tuma, and P.L. Tuma. 2008. Microtubule acetylation and stability may explain alcohol-induced alterations in hepatic protein trafficking. *Hepatology*. 47:1745-53.
- Kannarkat, G.T., D.J. Tuma, and P.L. Tuma. 2006. Microtubules are more stable and more highly acetylated in ethanol-treated hepatic cells. *J Hepatol*. 44:963-70.
- Klassen, L.W., G.M. Thiele, M.J. Duryee, C.S. Schaffert, A.L. DeVeney, C.D. Hunter, P. Olinga, and D.J. Tuma. 2008. An in vitro method of alcoholic liver injury using precision-cut liver slices from rats. *Biochem Pharmacol*. 76:426-36.
- Kouzarides, T. 2000. Acetylation: a regulatory modification to rival phosphorylation? *Embo J*. 19:1176-9.
- Lakshmanan, M.R., Ezekiel, M., Campbell, B.S., Muesing, R.A. 1986. Binding, uptake, and metabolism of chylomicron remnants by hepatocytes from control and chronic ethanol-fed rats. *Alcohol Clin Exp Res* 10: 412-418.
- Lee, S.M., C.A. Casey, and B.L. McVicker. 2009. Impact of asialoglycoprotein receptor deficiency on the development of liver injury. *World J Gastroenterol*. 15:1194-200.
- Lieber, C.S. 2003. Relationships between nutrition, alcohol use, and liver disease. *Alcohol Res Health*. 27:220-31.
- Lieber, C.S., and L.M. DeCarli. 1989. Liquid diet technique of ethanol administration: 1989 update. *Alcohol Alcohol*. 24:197-211.
- Liu. Y.W., Surka, M.C., Schroeter, T., Lukiyanchuk, V., Schmid, S.L. 2008. Isoform and splice-variant specific functions of dynamin-2 revealed by analysis of conditional knock-out cells. *Mol Biol Cell*. 19:5347-59.
- Liu, C., Tao, Q., Sun, M., Wu, J.Z., Yang, W., Jian, P., Peng, J., Hu, Y., Liu, C., Liu, P. 2010. Kupffer cells are associated with apoptosis, inflammation and fibrotic effects in hepatic fibrosis in rats. *Lab Invest*. Dec;90(12):1805-16.
- Lopez-Perez, M. and Salazar, E.P. 2006. A role for the cytoskeleton in STAT5 activation in MCF7 human breast cancer cells stimulated with EGF. *Int J Biochem Cell Biol* 38: 1716-1728.

- Matsuyama, A., T. Shimazu, Y. Sumida, A. Saito, Y. Yoshimatsu, D. Seigneurin-Berny, H. Osada, Y. Komatsu, N. Nishino, S. Khochbin, S. Horinouchi, and M. Yoshida. 2002. In vivo destabilization of dynamic microtubules by HDAC6-mediated deacetylation. *Embo J.* 21:6820-31.
- Mauch, T.J., Donohue, T.M., Jr., Zetterman, R.K., Sorrell, M.F., Tuma, D.J. 1986. Covalent binding of acetaldehyde selectively inhibits the catalytic activity of lysine-dependent enzymes. *Hepatology* 6: 263-269.
- Mauch, T.J., Tuma, D.J., Sorrell, M.F. 1987. The binding of acetaldehyde to the active site of ribonuclease: alterations in catalytic activity and effects of phosphate. *Alcohol* 22: 103-112.
- Mayor, S., and R.E. Pagano. 2007. Pathways of clathrin-independent endocytosis. *Nat Rev Mol Cell Biol.* 8:603-12.
- McNiven, M.A., and H.M. Thompson. 2006. Vesicle formation at the plasma membrane and trans-Golgi network: the same but different. *Science.* 313:1591-4.
- McVicker, B.L., and C.A. Casey. 1999. Effects of ethanol on receptor-mediated endocytosis in the liver. *Alcohol.* 19:255-60.
- McVicker, B.L., D.J. Tuma, J.L. Kubik, P.L. Tuma, and C.A. Casey. 2006. Ethanol-induced apoptosis in polarized hepatic cells possibly through regulation of the Fas pathway. *Alcohol Clin Exp Res.* 30:1906-15.
- McVicker, B.L., P.L. Tuma, K.K. Kharbanda, S.M.L. Lee, D.J. Tuma. 2009. Relationship between oxidative stress and hepatic glutathione levels in ethanol-mediated apoptosis of polarized hepatic cells. *World J Gastroenterol.* 15:2609-2616.
- Meads, T., and T.A. Schroer. 1995. Polarity and nucleation of microtubules in polarized epithelial cells. *Cell Motil Cytoskeleton.* 32:273-88.
- Medina, V.A., Donohue, T.M., Jr., Sorrell, M.F., Tuma, D.J. 1985. Covalent binding of acetaldehyde to hepatic proteins during ethanol oxidation. *J Lab Clin Med* 105: 5-10.
- Mezey, E. 1980. Alcoholic liver disease: roles of alcohol and malnutrition. *Am J Clin Nutr.* 33:2709-18.
- Mosselmans, R., Hepburn, A., Dumont, J.E., Fiers, W., Galand P. 1988. Endocytic pathway of recombinant murine tumor necrosis factor in L-929 cells. *J Immunol* 141: 3096-3100.

- Nyasae, L.K., A.L. Hubbard, and P.L. Tuma. 2003. Transcytotic efflux from early endosomes is dependent on cholesterol and glycosphingolipids in polarized hepatic cells. *Mol Biol Cell*. 14:2689-705.
- Nygren, A., Adner, N., Sundblad, L., Wiechel, K.L. 1985. Insulin uptake by the human alcoholic cirrhotic liver. *Metabolism* 34: 48-52.
- O'Rourke, M.F., Tuma, D.J., Casey, C.A. 1997. Decreased binding and autophosphorylation of the epidermal growth factor receptor in ethanol-fed rats. *Biochem Pharmacol* 53: 1445-1450.
- O'Shea, R.S., S. Dasarathy, and A.J. McCullough. 2010. Alcoholic liver disease. *Hepatology*. 51:307-28.
- Phung-Koskas, T., A. Pilon, C. Pous, C. Betzina, M. Sturm, M.L. Bourguet-Kondracki, G. Durand, and A. Drechou. 2005. STAT5B-mediated growth hormone signaling is organized by highly dynamic microtubules in hepatic cells. *J Biol Chem*. 280:1123-31.
- Polevoda, B., and F. Sherman. 2002. The diversity of acetylated proteins. *Genome Biol*. 3: reviews0006.
- Ponnambalam, S., and S.A. Baldwin. 2003. Constitutive protein secretion from the trans-Golgi network to the plasma membrane. *Mol Membr Biol*. 20:129-39.
- Potter, B.J., Chapman, R.W., Nunes, R.M., Sorrentino, D., Sherlock, S. 1985. Transferrin metabolism in alcoholic liver disease. *Hepatology*. 5:714-21.
- Pous, C., Chabin, K., Drechou, A., Barbot, L., Phung-Koskas, T., Settegrana, C., Bourguet-Kondracki, M.L., Maurice, M., Cassio, D., Guyot, M., Durand, G. 1998. Functional specialization of stable and dynamic microtubules in protein traffic in WIF-B cells. *J Cell Biol* 142: 153-165.
- Rahimi, R.S., Rockey, D.C. 2012. Complications of cirrhosis. *Curr Opin Gastroenterol*. May;28(3):223-9.
- Ramnarayanan, S.P., C.A. Cheng, M. Bastaki, and P.L. Tuma. 2007. Exogenous MAL reroutes selected hepatic apical proteins into the direct pathway in WIF-B cells. *Mol Biol Cell*. 18:2707-15.
- Ray, S., I. Boldogh, and A.R. Brasier. 2005. STAT3 NH2-terminal acetylation is activated by the hepatic acute-phase response and required for IL-6 induction of angiotensinogen. *Gastroenterology*. 129:1616-32.

- Rifkin, R.M., Todd, W.W., Toothaker, D.R., Sussman, A., Trowbridge, M., Draznin, B. 1983. Effects of in vivo and in vitro alcohol administration on insulin binding and glycogenesis in isolated rat hepatocytes. *Ann Nutr Metab* 27: 313-319.
- Rodriguez-Boulan, E., and A. Musch. 2005. Protein sorting in the Golgi complex: shifting paradigms. *Biochim Biophys Acta*. 1744:455-64.
- Rojkind, M, and Greenwel, P., 2001. Pathophysiology of Liver Fibrosis. *In The Liver: biology and pathobiology*. I.M. Arias, J.L. Boyer, F.V. Chisari, N. Fausto, D. Schachter, and D.A. Shafritz, editors. Lippincott Williams & Wilkins, Philadelphia.
- Sachse, M., van Kerkhof, P., Strous, G.J., Klumperman, J. 2001. The ubiquitin-dependent endocytosis motif is required for efficient incorporation of growth hormone receptor in clathrin-coated pits, but not clathrin-coated lattices. *J Cell Sci* 114: 3943-3952.
- Saucan L., Palade G.E., 1992. Differential colchicine effects on the transport of membrane and secretory proteins in rat hepatocytes in vivo: bipolar secretion of albumin, *Hepatology* 15: 714-721.
- Saucan, L., and G.E. Palade. 1994. Membrane and secretory proteins are transported from the Golgi complex to the sinusoidal plasmalemma of hepatocytes by distinct vesicular carriers. *J Cell Biol*. 125:733-41.
- Schachter, D. 2001. The hepatocyte plasma membrane: organization, differentiation, biogenesis, and turnover. *In The Liver: biology and pathobiology*. I.M. Arias, J.L. Boyer, F.V. Chisari, N. Fausto, D. Schachter, and D.A. Shafritz, editors. Lippincott Williams & Wilkins, Philadelphia.
- Schaffert, C.S., S.L. Todero, B.L. McVicker, P.L. Tuma, M.F. Sorrell, and D.J. Tuma. 2004. WIF-B cells as a model for alcohol-induced hepatocyte injury. *Biochem Pharmacol*. 67:2167-74.
- Seeley, R.R., Stephens, T.D., Tate, P. 2002. *Essentials of Anatomy and Physiology*, 4th ed. McGraw-Hill, NY, New York.
- Shanks, M.R., D. Cassio, O. Lecoq, and A.L. Hubbard. 1994. An improved polarized rat hepatoma hybrid cell line. Generation and comparison with its hepatoma relatives and hepatocytes in vivo. *J Cell Sci*. 107 (Pt 4):813-25.
- Sharma, R.J., and D.A. Grant. 1986. A differential effect between the acute and chronic administration of ethanol on the endocytotic rate constant, k_e , for the internalisation of asialoglycoproteins by hepatocytes. *Biochim Biophys Acta*. 862:199-204.

- Shepard, B.D., D.J. Fernandez, and P.L. Tuma. 2010. Alcohol consumption impairs hepatic protein trafficking: mechanisms and consequences. *Genes Nutr*.
- Shepard, B.D., R.A. Joseph, G.T. Kannarkat, T.M. Rutledge, D.J. Tuma, and P.L. Tuma. 2008. Alcohol-induced alterations in hepatic microtubule dynamics can be explained by impaired histone deacetylase 6 function. *Hepatology*.
- Shepard, B.D., and P.L. Tuma. 2010. Alcohol-induced alterations of the hepatocyte cytoskeleton. *World J Gastroenterol*. Mar 21;16(11):1358-65.
- Shepard, B.D., D.J. Tuma, and P.L. Tuma. 2009. Chronic Ethanol Consumption Induces Global Hepatic Protein Hyperacetylation. *Alcohol Clin Exp Res*.
- Shepard, B.D., D.J. Tuma, and P.L. Tuma. 2012. Lysine acetylation induced by chronic ethanol consumption impairs dynamin-mediated clathrin-coated vesicle release. *Hepatology*. 55(4):1260-70
- Smith, S.L., R.B. Jennett, M.F. Sorrell, and D.J. Tuma. 1992. Substoichiometric inhibition of microtubule formation by acetaldehyde-tubulin adducts. *Biochem Pharmacol*. 44:65-72.
- Sorkin, A., and Goh, L.K. 2009. Endocytosis and intracellular trafficking of ErbBs. *Exp Cell Res* 315: 683-696.
- Sorrell, M.F., D.J. Tuma, E.C. Schafer, and A.J. Barak. 1977. Role of acetaldehyde in the ethanol-induced impairment of glycoprotein metabolism in rat liver slices. *Gastroenterology*. 73:137-44.
- Stevens, V.J., Fantl, W.J., Newman, C.B., Sims, R.V., Cerami, A., Peterson, C.M. 1981. Acetaldehyde adducts with hemoglobin. *J Clin Invest* 67: 361-369
- Szasz, J., Burns, R., Sternlicht, H. 1982. Effects of reductive methylation on microtubule assembly. Evidence for an essential amino group in the alpha-chain. *J Biol Chem* 257: 3697-3704.
- Szasz, J., Yaffe, M.B., Elzinga, M., Blank, G.S., Sternlicht, H. 1986. Microtubule assembly is dependent on a cluster of basic residues in alpha-tubulin. *Biochemistry* 25: 4572-4582.
- Taub, R. 2003. Hepatoprotection via the IL-6/Stat3 pathway. *J Clin Invest*. 112:978-80.

- Thiel, S., Behrmann, I., Dittrich, E., Muys, L., Tavernier, J., Wijdenes, J., Heinrich, P.C., Graeve L. 1998. Internalization of the interleukin 6 signal transducer gp130 does not require activation of the Jak/STAT pathway. *Biochem J* 330 (Pt 1): 47-54.
- Tuma, D.J., Casey, C.A., Sorrell, M.F. 1991. Chronic ethanol-induced impairments in receptor-mediated endocytosis of insulin in rat hepatocytes. *Alcohol Clin Exp Res* 15: 808-813.
- Tuma, D.J., and C.A. Casey. 2003. Dangerous byproducts of alcohol breakdown--focus on adducts. *Alcohol Res Health*. 27:285-90.
- Tuma, D.J., Hoffman, T., Sorrell, M.F. 1991. The chemistry of acetaldehyde-protein adducts. *Alcohol Alcohol Suppl* 1: 271-276.
- Tuma, P.L., and A.L. Hubbard. 2003. Transcytosis: crossing cellular barriers. *Physiol Rev*. 83:871-932.
- Tuma, P.L., and A.L. Hubbard. 2001. The hepatocyte surface: dynamic polarity. In *The Liver: biology and pathobiology*. I.M. Arias, J.L. Boyer, F.V. Chisari, N. Fausto, D. Schachter, and D.A. Shafritz, editors. Lippincott Williams & Wilkins, Philadelphia.
- Tuma, D.J., M.R. Newman, T.M. Donohue, Jr., and M.F. Sorrell. 1987. Covalent binding of acetaldehyde to proteins: participation of lysine residues. *Alcohol Clin Exp Res*. 11:579-84.
- Tuma, D.J., Todero, S.L., Barak-Bernhagen, M., Sorrell, M.F. 1996. Effects of chronic ethanol administration on the endocytosis of cytokines by rat hepatocytes. *Alcohol Clin Exp Res* 20: 579-583.
- Tworek, B.L., Tuma, D.J., Casey, C.A. 1996. Decreased binding of asialoglycoproteins to hepatocytes from ethanol-fed rats. Consequence of both impaired synthesis and inactivation of the asialoglycoprotein receptor. *J Biol Chem* 271: 2531-2538.
- Ujhazy, P., H. Kipp, S. Misra, Y. Wakabayashi, and I.M. Arias. 2001. The biology of the bile canaliculus. In *The Liver: biology and pathobiology*. I.M. Arias, J.L. Boyer, F.V. Chisari, N. Fausto, D. Schachter, and D.A. Shafritz, editors. Lippincott Williams & Wilkins, Philadelphia.
- Van de Wiel, A., Delacroix, D.L., van Hattum, J., Schuurman, H.J., Kater, L. 1987. Characteristics of serum IgA and liver IgA deposits in alcoholic liver disease. *Hepatology*. 7:95-9.

Van Kerkhof, P., Sachse, M., Klumperman, J., Strous G.J. 2001. Growth hormone receptor ubiquitination coincides with recruitment to clathrin-coated membrane domains, *J Biol Chem* 276: 3778-3784.

Volentine, G.D., K.A. Ogden, D.K. Kortje, D.J. Tuma, and M.F. Sorrell. 1987. Role of acetaldehyde in the ethanol-induced impairment of hepatic glycoprotein secretion in the rat in vivo. *Hepatology*. 7:490-5.

Watanabe, J., Kanamura, S., Asada-Kubota, M., Kanai, K., Oka M. 1984. Receptor-mediated endocytosis of glucagon in isolated mouse hepatocytes. *Anat Rec* 210: 557-567.

Westermann, S., and K. Weber. 2003. Post-translational modifications regulate microtubule function. *Nat Rev Mol Cell Biol*. 4:938-47.

Xu, D.S., Jennett, R.B., Smith, S.L., Sorrell, M.F., Tuma, D.J. 1989. Covalent interactions of acetaldehyde with the actin/microfilament system. *Alcohol Alcohol* 24: 281-289.

Yoon, Y., Torok, N., Krueger, E., Oswald, B., McNiven, M.A. 1998. Ethanol-induced alterations of the microtubule cytoskeleton in hepatocytes. *Am J Physiol* 274: G757-766.

Zhang, J., R. Sprung, J. Pei, X. Tan, S. Kim, H. Zhu, C.F. Liu, N.V. Grishin, and Y. Zhao. 2008. Lysine acetylation is a highly abundant and evolutionarily conserved modification in *E. coli*. *Mol Cell Proteomics*.

Zhang X., Yuan Z., Zhang Y., Yong S., Salas-Burgos A., Koomen J., Olashaw N., Parsons J.T., Yang X.J., Dent S.R., Yao T.P., Lane W.S., Seto E., 2007 HDAC6 modulates cell motility by altering the acetylation level of cortactin, *Mol Cell* 27: 197-213.

Zhang, Y., N. Li, C. Caron, G. Matthias, D. Hess, S. Khochbin, and P. Matthias. 2003. HDAC-6 interacts with and deacetylates tubulin and microtubules in vivo. *Embo J*. 22:1168-79.